WEC PROPRIETARY CLASS 3

[redacted]

[redacted]

Westinghouse Energy Systems

WEC PROPRIETARY CLASS 3

[redacted]

[redacted]

WESTINGHOUSE CLASS 3

WCAP-12920

ANALYSIS OF THE SOUTHERN CALIFORNIA EDISON COMPANY SAN ONOFRE UNIT 3 REACTOR VESSEL SURVEILLANCE CAPSULE REMOVED FROM THE 97° LOCATION

E. Terek
E. P. Lippincott
A. Madeyski

March 1991

Work Performed Under Shop Order SJOP-106

Prepared by Westinghouse Electric Corporation
for the Southern California Edison Company

Approved by: T. A. Meyer

T. A. Meyer, Manager
Structural Reliability and
Plant Life Optimization

WESTINGHOUSE ELECTRIC CORPORATION
Nuclear and Advanced Technology Division
P.O. Box 355
Pittsburgh, Pennsylvania 15230-0355

PREFACE

This report has been technically reviewed and verified.

	Reviewer	
Sections 1 through 5, 7 and 8	J. M. Chicots	J. M. Chicots
Section 6	S. L. Anderson	S L Anderson

TABLE OF CONTENTS

LIST OF TABLES (Cont)

LIST OF TABLES (Cont)

LIST OF TABLES (Cont)

LIST OF TABLES (Cont)

LIST OF ILLUSTRATIONS

LIST OF ILLUSTRATIONS

LIST OF ILLUSTRATIONS

LIST OF ILLUSTRATIONS

SECTION 1.0
SUMMARY OF RESULTS

The analysis of the Southern California Edison Company San Onofre Unit 3 reactor vessel materials contained in the surveillance capsule removed from the 97° location, the first capsule to be removed from the San Onofre Unit 3 reactor pressure vessel, led to the following conclusions:

- The capsule received an average fast neutron fluence (E > 1.0 MeV) of 0.8×10^{19} n/cm^2 after 4.33 EFPY of plant operation.

- Irradiation of reactor vessel shell plate C-6802-1 Charpy specimens to 0.8×10^{19} n/cm^2 (E > 1.0 MeV) at 550°F resulted in a 30 and 50 ft-lb transition temperature increase of 55 and 67°F, respectively, for specimens oriented normal to the major working direction (transverse orientation).

- Irradiation of reactor vessel shell plate C-6802-1 Charpy specimens to 0.8×10^{19} n/cm^2 (E > 1.0 MeV) at 550°F resulted in a 30 and 50 ft-lb transition temperature increase of 50 and 45°F, respectively, for specimens oriented parallel to the major working direction (longitudinal orientation).

- The weld metal Charpy specimens irradiated to 0.8×10^{19} n/cm^2 (E > 1.0 MeV) at 550°F resulted in a 30 ft-lb transition temperature increase of 32°F and a 50 ft-lb transition temperature increase of 25°F.

- Irradiation of the reactor vessel weld Heat-Affected-Zone (HAZ) metal Charpy specimens to 0.8×10^{19} n/cm^2 (E > 1.0 MeV) at 550°F resulted in a 30 ft-lb transition temperature increase of 45°F and a 50 ft-lb transition temperature increase of 70°F.

- The average upper shelf energy of shell plate C-6802-1 showed a decrease of 16 ft-lbs after irradiation to 0.8×10^{19} n/cm^2 (E > 1.0 MeV) at 550°F for specimens oriented normal to the major working direction (transverse orientation).

- The average upper shelf energy of shell plate C-6802-1 showed a decrease of 22 ft-lbs after irradiation to 0.8×10^{19} n/cm^2 (E > 1.0 MeV) at 550°F for specimens oriented parallel to the major working direction (longitudinal orientation).

- The average upper shelf energy of the weld metal showed a decrease of 12 ft-lbs after irradiation to 0.8×10^{19} n/cm^2 (E > 1.0 MeV) at 550°F.

- The average upper shelf energy of the weld Heat-Affected-Zone (HAZ) metal showed a decrease of 11 ft-lbs after irradiation to 0.8×10^{19} n/cm^2 (E > 1.0 MeV) at 550°F.

- The calculated end-of-life (32 EFPY) maximum neutron fluence (E > 1.0 MeV) for the San Onofre Unit 3 reactor vessel is as follows:

  Vessel inner radius * = 4.20×10^{19} n/cm^2
  Vessel 1/4 thickness = 2.24×10^{19} n/cm^2
  Vessel 3/4 thickness = 4.58×10^{18} n/cm^2

  * Clad/base metal interface

- Based on an EOL (32 EFPY) peak clad/base metal interface fluence of 4.20×10^{19} n/cm^2 (E > 1.0 MeV), Regulatory Guide 1.99 Revision 2 and 10 CFR Part 50, the reactor vessel surveillance material, plate C-6802-1 and weld metal, are expected to meet the screening criteria of at least 50 ft-lb of upper shelf energy and an RT_{NDT} of less than 270°F for plate material and axial welds and less than 300°F for circumferential welds through EOL (32 EFPY).

SECTION 2.0
INTRODUCTION

This report presents the results of the examination of the capsule located at 97°, the first surveillance capsule to be removed from the San Onofre Unit 3 reactor vessel in the continuing surveillance program which monitors the effects of neutron irradiation on the Southern California Edison Company San Onofre Unit 3 reactor pressure vessel materials under actual operating conditions.

The surveillance program for the San Onofre Unit 3 reactor pressure vessel materials was designed by Combustion Engineering, Inc.[1] to the requirements of ASTM 185-73 "Standard Recommended Practice for Surveillance Tests for Nuclear Reactor Vessels". A complete description of the surveillance program has been reported by Combustion Engineering, Inc.[1]

Westinghouse Power Systems personnel were contracted to aid in the preparation of procedures for removing the capsule located at 97° from the reactor and its shipment to the Westinghouse Science and Technology Center Metallographic Hot Cell Facility, where the postirradiation mechanical testing of the Charpy V-notch impact and tensile surveillance specimens was performed.

This report summarizes the testing of and the postirradiation data obtained from the first surveillance capsule to be removed from the San Onofre Unit 3 reactor vessel and discusses the analysis of these data. The data are compared to the results of tests performed on unirradiated material from the reactor vessel.[2]

SECTION 3.0
BACKGROUND

The ability of the large steel pressure vessel containing the reactor core and its primary coolant to resist fracture constitutes an important factor in ensuring safety in the nuclear industry. The beltline region of the reactor pressure vessel is the most critical region of the vessel because it is subjected to significant fast neutron bombardment. The overall effects of fast neutron irradiation on the mechanical properties of low alloy, ferritic pressure vessel steels such as SA533 Grade B Class 1 (base material of the San Onofre Unit 3 reactor pressure vessel beltline) are well documented in the literature. Generally, low alloy ferritic materials show an increase in hardness and tensile properties and a decrease in ductility and toughness under certain conditions of irradiation.

A method for performing analyses to guard against fast fracture in reactor pressure vessels has been presented in "Protection Against Nonductile Failure," Appendix G to Section III of the ASME Boiler and Pressure Vessel Code. The method uses fracture mechanics concepts and is based on the reference nil-ductility temperature (RT_{NDT}).

RT_{NDT} is defined in the ASME Code as follows:

> Determine a temperature T_{NDT} that is at or above the nil-ductility transition temperature by drop weight tests.
>
> At a temperature not greater than T_{NDT}+60°F, each specimen of the Charpy V-notch (C_V) test (NB-2321.2) shall exhibit at least 35 mils lateral expansion and not less than 50 ft-lb absorbed energy. When these requirements are met, T_{NDT} is the reference temperature RT_{NDT}.

In the event that the above requirements are not met, conduct additional C_v tests in groups of three specimens to determine the temperature T_{C_v} at which they are met. In this case the reference temperature $RT_{NDT} = T_{C_v} - 60°F$. Thus, the reference temperature RT_{NDT} is the higher of T_{NDT} and $(T_{C_v} - 60°F)$.

When a C_v test has not been performed at $T_{NDT} + 60°F$ or when the C_v test at $T_{NDT} + 60°F$ does not exhibit a minimum of 50 ft-lb and 35 mils lateral expansion, a temperature representing a minimum of 50 ft-lb and 35 mils lateral expansion may be obtained from a full C_v impact curve developed from the minimum data points of all the C_v tests performed.

The RT_{NDT} of a given material is used to index that material to a reference stress intensity factor curve (K_{IR} curve) which appears in Appendix G of the ASME Code. The K_{IR} curve is a lower bound of dynamic, crack arrest, and static fracture toughness results obtained from several heats of pressure vessel steel. When a given material is indexed to the K_{IR} curve, allowable stress intensity factors can be obtained for this material as a function of temperature. Allowable operating limits can then be determined using these allowable stress intensity factors.

RT_{NDT} and, in turn, the operating limits of nuclear power plants can be adjusted to account for the effects of radiation on the reactor vessel material properties. The radiation embrittlement changes in mechanical properties of a given reactor pressure vessel steel can be monitored by a reactor vessel surveillance program such as the Program for Irradiation Surveillance of San Onofre Unit 3 Reactor Vessel Materials[1], in which a surveillance capsule is periodically removed from the operating nuclear reactor and the encapsulated specimens are tested. The increase in the average Charpy V-notch 30 ft-lb temperature (ΔRT_{NDT}) due to irradiation is added to the original RT_{NDT} to adjust the RT_{NDT} for radiation embrittlement. This adjusted RT_{NDT} (RT_{NDT} initial + ΔRT_{NDT}) is used to index the material to the K_{IR} curve and, in turn, to set operating limits for the nuclear power plant which take into account the effects of irradiation on the reactor vessel materials.

SECTION 4.0
DESCRIPTION OF PROGRAM

Six surveillance capsules for monitoring the effects of neutron radiation exposure on the San Onofre Unit 3 reactor pressure vessel core region material were inserted in the reactor vessel prior to initial plant start-up. A typical surveillance capsule assembly is shown in Figure 4-1. The six irradiation capsule assemblies are located at radial positions about the core, with their axial positions bisected by the midplane of the core. The capsule assemblies are contained in capsule holders positioned circumferentially about the core at locations which include regions of maximum flux as shown in Figure 4-2. The six vessel surveillance capsule assemblies are located near the inside wall of the reactor vessel.

The first surveillance capsule, located at 97°F, was removed after 4.33 effective full power years of plant operation. This capsule contained Charpy V-notch and tensile specimens from intermediate shell plate C-6802-1, weld metal and weld Heat-Affected-Zone (HAZ) material.

The chemical composition of the San Onofre Unit 3 beltline materials is presented in Table 4-1[2]. The chemical analysis reported in Table 4-1 was obtained from unirradiated material used in the San Onofre Unit 3 surveillance program [2]. In addition, a chemical analysis using Inductively Coupled Plasma Spectrometry (ICPS) was performed on irradiated weld metal specimens 37B and 367, intermediate shell plate C-6802-1 specimen 22B and HAZ metal specimen 46T and is reported in Table 4-2. The chemistry results from the NBS certified reference standards are reported in Table 4-3.

The San Onofre Unit 3 reactor vessel intermediate shell plate C-6802-1 was fabricated from SA 533 Grade B, Class 1 steel plate. The San Onofre Unit 3 surveillance materials are made from the same material. The steel plate was manufactured by Combustion Engineering and heat treated as follows:

The heat treatment for the plate material consisted of austenitization at 1600°F ± 25°F for 4 hours; water quenched and tempered at 1225°F ± 25°F for 4 hours. After a 40-hour stress relief at 1150°F ± 25°F the plates were furnace cooled to 600°F. The weldment received a final 41-hour and 45-minute stress relief at 1100 to 1150°F.

Because the lower and intermediate shell courses of the reactor vessel experience the highest fluences in the entire vessel, selection of the candidate surveillance base materials was restricted to the six plates in the intermediate and lower shell courses. Selection criteria followed the general guidelines of ASTM E185-73, "Standard Recommended Practice for Surveillance Tests for Nuclear Reactor Vessels".

The San Onofre Unit 3 surveillance materials consist of intermediate shell plate C-6802-1 which was made of SA 533 Grade B Class 1 plate, Mil B-4 submerged arc-weld with Linde 124 flux and Heat-Affected-Zone (HAZ) metal from plate C-6802-1.

All test specimens were machined from the 1/4 thickness location of the plate material. Test specimens represent material taken at least one plate thickness from the quenched end.

The longitudinal base metal Charpy V-notch test specimens were oriented with the longitudinal axis of the specimen parallel to the major rolling direction of the plate whereas transverse base metal specimens were oriented with the longitudinal axis perpendicular to the major rolling direction and parallel to the surface of the plate. The axis of the notch of the Charpy specimens was machined perpendicular to the major surfaces of the plate.

The weld metal Charpy impact test specimens were oriented transversely with their major axis perpendicular to the direction of the weld and parallel to the surface of the plate. The notch in each of the test specimens was oriented perpendicular to the surface of the weld.

The Heat-Affected-Zone (HAZ) metal Charpy V-notch test specimens were oriented transversely with the longitudinal axis of the specimen perpendicular to the direction of the weld and parallel to the surface of the plate. The notch in each of the test specimens was oriented perpendicular to the surface of the weld and the root of the notch was centered on a line parallel to and 1/32 inch from the weld fusion line on the Heat-Affected-Zone side.

The longitudinal base metal tensile test specimens were oriented with the longitudinal axis of the specimen parallel to the major rolling direction of the plate whereas transverse base metal specimens were oriented with the longitudinal axis perpendicular to the major rolling direction and parallel to the surface of the plate.

The weld metal tensile test specimens were oriented transversely with their major axis perpendicular to the direction of the weld and parallel to the surface of the plate.

The Heat-Affected-Zone (HAZ) metal tensile test specimens were oriented transversely with the longitudinal axis of the specimen perpendicular to the direction of the weld and parallel to the surface of the plate. The test specimens were positioned so that the HAZ was centered as closely as possible in the gage length of the specimen.

The capsule contained fission threshold detectors (U-238) and threshold detectors of nickel (Ni), titanium (Ti), iron (Fe), sulfur (S), copper (Cu) with known cobalt (Co) content and Cobalt (Co) to monitor the thermal neutron exposure. The flux monitors were located in the three tensile-monitor compartment assemblies as shown in Figure 4-3.

Thermal monitors made from low-melting eutectic alloys sealed in quartz tubes were included in the capsule and were also located in the three tensile-monitor compartment assemblies as shown in Figure 4-3. The composition of the alloys and their melting points are as follows:

Chemical Composition	Melting Temperature (°C)	(°F)
80% Au, 20% Sn	280	536
90% Pb, 5% Sn, 5% Ag	292	558
97.5% Pb, 2.5% Ag	304	580
97.5% Pb, 0.75% Sn, 1.75% Ag	310	590

Contained in Figure 4-4 is A typical Charpy impact compartment assembly.

TABLE 4-1

Chemical Composition of the Unirradiated San Onofre Unit 3 Reactor Vessel Surveillance Program Materials *

	Weight Percent	
	Plate	Weld
Element	C-6802-1	C-6802-2 & 3
Si	0.23	0.39
S	0.014	0.009
P	0.008	0.004
Mn	1.38	1.54
C	0.24	0.12
Cr	0.07	0.05
Ni	0.57	0.08
Mo	0.58	0.55
V	0.005	0.005
Cb	<.01	<.01
B	0.0005	0.001
Co	0.010	0.015
Cu	0.05	0.03
Al	0.033	0.006
W	<.01	0.01
Ti	<.01	<.01
As	0.009	<.001
Sn	0.005	0.002
Zr	0.002	<.001
N	0.010	0.006
Sb	---	0.0012
Pb	---	<.001

* Chemical Composition as Reported in Reference 2.

TABLE 4-2

Chemical Compostion of Four San Onofre Unit 3 Charpy Specimens Removed from Surveillance Capsule W-97*

	Chemical Composition (wt.%)			
	Standard Reference Metal		Weld Metal	
Specimen No.	37B	36T	46T	22B
Material	WELD	WELD	HAZ	BASE
Fe	MATRIX ELEMENT: Remainder by Difference			
Mn	1.430	1.464	1.295	1.307
Cr	0.063	0.061	0.102	0.101
Ni	0.108	0.094	0.567	0.575
Mo	0.563	0.544	0.527	0.531
Co	0.010	0.012	<0.010	<0.010
Cu	0.034	0.032	0.057	0.058
P	0.014	0.011	0.012	0.009
V	0.015	0.014	0.007	0.014
C	0.116	0.111	0.221	0.237
S	0.0075	0.0075	0.0136	0.0135
Si	0.411	0.355	0.244	0.048

Analyses	Method of Analysis
Metals	ICPS, Inductively Coupled Plasma Spectrometry
Carbon	EC-12, LECO Carbon Analyzer
Sulfur	Combustion/titration
Silicon	Dissolution/gravimetric

TABLE 4-3

Chemistry Results from the NBS

Certified Reference Standards

Material ID		Low Alloy Steel: NBS Certified Reference Standards			
		NBS 361		NBS 362	
		Certified	Measured	Certified	Measured
Metals		Concentration in Weight Percent			
Fe	*	95.60	(matrix)	95.30	(matrix)
Mn		0.66	0.671	1.04	1.075
Cr		0.694	0.701	0.30	0.310
Ni		2.00	2.12	0.59	0.615
Mo		0.19	0.195	0.068	0.065
Co		0.032	0.015	0.30	0.347
Cu		0.042	0.043	0.50	0.519
P		0.014	0.0141	0.041	0.0395
V		0.011	0.014	0.040	0.0355
C		0.383	0.3844	0.160	0.1620
S		0.014	N.A.	0.036	0.0362
Si		0.222	0.228	0.39	N.A.

Material ID		Low Alloy Steel: NBS Certified Reference Standards			
		NBS 363		NBS 364	
		Certified	Measured	Certified	Measured
Metals		Concentration in Weight Percent			
Fe	*	94.4	(matrix)	96.7	(matrix)
Mn		1.50	1.556	0.255	0.251
Cr		1.31	1.366	0.063	0.061
Ni		0.30	0.321	0.144	0.142
Mo		0.028	0.029	0.49	0.495
Co		0.048	0.040	0.15	0.160
Cu		0.10	0.102	0.249	0.253
P		0.029	0.0316	0.01	0.0094
V		0.31	0.251	0.105	0.106
C		0.62	N.A.	0.87	N.A.
S		0.0068	N.A.	0.0250	0.0249
Si		0.74	N.A.	0.065	N.A.

* Matrix element calculated as difference for material balance. ( )

N.A. - Not analyzed

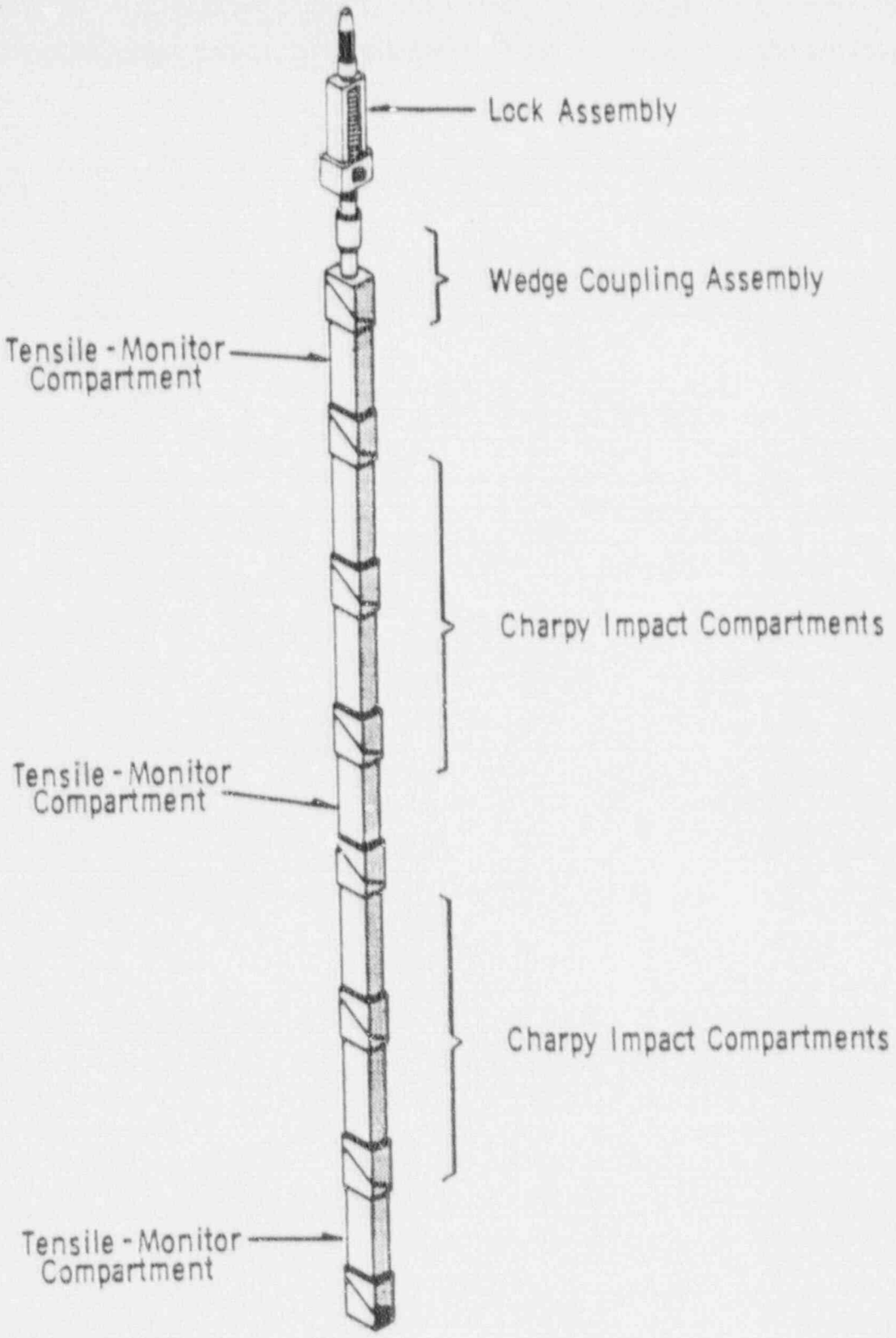

Figure 4-1. Typical Surveillance Capsule Assembly

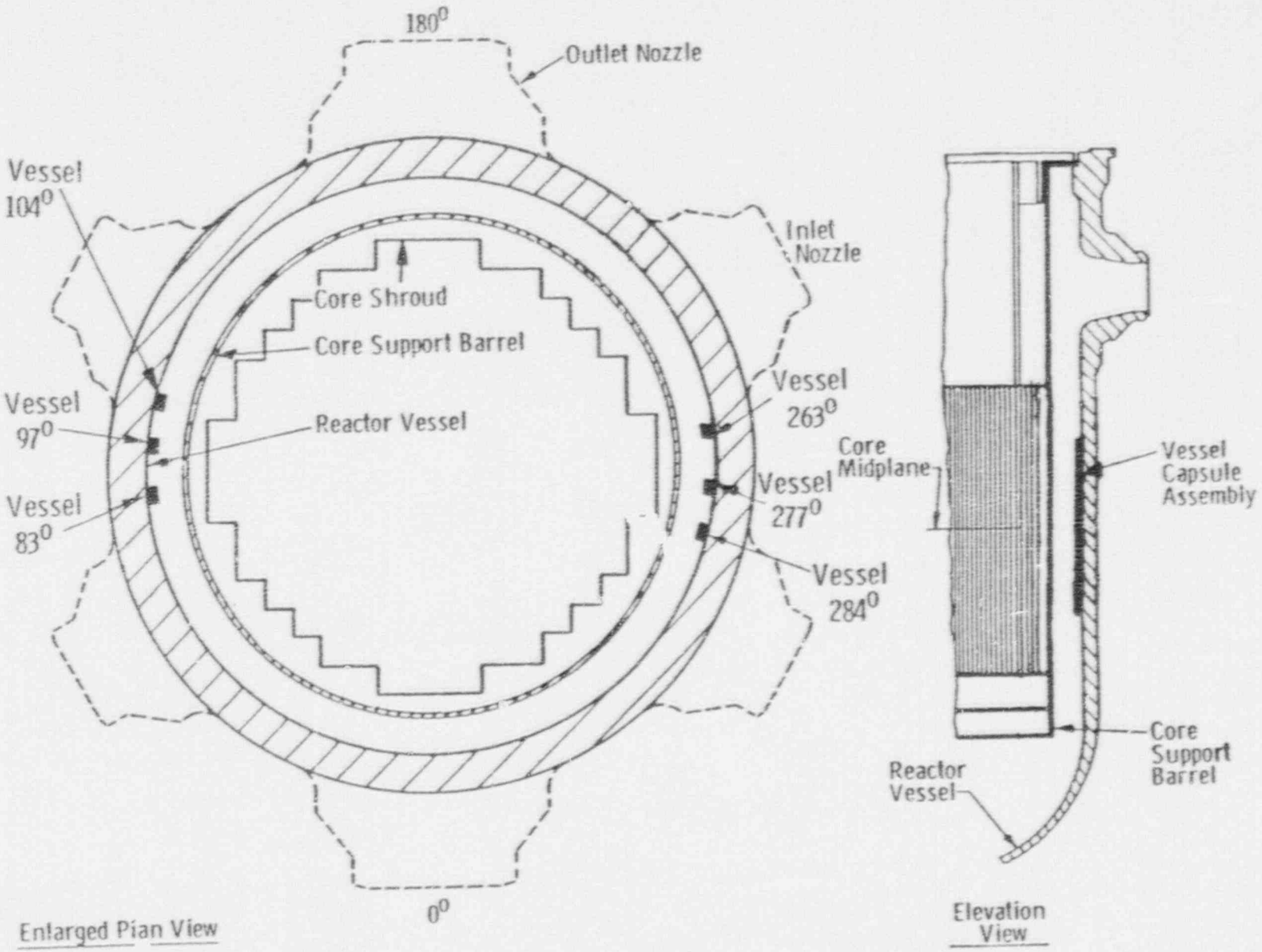

Figure 4-2. Typical Locations of San Onofre Unit 3 Surveillance Capsule Assemblies

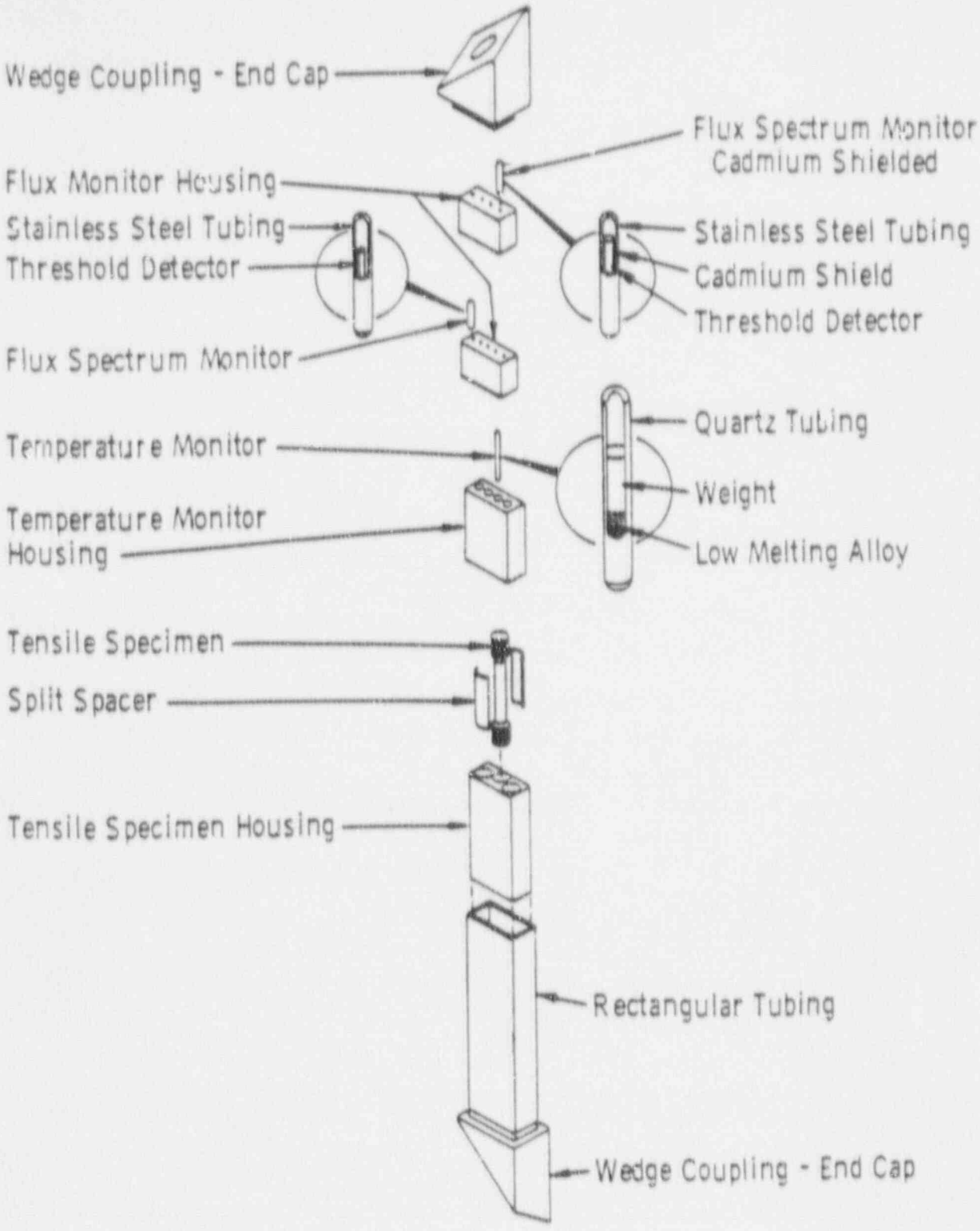

Figure 4-3. Typical Tensile-Monitor Compartment Assembly

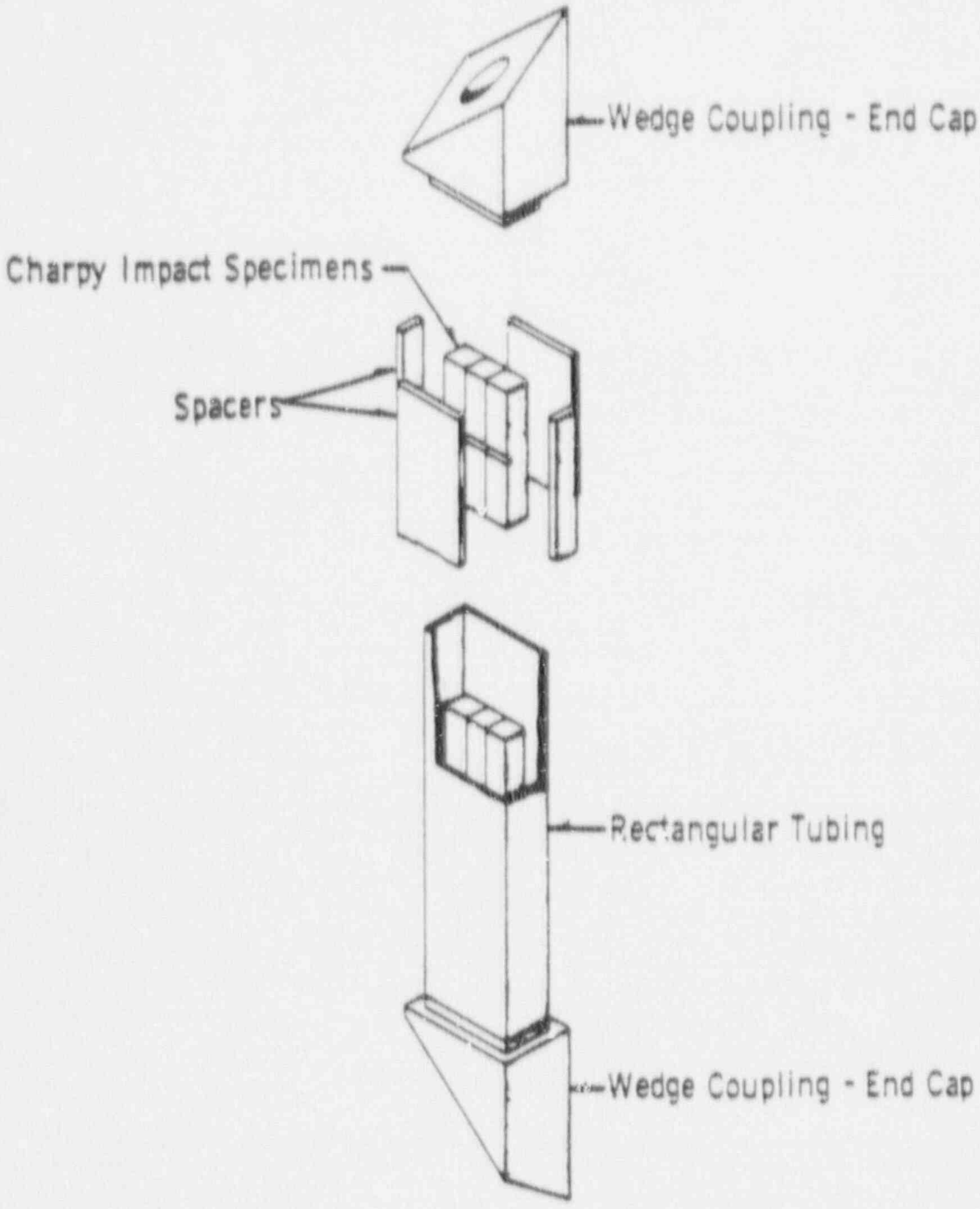

Figure 4-4. Typical Charpy Impact Compartment Assembly

SECTION 5.0
TESTING OF SPECIMENS FROM THE SURVEILLANCE CAPSULE LOCATED AT 97°

5.1 Overview

The post-irradiation mechanical testing of the Charpy V-notch and tensile specimens, contained in the surveillance capsule removed from the 97° location, was performed at the Westinghouse Science and Technology Center Hot Cell Laboratory with consultation by Westinghouse Power Systems personnel. Testing was performed in accordance with 10CFR50, Appendices G and H[3], ASTM Specification E185-82[4] and Westinghouse Procedure MHL 8402, Revision 1 as modified by RMF Procedures 8102, Revision 1 and 8103, Revision 1.

Upon receipt of the capsule at the laboratory, the specimens and spacer blocks were carefully removed, inspected for identification number, and checked against the master list supplied by the Southern California Edison Company. No discrepancies were found.

The surveillance capsule had four low melting eutectic alloy thermal monitors which were removed from Blocks C214, C242, and C273. The thermal monitors were encapsulated in quartz tubes of 1, 1.25, 1.50, and 1.75 inches long and had melting temperatures of 536°, 558°, 580° and 590°F, respectively. Examination of the four low-melting, 536°, 558°, 580° and 590°F eutectic alloys indicated melting of the 536°F monitor, but not of the three remaining thermal monitors in blocks C214 and C242. Based on this examination, the maximum temperature to which these blocks were exposed was less than 558°F but more than 536°F. At block C273 both the 536°F and the 558°F melting point alloys melted, indicating that the temperature of this block reached the range from 558°F to 580°F. Figure 5-1 shows the condition of the thermal monitors.

The Charpy impact tests were performed per ASTM Specification E23-88[5] and RMF Procedure 8103, Revision 1 on a Tinius-Olsen Model 74, 358J machine. The tup (striker) of the Charpy machine is instrumented with an Effects Technology Model 500 instrumentation system. With this system, load-time and energy-time signals can be recorded in addition to the standard measurement of Charpy

energy (E_D). From the load-time curve, the load of general yielding (P_{GY}), the time to general yielding (t_{GY}), the maximum load (P_M) and the time to maximum load (t_M) can be determined. Under some test conditions, a sharp drop in load indicative of fast fracture was observed. The load at which fast fracture was initiated is identified as the fast fracture load (P_F), and the load at which fast fracture terminated is identified as the arrest load (P_A).

The energy at maximum load (E_M) was determined by comparing the energy-time record and the load-time record. The energy at maximum load is roughly equivalent to the energy required to initiate a crack in the specimen. Therefore, the propagation energy for the crack (E_p) is the difference between the total energy to fracture (E_D) and the energy at maximum load.

The yield stress (σ_Y) is calculated from the three-point bend formula having the following expression:

$$\sigma_Y = P_{GY} * [L / (B * (W-a)^2 * C)] \qquad (1)$$

where the constant C is dependent on the notch flank angle (ϕ), notch root radius (ρ), and the type of loading (i.e. pure bending or three-point bending). In three-point bending, a Charpy specimen in which $\phi = 45°$ and $\rho = 0.010"$, Equation 1 is valid with with C = 1.21. Therefore (for L = 4W),

$$\sigma_Y = P_{GY} * [L/(B*(W-a)^2 * 1.21)] = [3.3 P_{GY} W]/[B(W-a)^2] \qquad (2)$$

For the Charpy specimens, B = 0.394 in., W = 0.394 in. and a = 0.079 in. Equation 2 then reduces to:

$$\sigma_Y = 33.3 \times P_{GY} \qquad (3)$$

where σ_Y is in units of psi and P_{GY} is in units of lbs. The flow stress was calculated from the average of the yield and maximum loads, also using the three-point bend formula.

Percent shear was determined from post-fracture photographs using the ratio-of-areas methods in compliance with ASTM Specification A370-89[6]. The lateral expansion was measured using a dial gage rig similar to that shown in the same specification.

Tension tests were performed on a 20,000-pound Instron, split-console test machine (Model 1115) per ASTM Specification E8-89b[7] and E21-79(1988)[8], and RMF Procedure 8102, Revision 1. All pull rods, grips, and pins were made of Inconel 718 hardened to HRC45. The upper pull rod was connected through a universal joint to improve axiality of loading. The tests were conducted at a constant crosshead speed of 0.05 inches per minute throughout the test.

Extension measurements were made with a linear variable displacement transducer (LVDT) extensometer. The extensometer knife edges were spring-loaded to the specimen and operated through specimen failure. The extensometer gage length is 1.00 inch. The extensometer is rated as Class B-2 per ASTM E83-85[9].

Elevated test temperatures were obtained with a three-zone electric resistance split-tube furnace with a 9-inch hot zone. All tests were conducted in air.

Because of the difficulty in remotely attaching a thermocouple directly to the specimen, the following procedure was used to monitor specimen temperature: Chromel-alumel thermocouples were inserted in shallow holes in the center and each end of the gage section of a dummy specimen and in each grip. In the test configuration, with a slight load on the specimen, a plot of specimen temperature versus upper and lower grip and controller temperatures was developed over the range of room temperature to 550°F (288°C). The upper grip was used to control the furnace temperature. During the actual testing, the grip temperatures were used to obtained desired specimen temperatures. Experiments indicated that this method is accurate to ±2°F.

The yield load, ultimate load, fracture load, total elongation, and uniform elongation were determined directly from the load-extension curve. The yield strength, ultimate strength and fracture strength were calculated using the original cross-sectional area. The final diameter and final gage length were determined from post-fracture photographs. The fracture area used to calculate the fracture stress (true stress at fracture) and percent reduction in area was computed using the final diameter measurement.

Rockwell B hardness values were obtained with a RAMS Rockwell Hardness Tester Model No. 30-R.

5.2 Charpy V-Notch Impact Test Results

The results of Charpy V-notch impact tests performed on the various materials contained in the San Onofre Unit 3 surveillance capsule located at 97° irradiated at 550°F to 0.8 x 10^{19} n/cm^2 (E > 1.0 MeV) are presented in Tables 5-1 through 5-4 and are compared with unirradiated results[2] as shown in Figures 5-2 through 5-5. The transition temperature increases and upper shelf energy decreases for the various materials contained in the San Onofre Unit 3 surveillance capsule located at 97° are summarized in Table 5-5.

Irradiation of the reactor vessel intermediate shell plate C-6802-1 Charpy specimens to 0.8 x 10^{19} n/cm^2 (E > 1.0 MeV) at 550°F (Figure 5-2) resulted in a 30 ft-lb transition temperature increase of 55°F and a 50 ft-lb transition temperature increase of 67°F for specimens oriented with the longitudinal axis perpendicular to the major rolling direction and parallel to the surface of the plate (transverse orientation). This results in a 30 ft-lb transition temperature of 105°F and a 50 ft-lb transition temperature of 160°F.

The average upper shelf energy (USE) of the intermediate shell plate C-6802-1 Charpy specimens (transverse orientation) resulted in a decrease of 16 ft-lbs after irradiation to 0.8 x 10^{19} n/cm^2 (E > 1.0 MeV) at 550°F. This results in an average USE of 76 ft-lbs (Figure 5-2).

Irradiation of the reactor vessel intermediate shell plate C-6802-1 Charpy specimens to 0.8 x 10^{19} n/cm^2 (E > 1.0 MeV) at 550°F (Figure 5-3) resulted in a 30 ft-lb transition temperature increase of 50°F and a 50 ft-lb transition temperature increase of 45°F for specimens oriented with the longitudinal axis parallel to the major rolling direction (longitudinal orientation). This results in a 30 ft-lb transition temperature of 130°F and a 50 ft-lb transition temperature of 170°F.

The average upper shelf energy (USE) of the intermediate shell plate C-6802-1 Charpy specimens (longitudinal orientation) resulted in a decrease of 22 ft-lbs after irradiation to 0.8 x 10^{19} n/cm^2 (E > 1.0 MeV) at 550°F. This results in an average USE of 70 ft-lbs (Figure 5-3).

Irradiation of the reactor vessel surveillance weld metal Charpy specimens to 0.8 x 10^{19} n/cm^2 (E > 1.0 MeV) at 550°F (Figure 5-4) resulted in a 30 ft-lb transition temperature increase of 32°F and a 50 ft-lb transition temperature increase of 25°F. This resulted in a 30 ft-lb transition temperature of 5°F and a 50 ft-lb transition temperature of 45°F.

The average upper shelf energy (USE) of the reactor vessel surveillance weld metal resulted in a energy decrease of 12 ft-lbs after irradiation to 0.8 x 10^{19} n/cm^2 (E > 1.0 MeV) at 550°F. This resulted in an average USE of 70 ft-lb (Figure 5-4).

Irradiation of the reactor vessel weld metal Heat-Affected-Zone (HAZ) specimens to 0.8 x 10^{19} n/cm^2 (E > 1.0 MeV) at 550°F (Figure 5-5) resulted in a 30 ft-lb transition temperature increase of 45°F and a 50 ft-lb transition temperature increase of 70°F. This results in a 30 ft-lb transition temperature of 35°F and a 50 ft-lb transition temperature of 120°F.

The average upper shelf energy (USE) of the reactor vessel HAZ metal resulted in a decrease of 11 ft-lbs after irradiation to 0.8 x 10^{19} n/cm^2 (E > 1.0 MeV) at 550°F. This resulted in an average USE of 74 ft-lb (Figure 5-4).

The fracture appearance of each irradiated Charpy specimen from the various materials are shown in Figures 5-6 through 5-9 and show an increasingly ductile or tougher appearance with increasing test temperature.

A comparison of the 30 ft-lb transition temperature increases and the upper shelf energy decreases for the various San Onofre Unit 3 surveillance materials with predicted increases using the methods of NRC Regulatory Guide 1.99, Revision 2[10] is presented in Table 5-8. This comparison indicates that the 30 ft-lb transition temperature increases resulting from irradiation to 0.8 x 10^{19} n/cm^2 (E > 1.0 MeV) are higher than the NRC Regulatory Guide 1.99, Revision 2 predictions and the average USE decreases resulting from irradiation to 0.8 x 10^{19} n/cm^2 (E > 1.0 MeV) are in close agreement with Regulatory Guide 1.99, Revision 2 predictions.

5.3 Tension Test Results

The results of tension tests performed on the reactor vessel intermediate shell plate C-6802-1, weld metal and weld HAZ metal irradiated to 0.8 x 10^{19} n/cm^2 (E > 1.0 MeV) at 550°F are shown in Table 5-7 and are compared with unirradiated results[2] as shown in Figures 5-10, 5-11 and 5-12.

Irradiation of the reactor vessel intermediate shell plate C-6802-1 tensile specimens to 0.8 x 10^{19} n/cm^2 (E > 1.0 MeV) at 550°F (Figure 5-10) resulted in an increase of 2 to 8 ksi in 0.2 percent offset yield strength and an increase of 0 to 4 ksi in ultimate tensile strength for specimens oriented with the longitudinal axis perpendicular to the major working direction of the plate (transverse orientation).

Irradiation of the reactor vessel weld metal tensile specimens to 0.8 x 10^{19} n/cm^2 (E > 1.0 MeV) at 550°F (Figure 5-11) resulted in an increase of 0 to 14 ksi for the 0.2 percent offset yield strength and an increase of 0 to 22 ksi for the ultimate tensile strength.

Irradiation of the reactor vessel weld HAZ metal tensile specimens to 0.8 x 10^{19} n/cm^2 (E > 1.0 MeV) at 550°F (Figure 5-12) resulted in an increase of 2 to 7 ksi for the 0.2 percent offset yield strength and an increase of 0 to 3 ksi for the ultimate tensile strength.

The fractured tension specimens for the reactor vessel intermediate shell plate C-6802-1 tensile specimens are shown in Figure 5-13.

The fractured tension specimens for the weld metal are shown in Figure 5-14.

The fractured tension specimens for the weld HAZ metal are shown in Figure 5-15.

True stress-strain curves for the tension specimens are shown in Figures 5-16 through 5-20.

Engineering stress-strain curves for the tension specimens are shown in Figures 5-21 through 5-25.

5.4 Hardness Test Results

The results of Rockwell B hardness tests are presented in Table 5-8.

5.5 Projected EOL Properties

The projected EOL (32 EFPY) RT_{NDT}, RT_{PTS} and USE for the materials contained in the capsule removed from the 97° location are presented in Table 5-9. Table 5-9 was generated using the projected EOL (32 EFPY) peak vessel fluence of 4.2 x 10^{19} n/cm^2 (E > 1.0 MeV).

TABLE 5-1

CHARPY V-NOTCH IMPACT DATA FOR THE SAN ONOFRE UNIT 3
REACTOR VESSEL INTERMEDIATE SHELL PLATE C-6802-1 IRRADIATED
AT 550°F, FLUENCE 0.8 x 10^{19} n/cm^2 (E > 1.0 MeV)

Sample No.	Temperature (°F)	(°C)	Impact Energy (ft-lb)	(J)	Lateral Expansion (mils)	(mm)	Shear (%)
			Longitudinal Orientation				
147	50	(10)	6.0	(8.0)	5.0	(0.13)	5
153	75	(24)	22.0	(30.0)	15.0	(0.38)	15
15K	100	(38)	29.0	(39.5)	24.0	(0.61)	25
113	125	(52)	35.0	(47.5)	32.0	(0.81)	30
14Y	150	(66)	32.0	(43.5)	26.0	(0.66)	30
15B	165	(74)	45.0	(61.0)	43.0	(1.09)	45
14A	175	(79)	30.0	(40.5)	27.0	(0.69)	45
14E	200	(93)	46.0	(62.5)	46.0	(1.17)	55
11T	225	(107)	75.0	(101.5)	66.0	(1.68)	80
12K	250	(121)	45.0	(61.0)	48.0	(1.22)	80
12L	250	(121)	48.0	(65.0)	46.0	(1.17)	95
14M	275	(135)	90.0	(122.0)	76.0	(1.93)	100
			Transverse Orientation				
25U	0	(-18)	19.0	(26.0)	18.0	(0.46)	10
23K	25	(- 4)	16.0	(21.5)	11.0	(0.28)	10
21A	50	(10)	9.0	(12.0)	12.0	(0.31)	10
23L	75	(24)	21.0	(28.5)	20.0	(0.51)	15
22B	100	(38)	25.0	(34.0)	25.0	(0.64)	20
25J	115	(46)	55.0	(74.5)	48.0	(1.22)	45
25L	130	(54)	50.0	(68.0)	44.0	(1.12)	50
247	150	(66)	33.0	(44.5)	33.0	(0.84)	50
223	165	(74)	36.0	(49.0)	37.0	(0.94)	65
25C	200	(93)	92.0	(124.5)	73.0	(1.85)	100
245	225	(107)	62.0	(84.0)	59.0	(1.50)	100
23M	250	(121)	73.0	(99.0)	77.0	(1.96)	100

TABLE 5-2

CHARPY V-NOTCH IMPACT DATA FOR THE SAN ONOFRE UNIT 3 REACTOR VESSEL WELD METAL AND HAZ METAL IRRADIATED AT 550°F, FLUENCE 0.8 x 10^{19} n/cm^2 (E > 1.0 MeV)

Sample No.	Temperature (°F)	(°C)	Impact Energy (ft-lb)	(J)	Lateral Expansion (mils)	(mm)	Shear (%)
			Weld Metal				
363	-50	(-46)	23.0	(31.0)	20.0	(0.51)	15
33L	-25	(-32)	27.0	(36.5)	25.0	(0.64)	20
31D	0	(-18)	5.0	(7.0)	6.0	(0.15)	5
37B	10	(-12)	42.0	(57.0)	34.0	(0.86)	60
367	25	(- 4)	42.0	(57.0)	44.0	(1.12)	65
331	50	(10)	44.0	(59.5)	44.0	(1.12)	70
37U	60	(16)	61.0	(82.5)	57.0	(1.45)	95
371	80	(27)	65.0	(88.0)	59.0	(1.50)	95
365	105	(41)	67.0	(91.0)	60.0	(1.52)	100
34P	150	(66)	75.0	(101.5)	73.0	(1.85)	100
33D	190	(88)	77.0	(104.5)	76.0	(1.93)	100
377	225	(107)	63.0	(85.5)	58.0	(1.47)	100
			HAZ Metal				
441	-75	(-59)	9.0	(12.0)	8.0	(0.20)	5
42L	-50	(-46)	18.0	(24.5)	16.0	(0.41)	15
45C	-20	(-29)	3.0	(4.0)	4.0	(0.10)	5
43P	0	(-18)	26.0	(35.5)	23.0	(0.58)	35
464	25	(- 4)	35.0	(47.5)	37.0	(0.94)	45
41C	60	(16)	33.0	(44.5)	33.0	(0.84)	50
47E	95	(35)	43.0	(58.5)	44.0	(1.12)	75
46T	125	(52)	41.0	(55.5)	38.0	(0.97)	70
45M	145	(63)	45.0	(61.0)	44.0	(1.12)	80
437	165	(74)	63.0	(85.5)	61.0	(1.55)	100
45P	200	(93)	84.0	(114.0)	68.0	(1.73)	100
434	250	(121)	75.0	(101.5)	65.0	(1.65)	100

TABLE 5-3

INSTRUMENTED CHARPY IMPACT TEST RESULTS FOR THE SAN ONOFRE UNIT 3 REACTOR VESSEL SHELL C-6802-1 IRRADIATED AT 550°F, FLUENCE 0.8 x 10^{19} n/cm^2 (E > 1.0 MeV)

Sample Number	Test Temp (°F)	Charpy Energy (ft-lb)	Normalized Energies (ft-lb/in^2) Charpy Ed/A	Maximum Em/A	Prop Ep/A	Yield Load (kips)	Time to Yield (μsec)	Maximum Load (kips)	Time to Maximum (μsec)	Fracture Load (kips)	Arrest Load (kips)	Yield Stress (ksi)
Longitudinal Orientation												
147	50	6.0	48	COMPUTER MALFUNCTION **								
153	75	22.0	177	38	140	4.25	75	4.40	55	4.30	0.25	141
15K	100	29.0	234	124	110	3.60	45	4.10	240	3.75	0.70	120
113	125	35.0	282	173	109	3.15	25	3.80	375	3.75	0.80	104
14Y	150	32.0	258	128	131	3.30	5	4.00	250	4.00	1.40	109
15B	165	45.0	382	175	188	3.80	135	4.00	350	3.75	1.60	126
14A	175	30.0	242	70	171	3.25	20	3.65	145	3.70	1.55	107
14E	200	48.0	370	156	215	3.50	20	4.25	300	4.10	2.55	115
11T	225	75.0	604	205	399	3.00	50	3.65	470	3.10	2.15	100
12K	250	45.0	382	110	253	3.50	55	3.70	225	3.70	3.45	116
12L	250	48.0	387	134	252	2.90	25	3.60	305	3.40	2.70	96
14M	275	90.0	726	203	522	3.40	65	3.85	425	-*	-*	113
Transverse Orientation												
25U	0	19.0	153	20	133	4.25	0	4.25	25	4.20	-*	141
23K	25	16.0	129	21	108	3.90	15	4.00	30	4.00	0.15	130
21A	50	9.0	73	COMPUTER MALFUNCTION **								
23L	75	21.0	169	65	104	4.40	30	4.50	105	4.50	0.60	145
22B	100	25.0	201	69	132	3.65	20	4.00	130	3.95	0.55	120
25J	115	55.0	443	224	219	3.30	5	4.05	455	3.90	1.55	109
25L	130	50.0	403	159	244	3.55	25	4.30	300	4.25	2.35	118
247	150	33.0	266	53	212	3.55	150	3.75	100	3.75	1.85	118
223	165	38.0	290	121	169	3.05	35	3.60	270	3.60	1.55	100
25C	200	92.0	741	257	483	3.65	65	4.30	500	-*	-*	121
245	225	62.0	499	146	354	3.55	50	3.85	295	-*	-*	117
22J	250	73.0	588	177	411	3.25	130	3.60	405	-*	-*	107

*Fully ductile fracture; no arrest load

** When test was run data did not transfer to computer disk

TABLE 5-4

INSTRUMENTED CHARPY IMPACT TEST RESULTS FOR THE SAN ONOFRE UNIT 3 SURVEILLANCE WELD AND HAZ METAL IRRADIATED AT 550°F, FLUENCE 0.8 x 10^{19} n/cm^2 (E > 1.0 MeV)

Sample Number	Test Temp (°F)	Charpy Energy (ft-lb)	Normalized Energies Charpy Ed/A (ft-lb/in²)	Maximum Em/A (ft-lb/in²)	Prop Ep/A (ft-lb/in²)	Yield Load (kips)	Time to Yield (μsec)	Maximum Load (kips)	Time to Maximum (μsec)	Fracture Load (kips)	Arrest Load (kips)	Yield Stress (ksi)
					Weld Metal							
383	- 50	23.0	185	53	132	4.40	0	4.55	80	4.55	0.55	146
33L	- 25	27.0	217	146	71	4.10	35	4.55	250	4.55	0.35	136
31D	0	5.0	40	COMPUTER MALFUNCTION **								
37B	10	42.0	338	146	192	4.45	65	4.75	240	4.70	2.25	147
387	25	42.0	338	134	204	4.40	45	4.75	220	4.70	1.95	146
331	50	44.0	354	155	199	3.50	45	4.00	315	3.85	1.40	115
37U	80	61.0	491	159	332	3.80	70	4.25	305	4.15	2.70	126
371	80	65.0	523	168	355	4.30	120	4.45	295	4.20	3.80	142
385	105	67.0	540	167	373	3.95	135	4.25	315	-*	-*	131
34P	150	75.0	604	192	412	3.65	125	4.05	390	-*	-*	121
33D	190	77.0	620	199	421	2.90	80	3.55	470	-*	-*	96
377	225	63.0	507	151	357	3.75	140	4.00	305	-*	-*	124
					HAZ Metal							
441	- 75	9.0	73	COMPUTER MALFUNCTION **								
42L	- 50	18.0	145	76	70	4.35	40	4.55	120	4.55	0.01	144
45C	- 20	3.0	24	COMPUTER MALFUNCTION **								
43P	0	26.0	209	85	125	4.40	70	4.55	140	4.35	1.10	145
484	25	35.0	282	158	123	3.95	10	4.60	275	4.60	0.70	131
41C	80	33.0	266	58	208	3.30	40	3.55	120	3.55	2.65	109
47E	95	43.0	346	110	236	3.20	65	3.55	245	3.50	0.25	106
46T	125	41.0	330	151	180	3.55	65	4.05	305	3.75	2.15	118
45M	145	45.0	362	125	237	3.90	130	4.05	240	3.55	1.75	129
437	185	83.0	507	138	369	3.35	65	3.65	300	-*	-*	111
45P	200	84.0	678	199	477	3.70	80	4.05	395	-*	-*	122
434	250	75.0	604	183	421	3.25	90	3.70	405	-*	-*	107

*Fully ductile fracture; no arrest load

** When test was run data did not transfer to computer disk

TABLE 5-5

EFFECT OF 550°F IRRADIATION TO 0.8×10^{19} n/cm^2 (E > 1.0 MeV)

ON NOTCH TOUGHNESS PROPERTIES OF THE SAN ONOFRE UNIT 3 REACTOR VESSEL SURVEILLANCE MATERIALS

Material	Average 30 ft-lb * Temperature (°F)			Average 35 mil * Lateral Expansion Temperature (°F)			Average 50 ft-lb * Temperature (°F)			Average Energy * Absorption at Full Shear (ft-lb)		
	Unirradiated	Irradiated	ΔT	Unirradiated	Irradiated	ΔT	Unirradiated	Irradiated	ΔT	Unirradiated	Irradiated	Δ(ft-lb)
Plate C-6802-1 (Transverse Orientation)	50	105	55	85	133	48	93	160	67	92	76	-16
Plate C-6802-1 (Longitudinal Orientation)	80	130	50	100	155	55	125	170	45	92	70	-22
Weld Metal	-27	5	32	-12	25	37	20	45	25	82	70	-12
HAZ Metal	-10	35	45	20	50	30	50	120	70	85	74	-11

* "AVERAGE" is defined as the value read from the curve fitted through the data points from the Charpy tests as shown in Figures 5-2 through 5-5.

TABLE 5-6

COMPARISON OF SAN ONOFRE UNIT 3 SURVEILLANCE MATERIAL 30 FT-LB TRANSITION TEMPERATURE SHIFTS AND UPPER SHELF ENERGY DECREASES WITH REGULATORY GUIDE 1.99 REVISION 2 PREDICTIONS

Material	Capsule	Fluence 10^{19} n/cm^2	30 ft-lb Transition Temp. Shift		Upper Shelf Energy Decrease	
			R.G. 1.99 Rev. 2 (Predicted) (°F)	Measured (°F)	R.G. 1.99 Rev. 2 (Predicted) (%)	Measured (%)
Plate C-6802-1 (Transverse Orientation)	W-97	0.8	31	55.0	18	17.0
Plate C-6802-1 (Longitudinal Orientation)	W-97	0.8	31	50.0	18	24.0
Weld Metal	W-97	0.8	27	32.0	18	15.0
HAZ Metal	W-97	0.8	---	45.0	---	13.0

TABLE 5-7

TENSILE PROPERTIES FOR SAN ONOFRE UNIT 3 REACTOR VESSEL SURVEILLANCE MATERIAL

IRRADIATED AT 550°F TO 0.8 x 10^{19} n/cm^2 (E > 1.0 MeV)

Material	Sample Number	Test Temp. (°F)	0.2% Yield Strength (ksi)	Ultimate Strength (ksi)	Fracture Load (kip)	Fracture Stress (ksi)	Fracture Strength (ksi)	Uniform Elongation (%)	Total Elongation (%)	Reduction in Area (%)
Plate C6802-1 (Transverse)	2KE	74	71.3	91.7	3.10	208.6	63.2	13.0	23.3	70
	2KC	200	67.7	86.6	2.95	215.6	60.1	10.5	23.0	72
	2K3	550	60.1	86.6	3.00	202.0	61.1	10.5	22.2	70
HAZ	4JD	74	67.2	87.6	2.85	185.1	58.1	12.0	24.5	69
	4JK	175	62.1	77.9	2.63	148.5	53.5	12.0	25.0	64
	4JA	550	60.1	84.5	2.75	172.4	56.0	12.0	24.5	68
Weld	3JC	74	51.4	75.4	2.60	168.9	53.0	11.4	20.4	69
	3JE	250	62.6	93.7	3.45	232.3	70.3	10.5	20.3	70
	3J4	550	54.5	94.7	3.60	203.7	73.3	13.5	22.7	64

TABLE 5-8

ROOM TEMPERATURE ROCKWELL B HARDNESS VALUES FOR THE SAN ONOFRE UNIT 3 SURVEILLANCE MATERIALS IRRADIATED AT 550°F, FLUENCE 0.8 X 10^{19} n/cm^2 (E > 1.0 MeV)

Specimen Identification	Rockwell B Hardness			Average
(1) Base Metal (Long.)				
15K	89	89	87	88.3
12K	87	87	85	86.3
12L	85	87	85	85.7
153	86	87	86	86.3
14Y	85	84	85	84.7
15B	88	88	87	87.7
11T	87	89	87	87.7
14E	89	91	90	90.0
14M	87	89	88	88.0
147	90	91	92	91.0
14A	89	90	89	89.3
113	89	89	90	89.3
(2) Base Metal (Trans.)				
245	84	89	88	87.0
21A	83	89	81	84.3
223	73	84	87	81.3
23K	88	86	81	85.0
23M	84	89	88	87.0
23L	86	89	86	87.0
22B	77	87	89	84.3
25U	90	91	91	90.7
247	87	91	90	89.3
25J	83	89	87	86.3
25C	81	85	88	84.7
25L	86	88	89	87.7

TABLE 5-B (cont)

ROOM TEMPERATURE ROCKWELL B HARDNESS VALUES FOR THE SAN ONOFRE UNIT 3 SURVEILLANCE MATERIALS IRRADIATED AT 550°F, FLUENCE 0.8 X 10^{19} n/cm^2 (E > 1.0 MeV)

Specimen Identification	Rockwell B Hardness			Average
(3) Weld Metal				
367	88	91	95	91.3
34P	88	83	84	85.0
33L	89	87	91	89.0
377	91	94	93	92.7
37U	92	92	93	92.3
37B	93	95	94	94.0
371	93	94	94	93.7
31D	81	81	82	81.3
33D	90	85	87	87.3
365	92	94	93	93.0
331	90	90	90	90.0
363	87	89	87	87.7
(4) HAZ Metal				
437	89	91	88	89.3
42L	88	86	84	86.0
41C	87	89	86	87.3
45M	89	89	89	89.0
434	92	92	89	91.0
45C	88	87	85	86.7
46T	86	88	84	86.0
464	88	89	88	88.3
45P	89	89	87	88.3
47E	86	87	86	86.3
43P	94	95	93	94.0
441	89	90	90	89.7

TABLE 5-9

PROJECTED EOL (32 EFPY) RT_{NDT}, RT_{PTS} AND USE
FOR THE SAN ONOFRE UNIT 3 SURVEILLANCE MATERIAL
CONTAINED IN CAPSULE W-97

SURVEILLANCE MATERIAL	CURRENT PTS[1] RULE RT_{PTS} AT 32 EFPY (°F)	PROPOSED PTS[1] RULE RT_{PTS} AT 32 EFPY (°F)	R.G. 1.99[1,2] REV. 2 32 EFPY CALCULATED RT_{NDT} (°F)	R.G. 1.99[3] REV. 2 32 EFPY CALCULATED USE (ft-lb)
PLATE C-6802-1 (Transverse Orientation)	127	120	120 (116)	71
WELD METAL	23	62	46 (39)	63

(1) The fluence value used for the above calculations was 4.2×10^{19} n/cm^2 ($E > 1.0$ MeV). This is the projected EOL (32 EFPY) peak vessel fluence.

(2) Values in () calculated using 1/4 T (32 EFPY) peak vessel fluence.

(3) Calculated using 1/4 T (32 EFPY) peak vessel fluence.

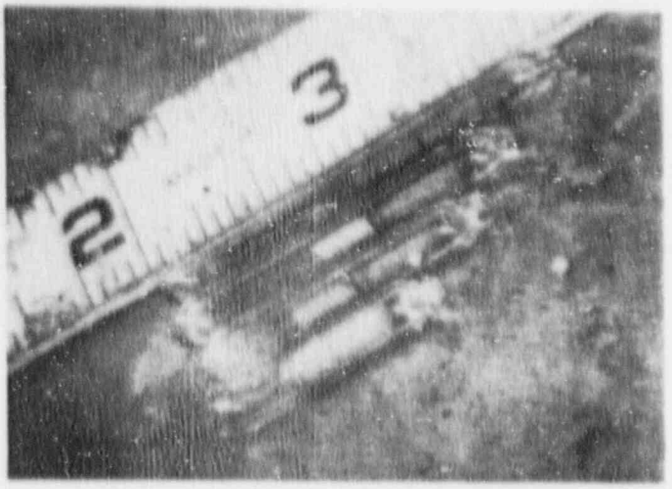

BLOCK C214

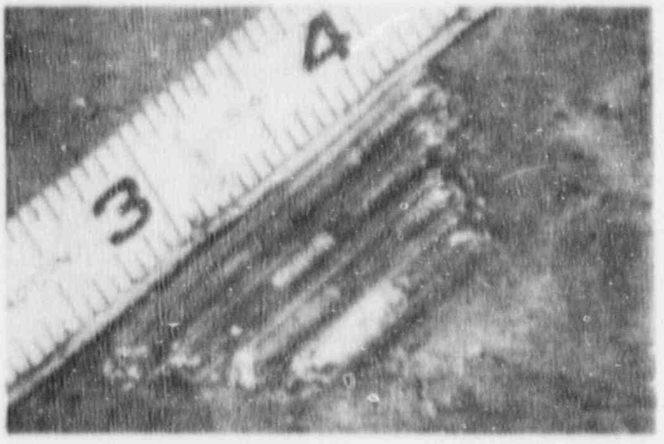

BLOCK C242

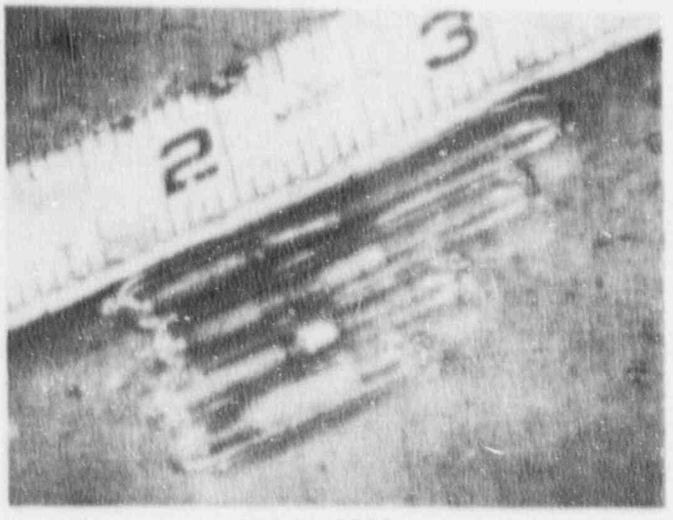

BLOCK C273

Figure 5-1. Appearance of the Thermal Monitors in the Various Quartz Tubes.

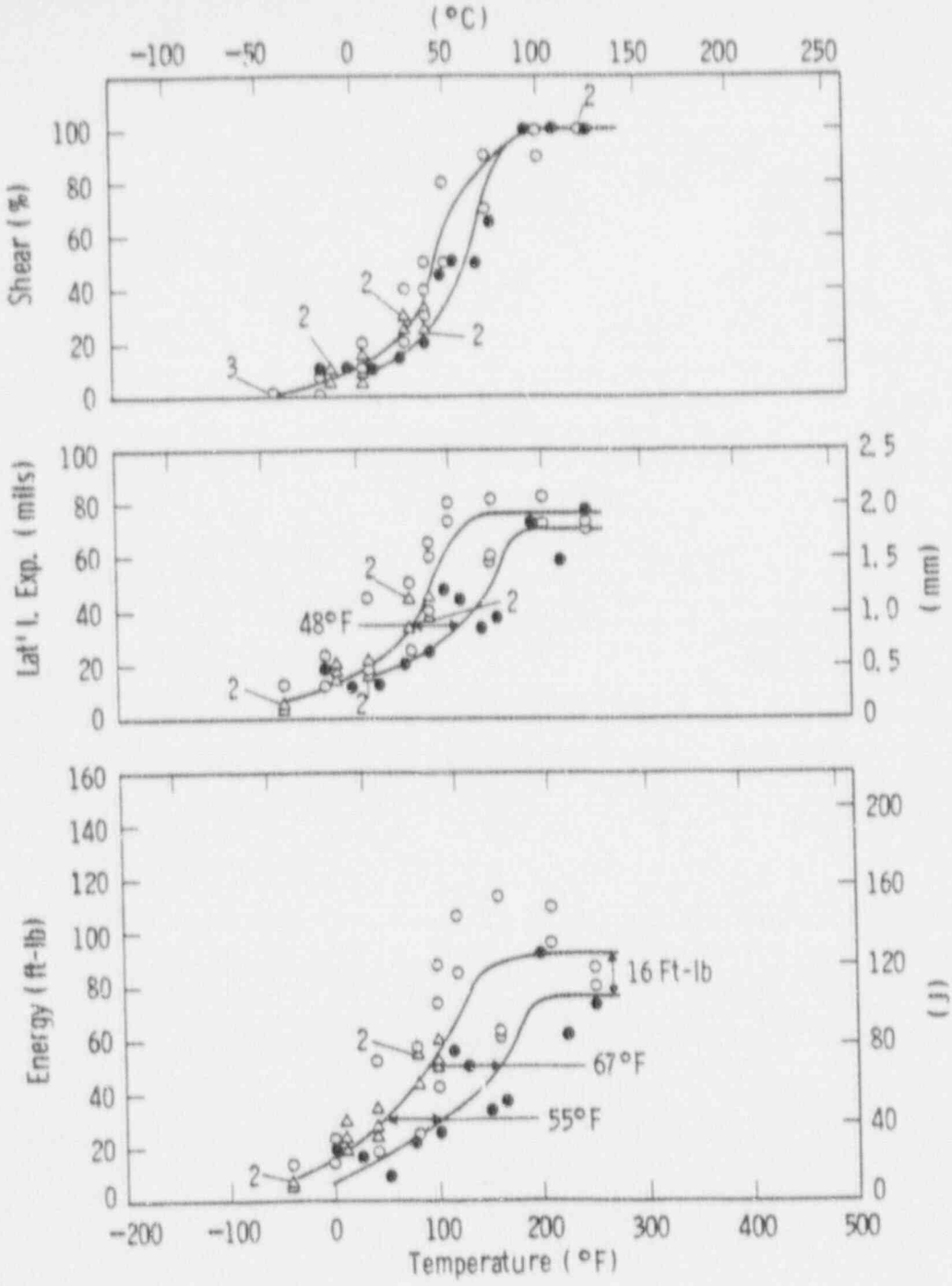

Figure 5-2. Charpy V-Notch Impact Properties for the San Onofre Unit 3 Reactor Vessel Intermediate Shell Plate C-6802-1 (Transverse Orientation)

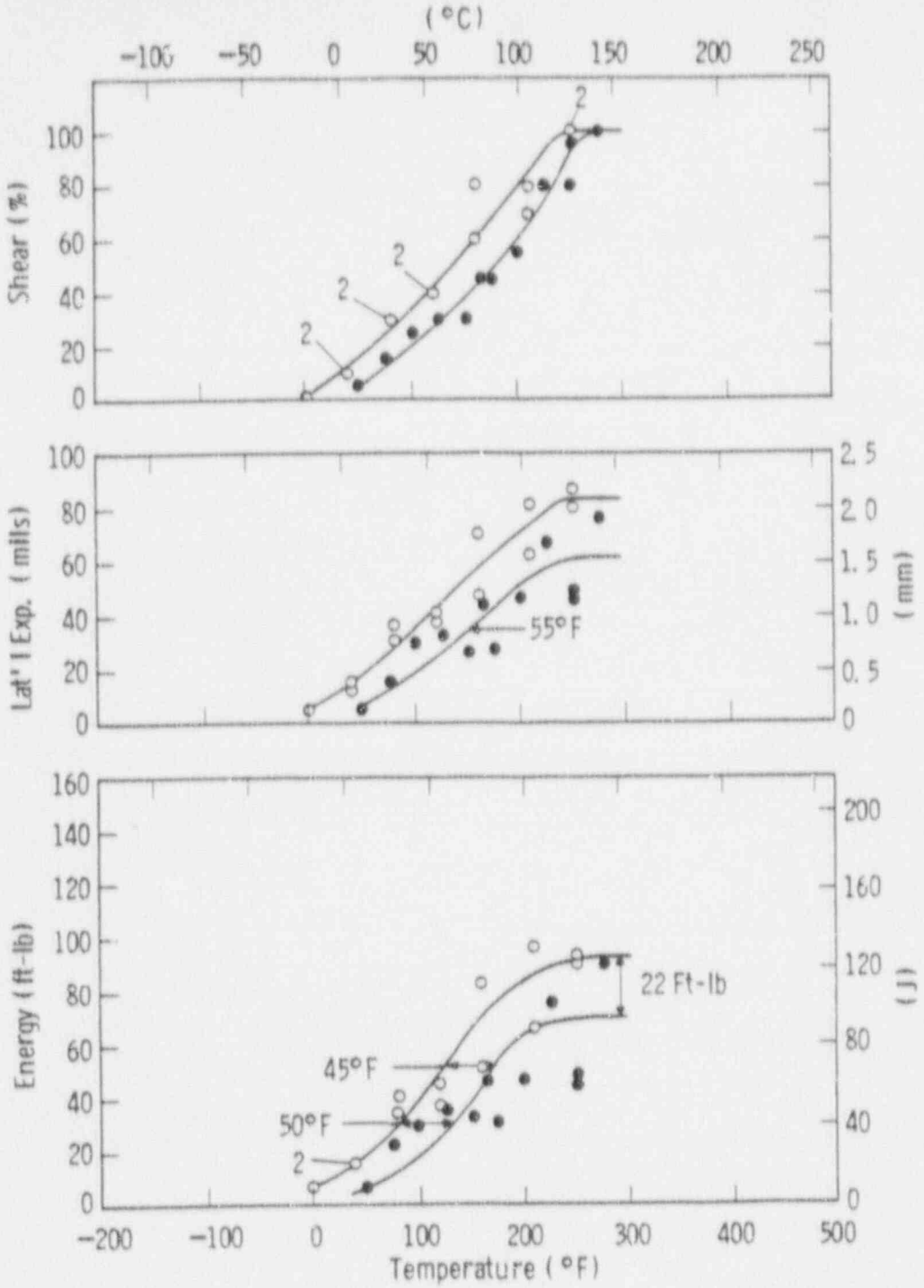

Figure 5-3. Charpy V-Notch Impact Properties for the San Onofre Unit 3 Reactor Vessel Intermediate Shell Plate C-6802-1 (Longitudinal Orientation)

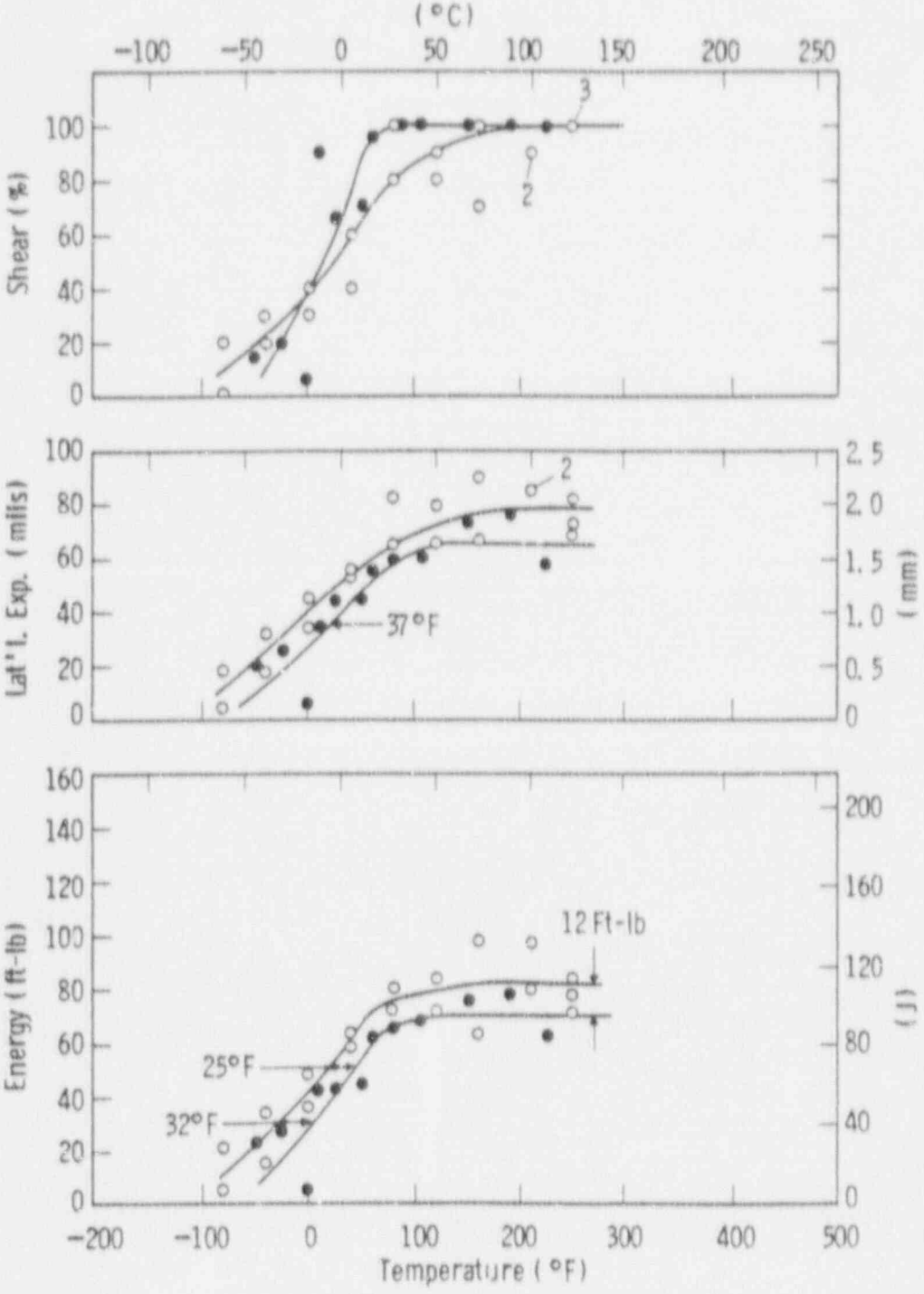

Figure 5-4. Charpy V-Notch Impact Properties for San Onofre Unit 3 Reactor Vessel Surveillance Weld Metal

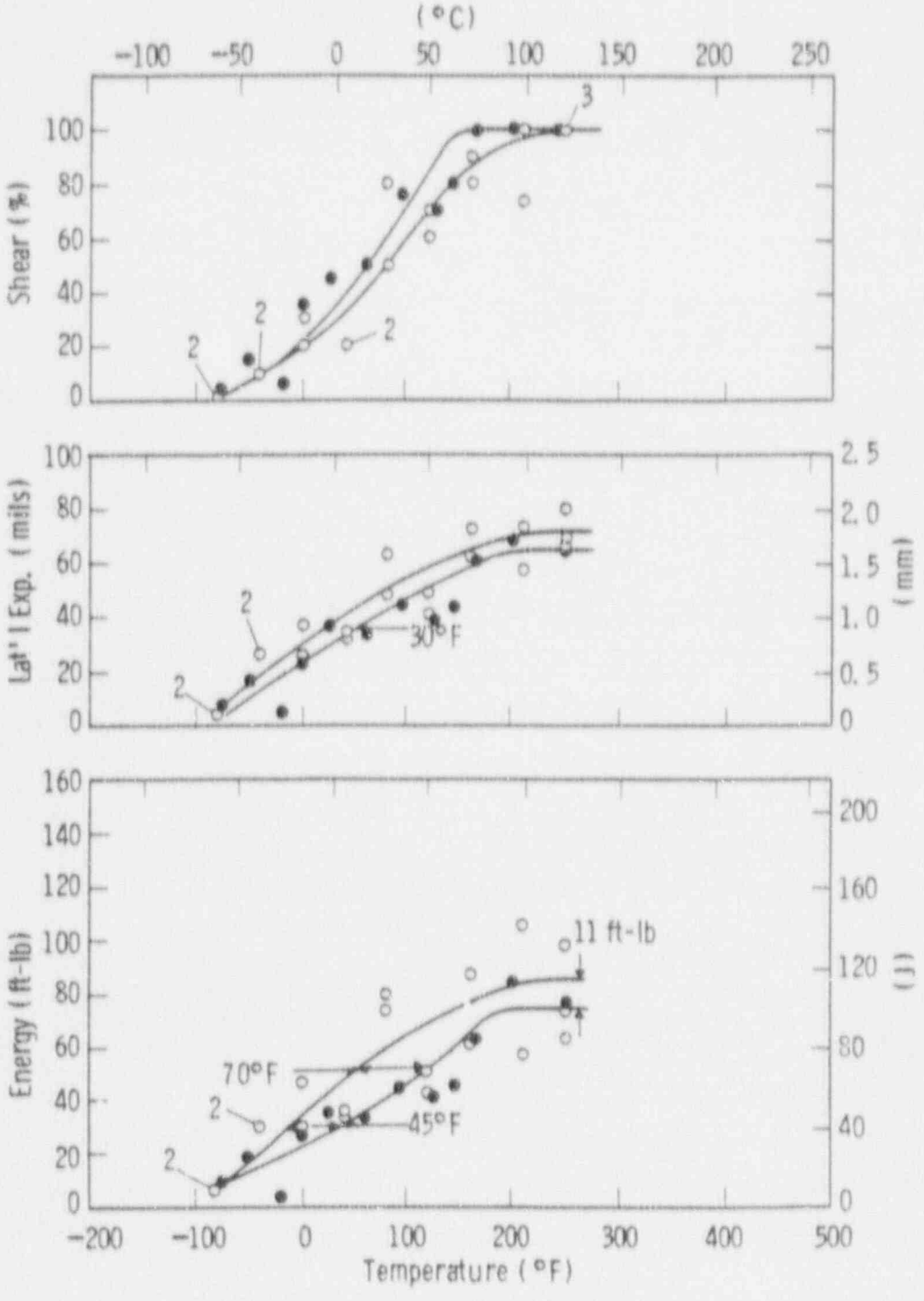

Figure 5-5. Charpy V-Notch Impact Properties for the San Onofre Unit 3 Reactor Vessel Surveillance HAZ Metal

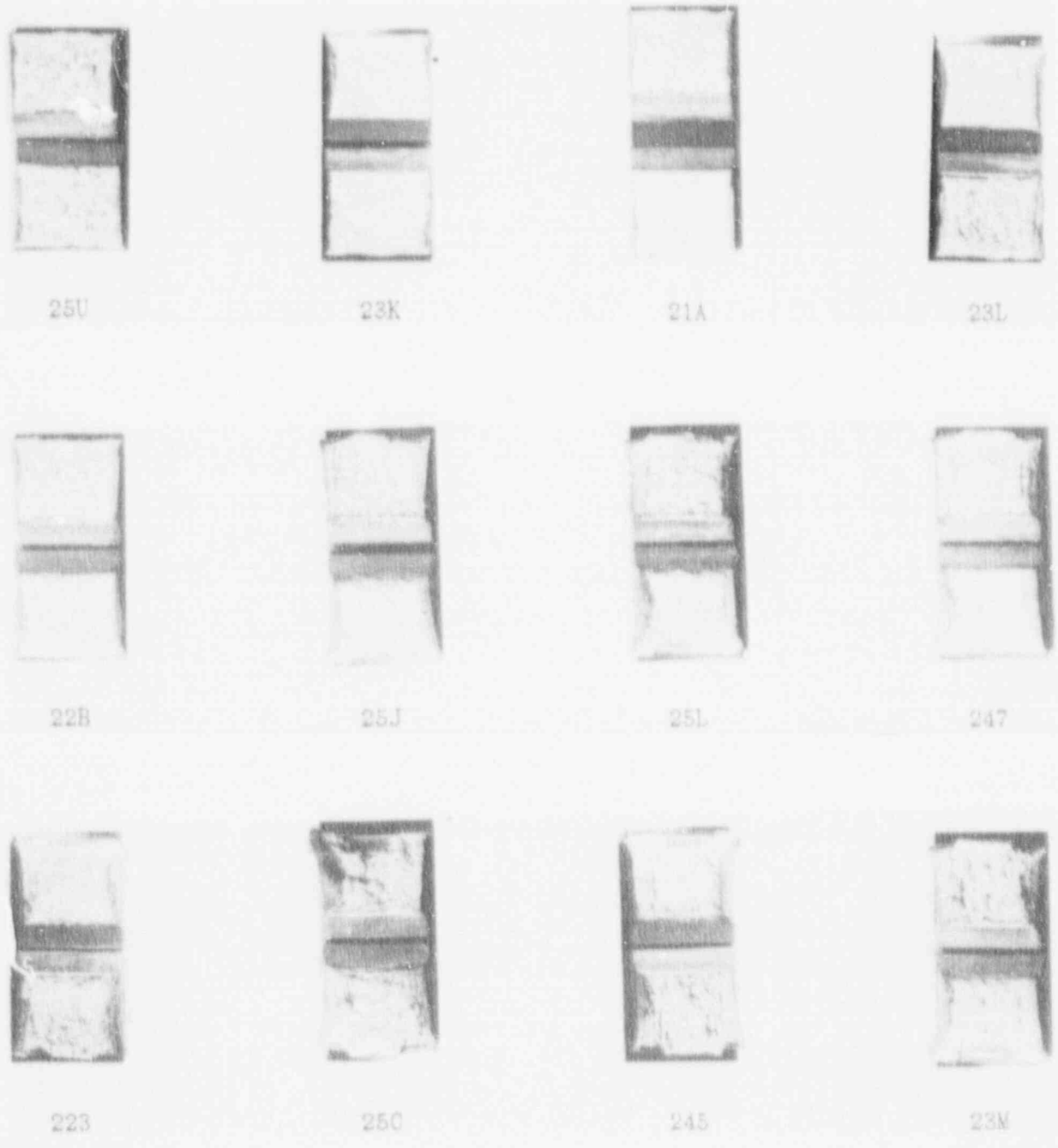

Figure 5-6. Charpy V-Notch Impact Specimen Fracture Surfaces for the San Onofre Unit 3 Reactor Vessel Intermediate Shell Plate C-6802-1 (Transverse Orientation)

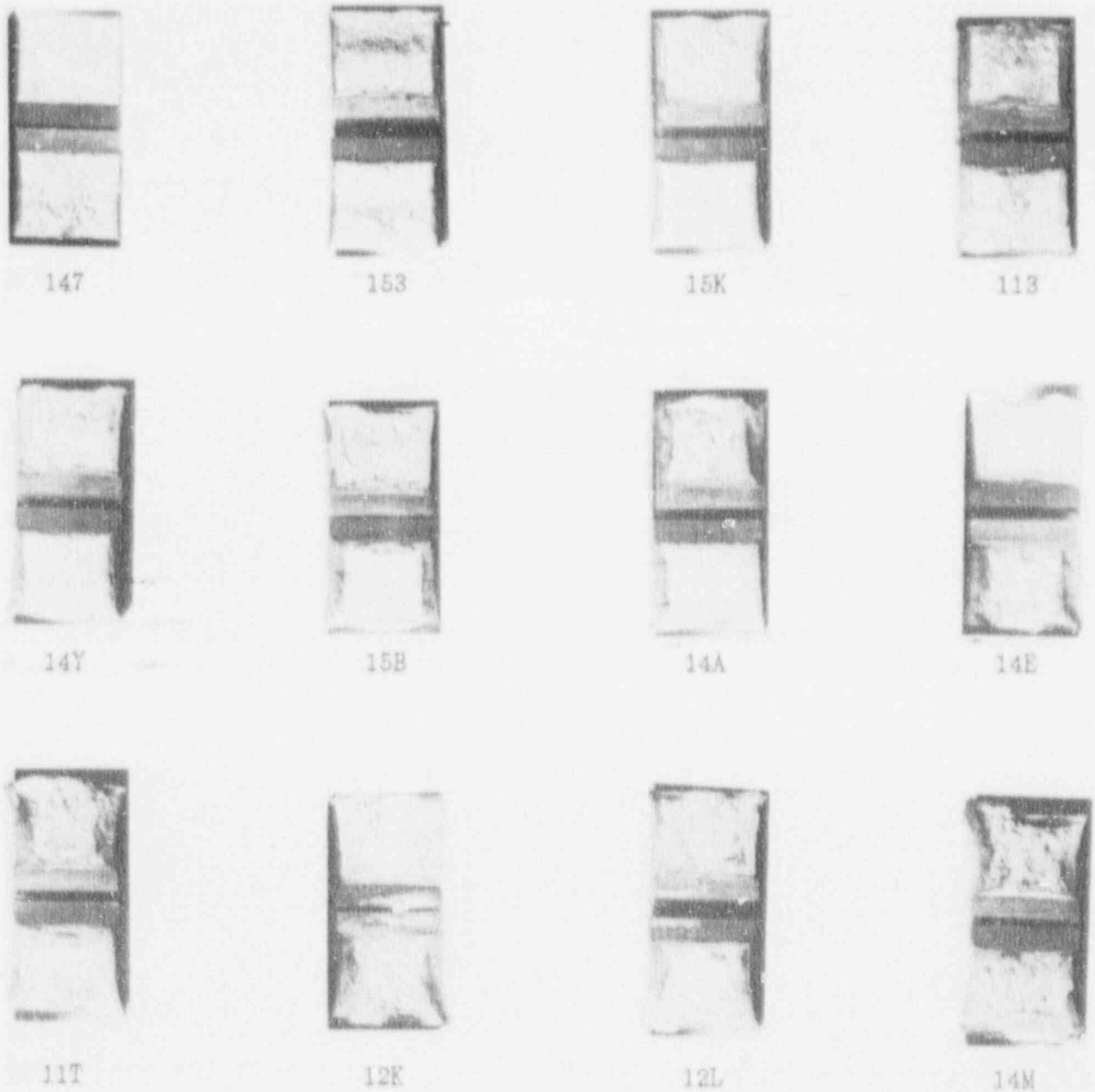

Figure 5-7. Charpy V-Notch Impact Specimen Fracture Surfaces for the San Onofre Unit 3 Reactor Vessel Intermediate Shell Plate C-6802-1 (Longitudinal Orientation)

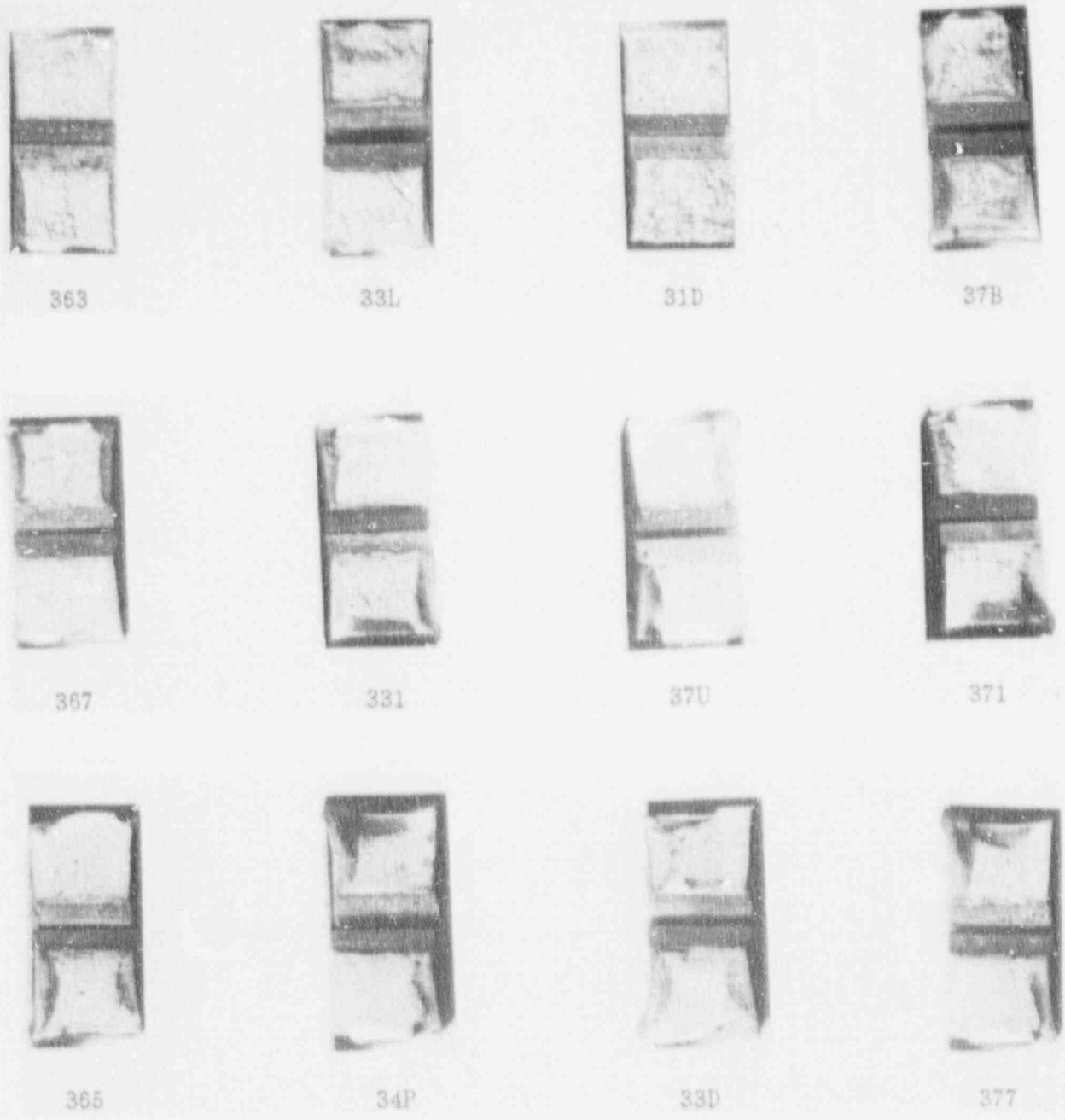

Figure 5-8. Charpy Impact Specimen Fracture Surfaces for San Onofre Unit 3 Reactor Vessel Surveillance Weld Metal

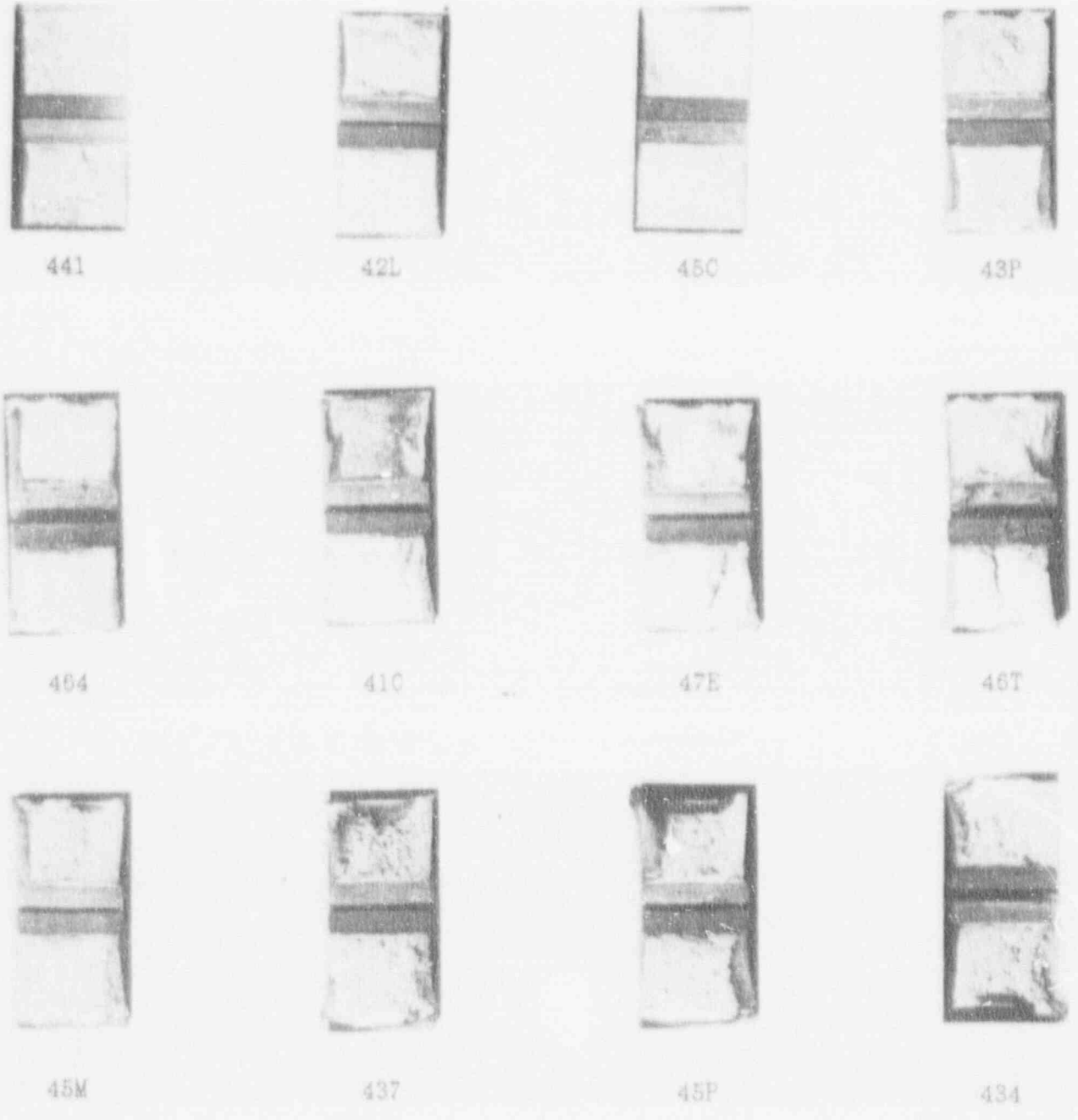

Figure 5-9. Charpy Impact Specimen Fracture Surfaces for San Onofre Unit 3 Reactor Vessel Surveillance HAZ Metal

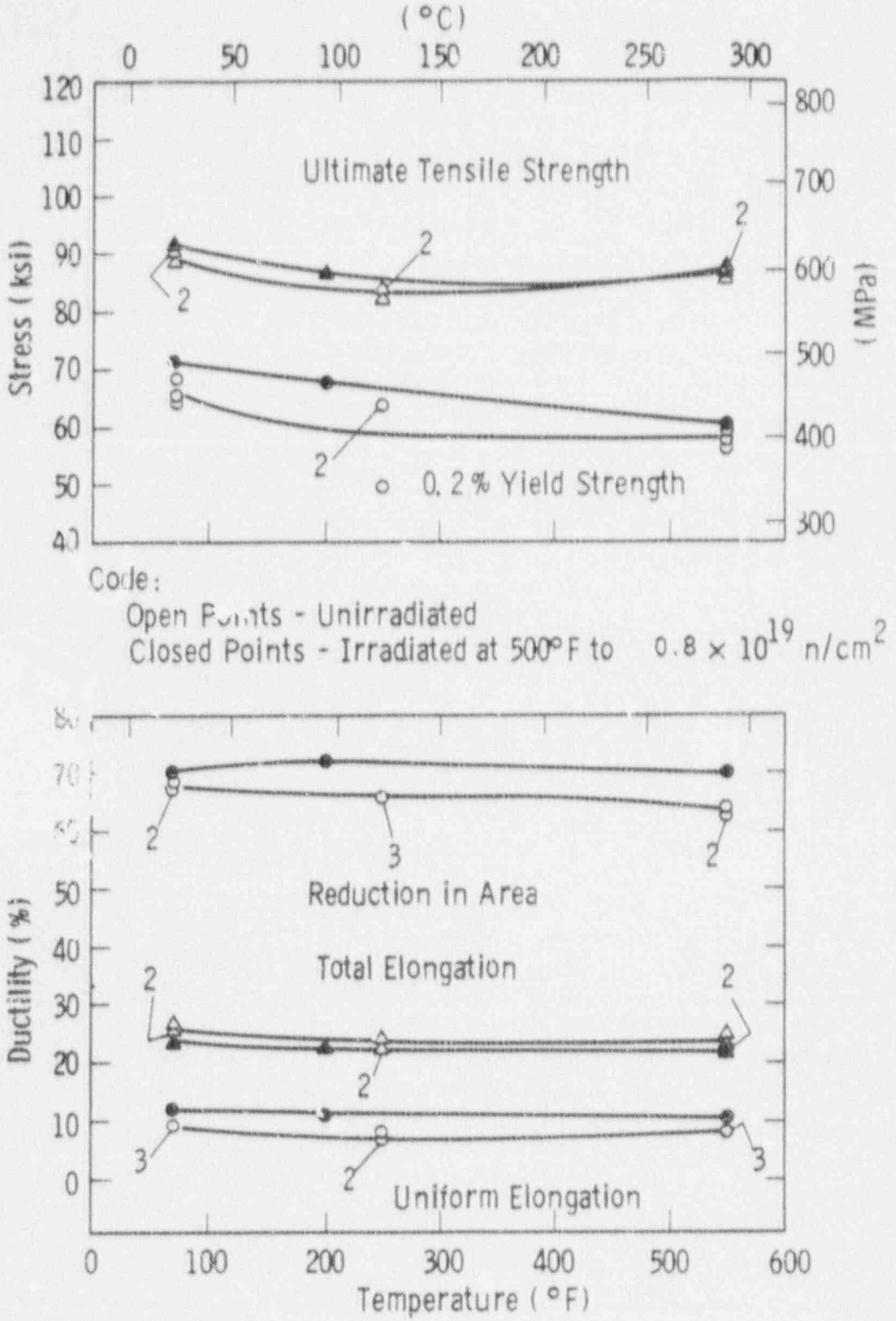

Figure 5-10. Tensile Properties for the San Onofre Unit 3 Reactor Vessel Intermediate Shell Plate C-6802-1 (Transverse Orientation)

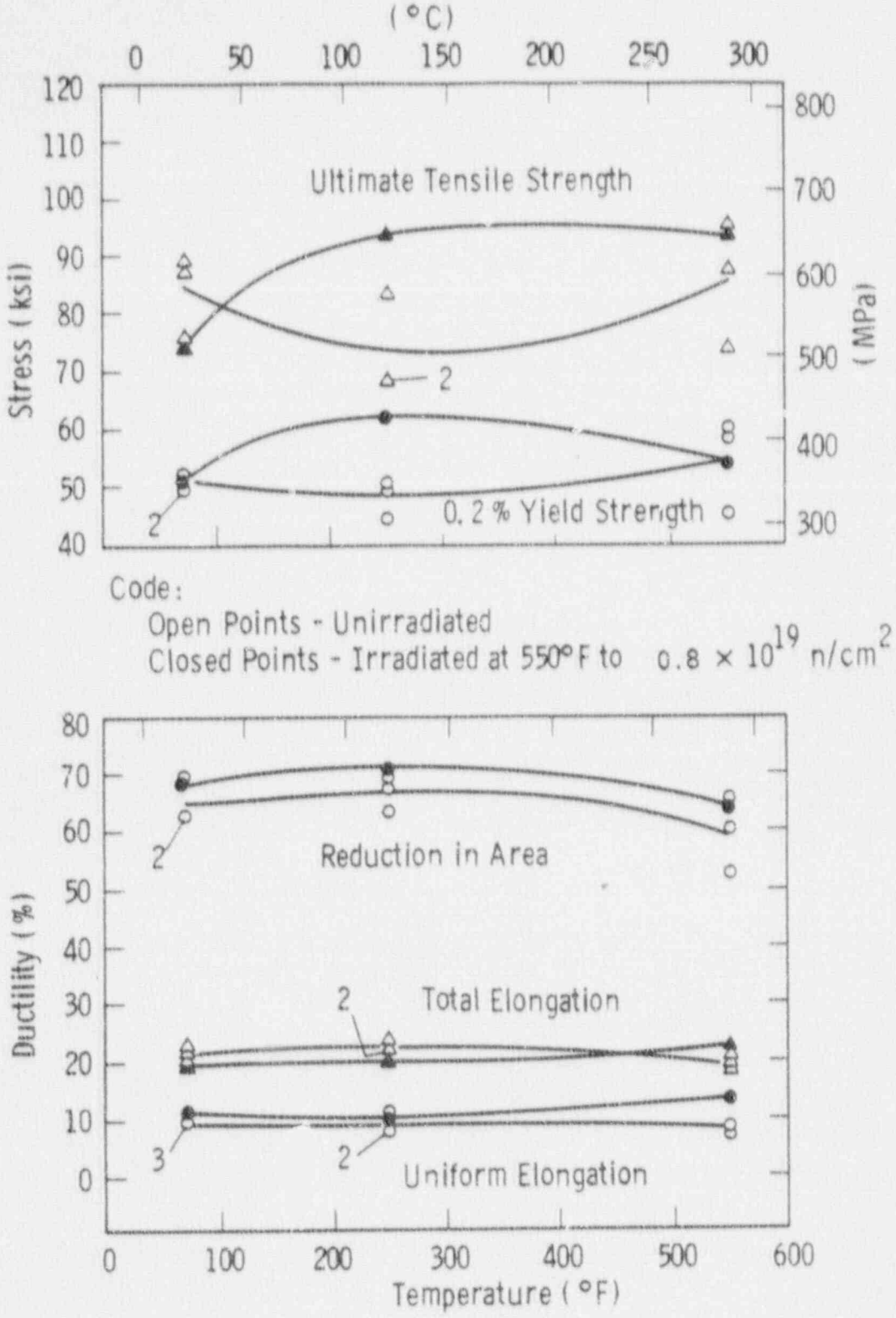

Figure 5-11. Tensile Properties for the San Onofre Unit 3 Reactor Vessel Weld Metal

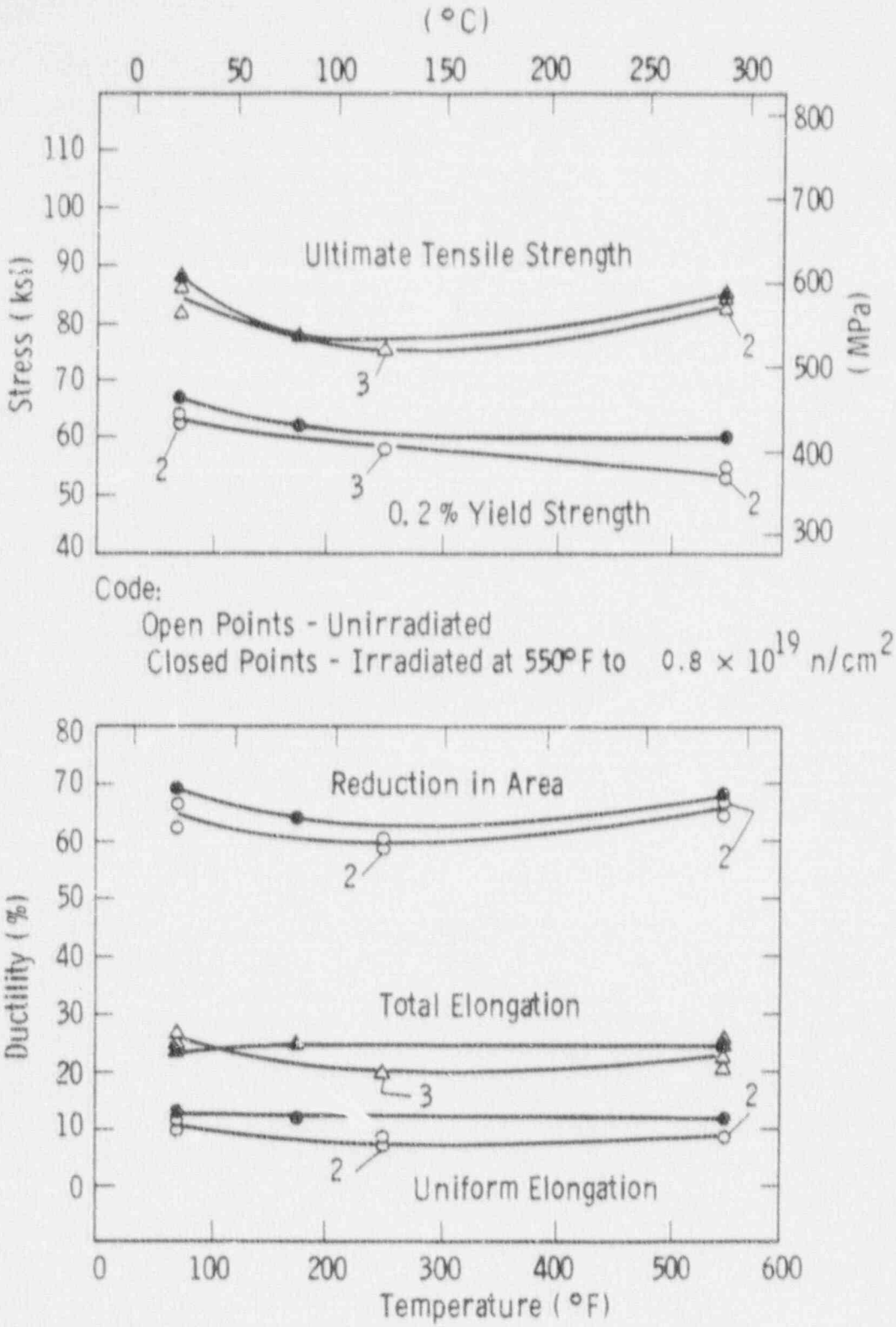

Figure 5-12. Tensile Properties for San Onofre Unit 3 Reactor Vessel HAZ Metal

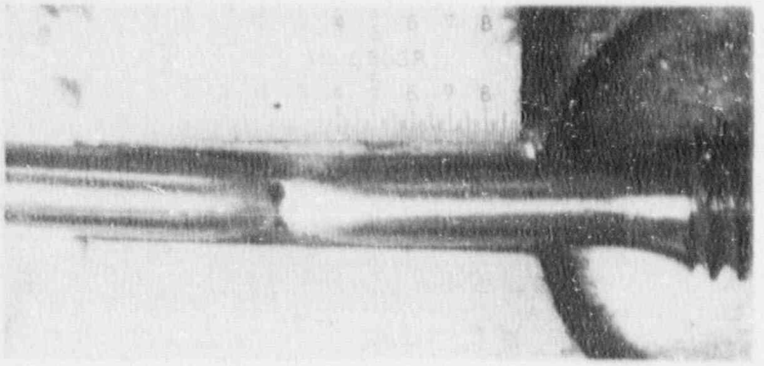

Specimen 2KE 74°F

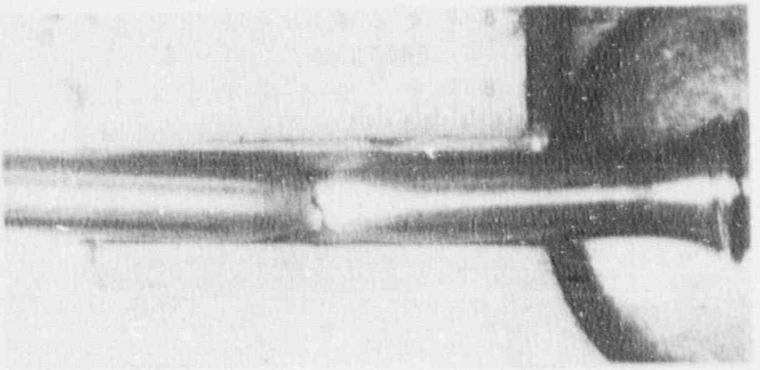

Specimen 2KC 200°F

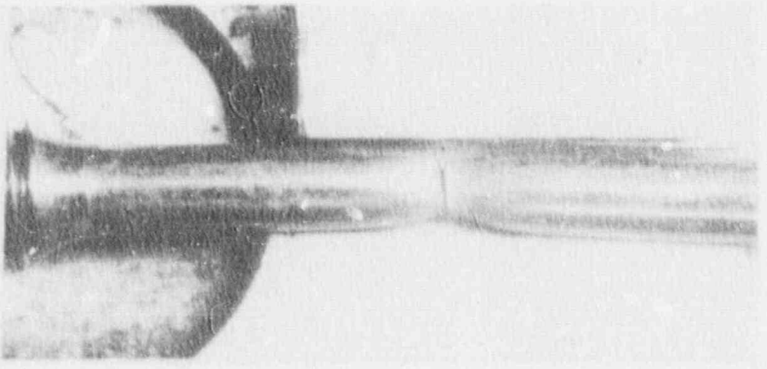

Specimen 2K3 550°F

Figure 5-13. Fractured Tensile Specimens from the San Onofre Unit 3 Reactor Vessel Intermediate Shell Plate C-6802-1 (Transverse Orientation)

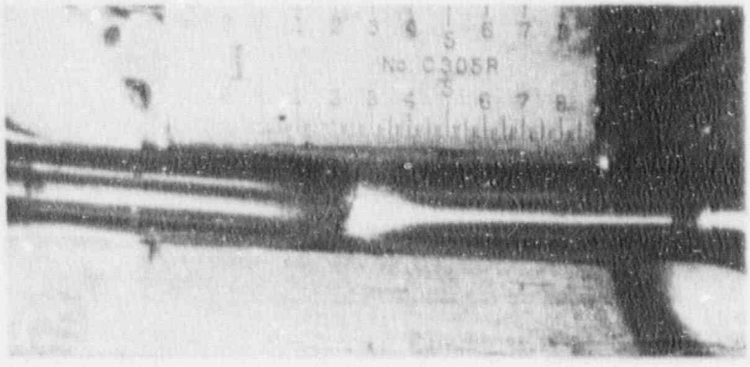

Specimen 3JC 74°F

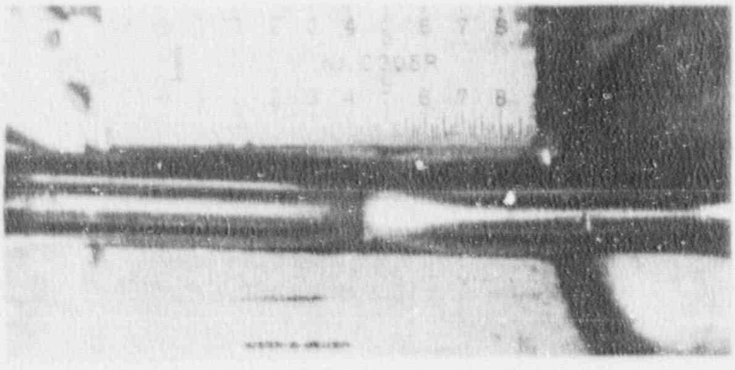

Specimen 3JE 250°F

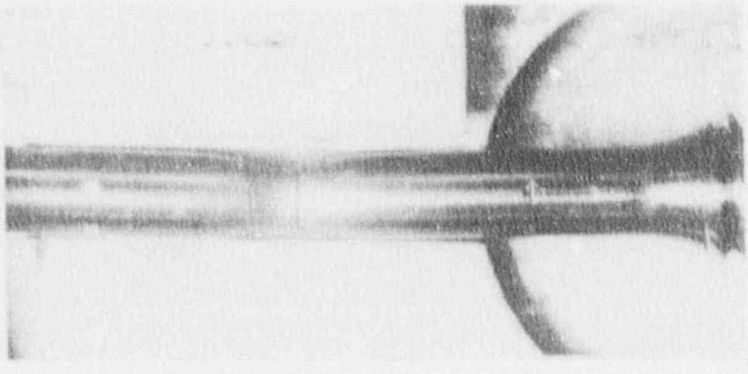

Specimen 3J4 550°F

Figure 5-14. Fractured Tensile Specimens from the San Onofre Unit 3 Reactor Vessel Weld Metal

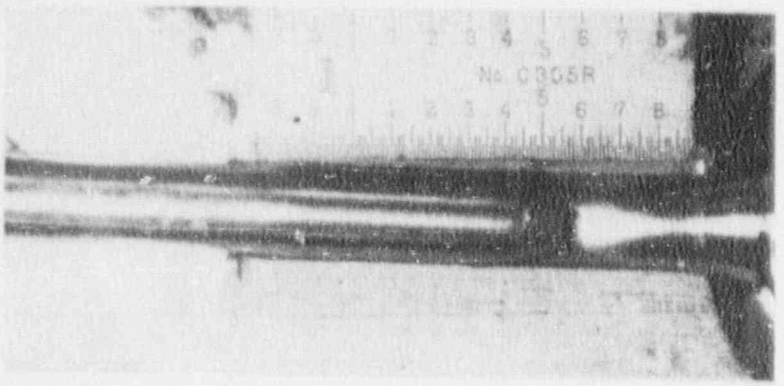

Specimen 4JD 74°F

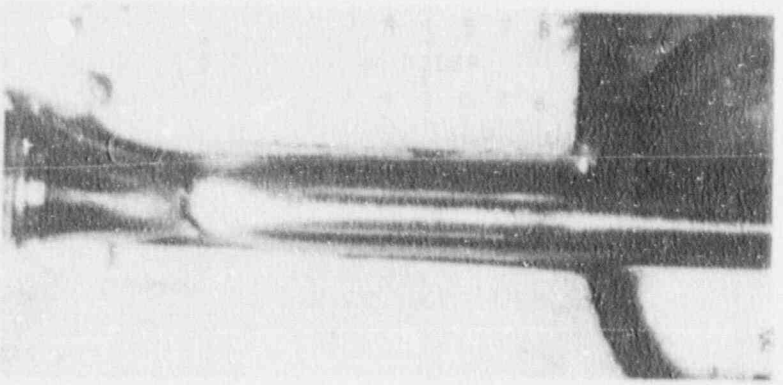

Specimen 4JK 175°F

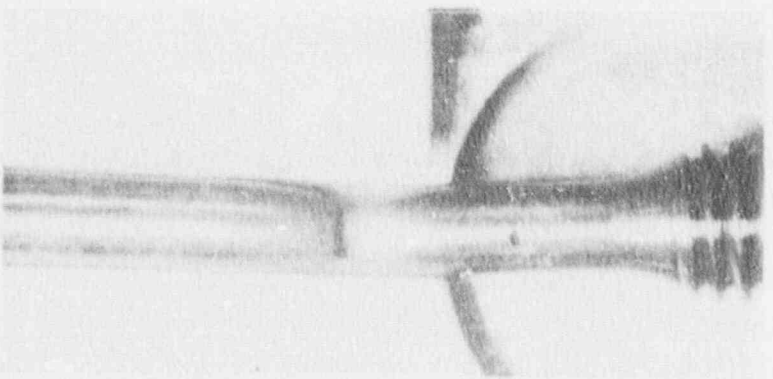

Specimen 4JA 550°F

Figure 5-15. Fractured Tensile Specimens from San Onofre Unit 3 Reactor Vessel HAZ Metal

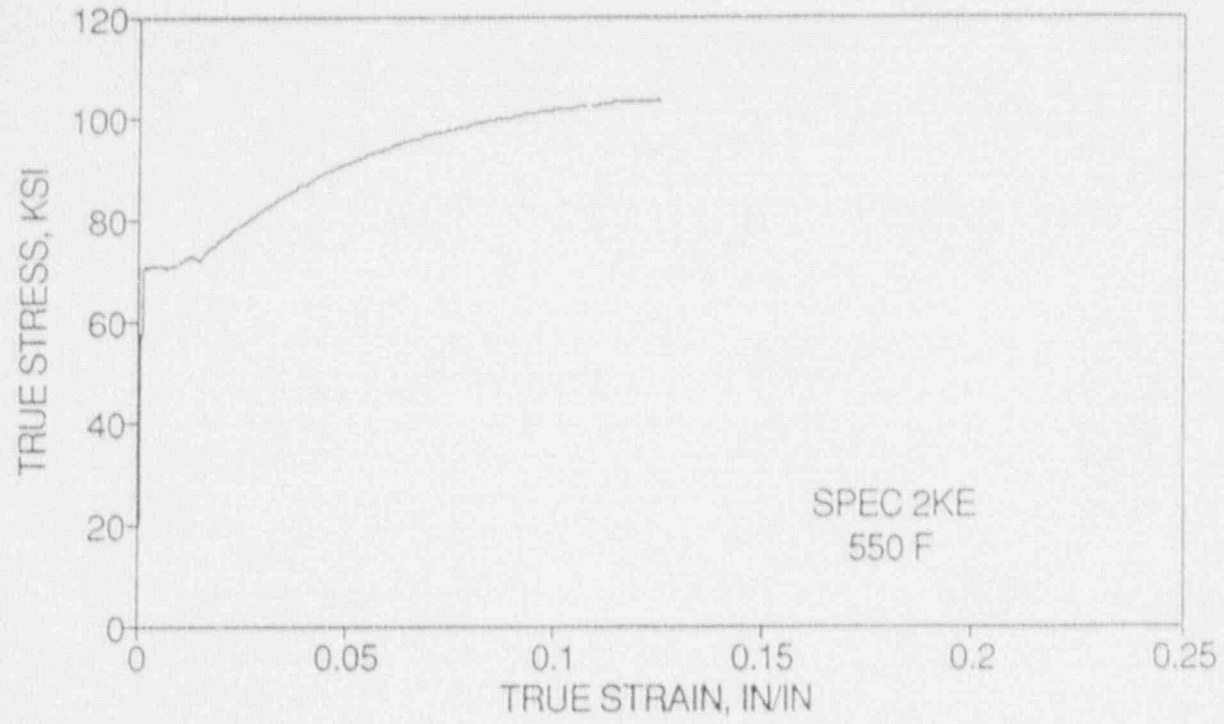

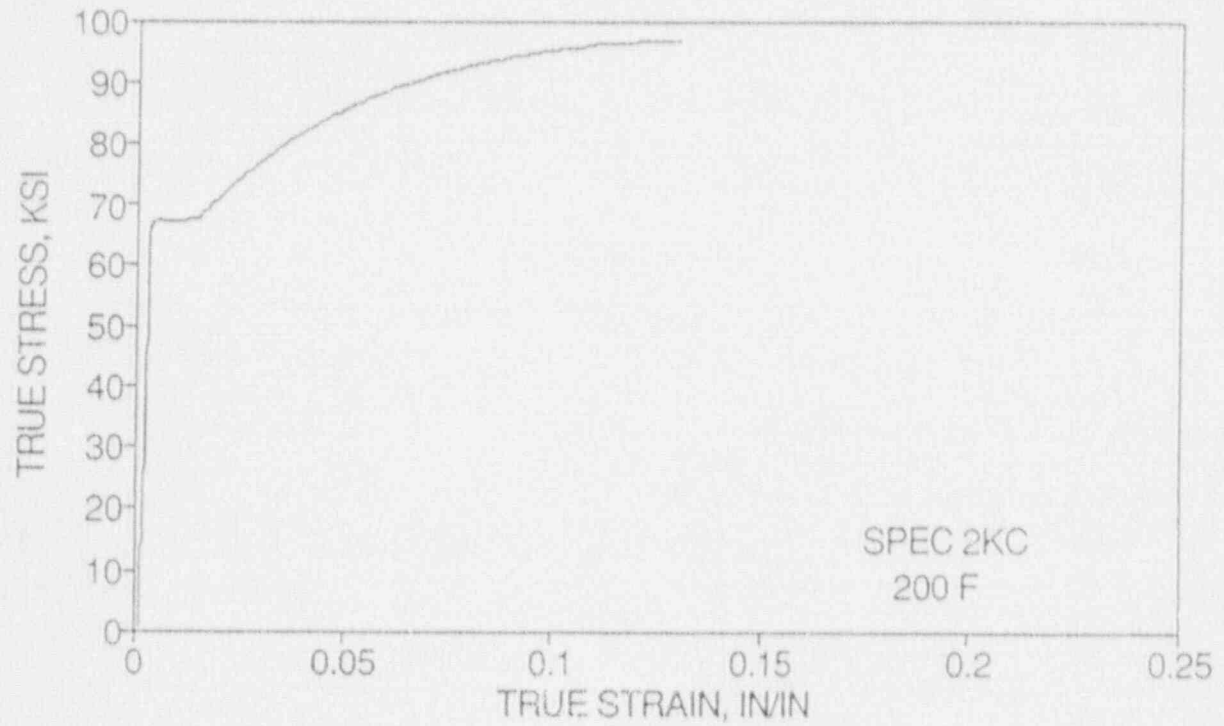

Figure 5-16. True Stress-Strain Curves for the San Onofre Unit 3 Reactor Vessel Shell Plate C-6802-1 Tension Specimens 2KE and 2KC

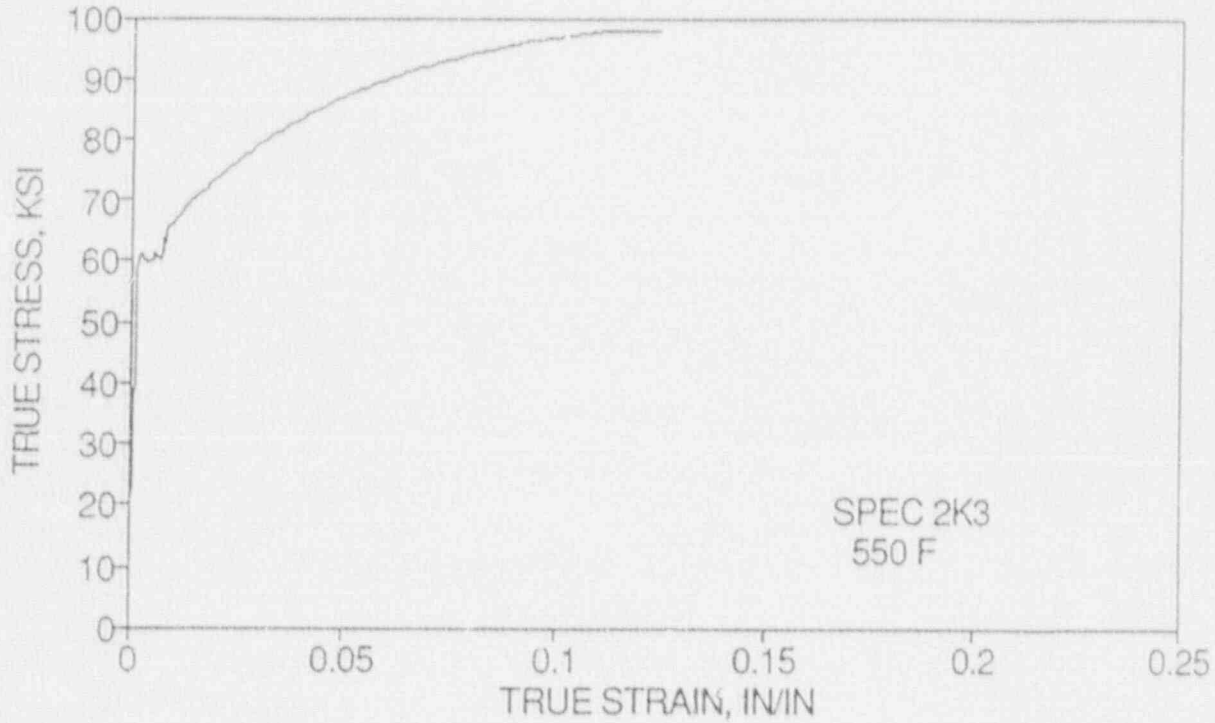

Figure 5-17. True Stress-Strain Curve for the San Onofre Unit 3 Reactor Vessel Shell Plate C-6802-1 Tension Specimen 2K3

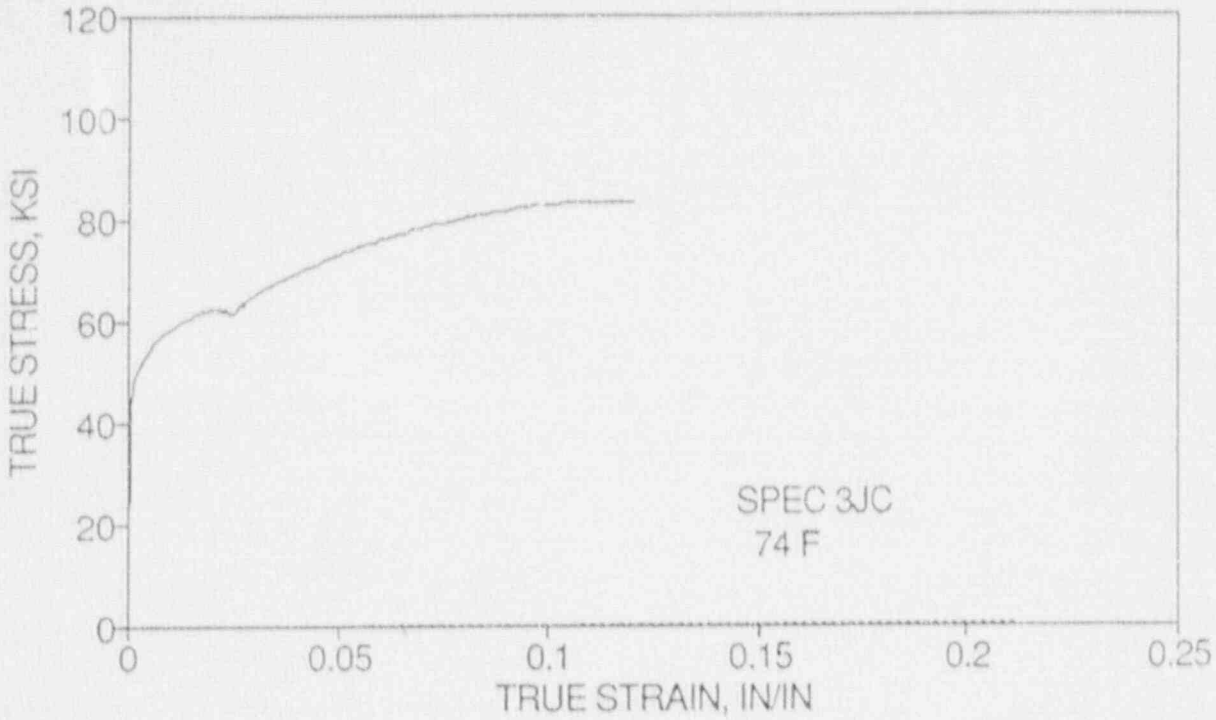

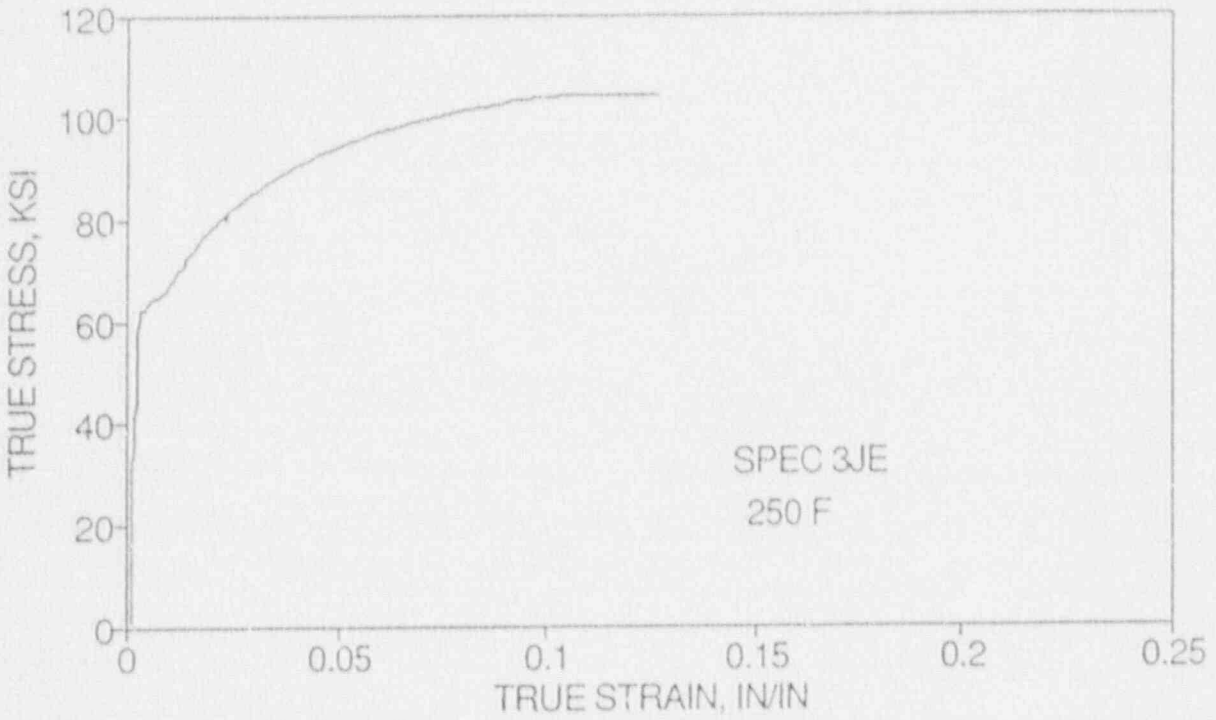

Figure 5-18. True Stress-Strain Curves for the San Onofre Unit 3 Reactor Vessel Weld Metal Tension Specimens 3JC and 3JE

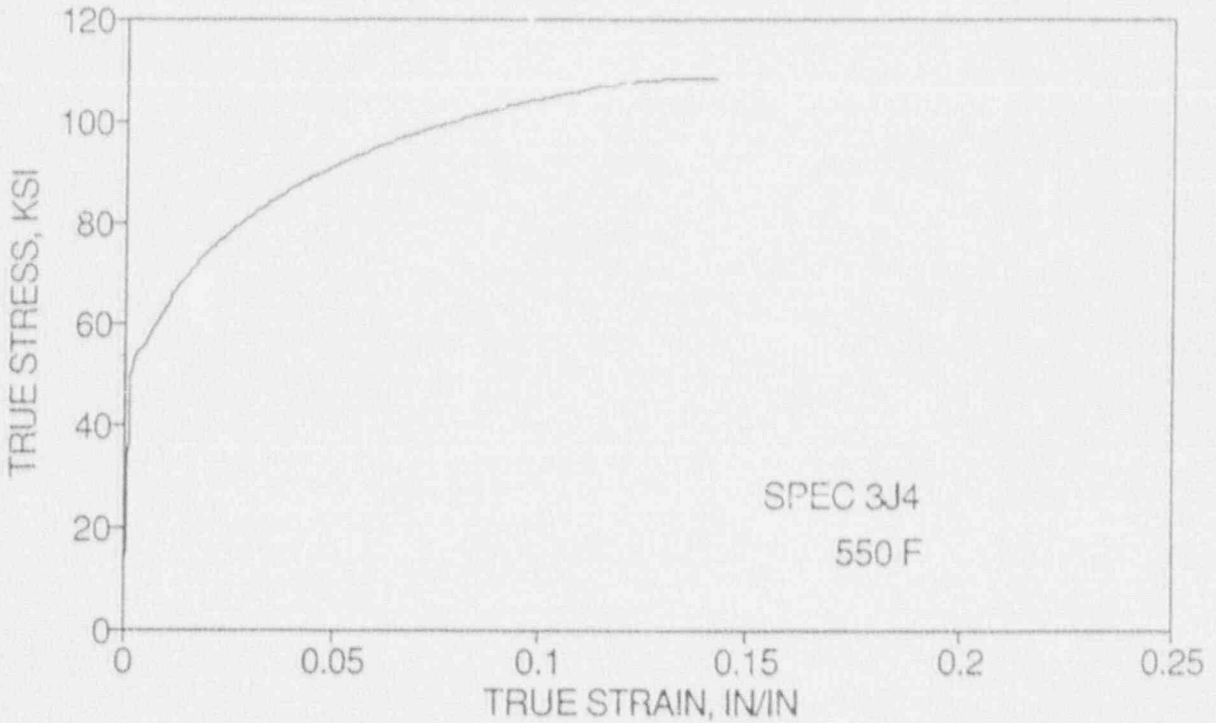

Figure 5-19. True Stress-Strain Curve for the San Onofre Unit 3 Reactor Vessel Weld Metal Tension Specimen 3J4

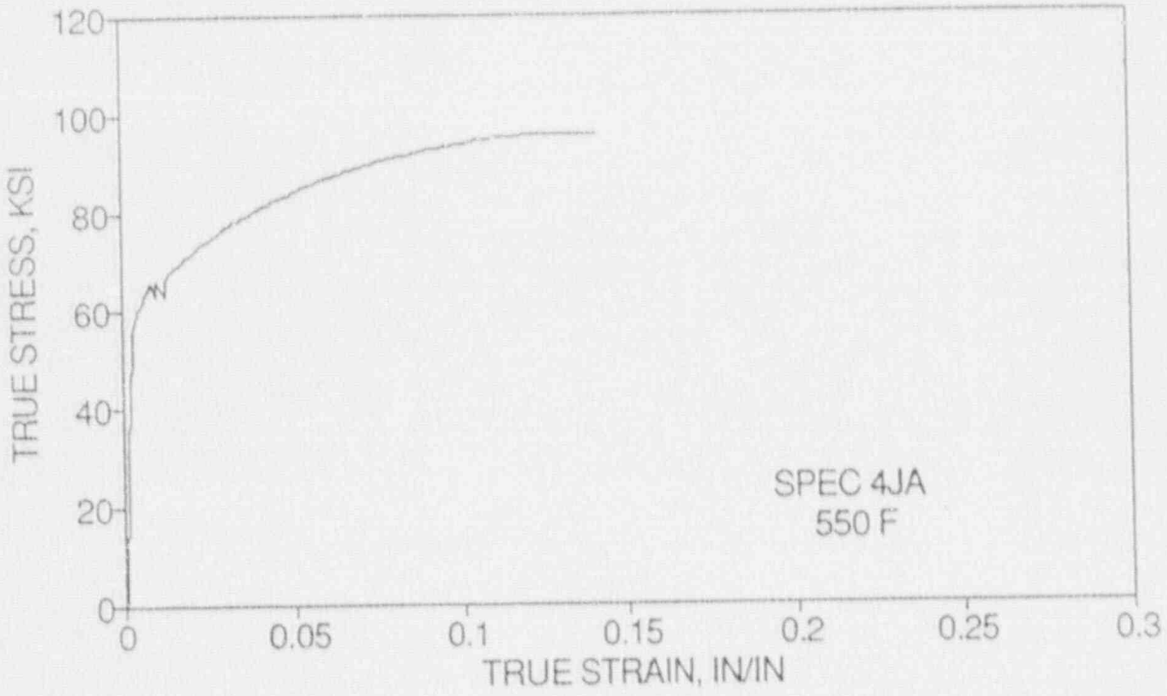

Figure 5-20. True Stress-Strain Curve for the San Onofre Unit 3 Reactor Vessel HAZ Metal Tension Specimen 4JA

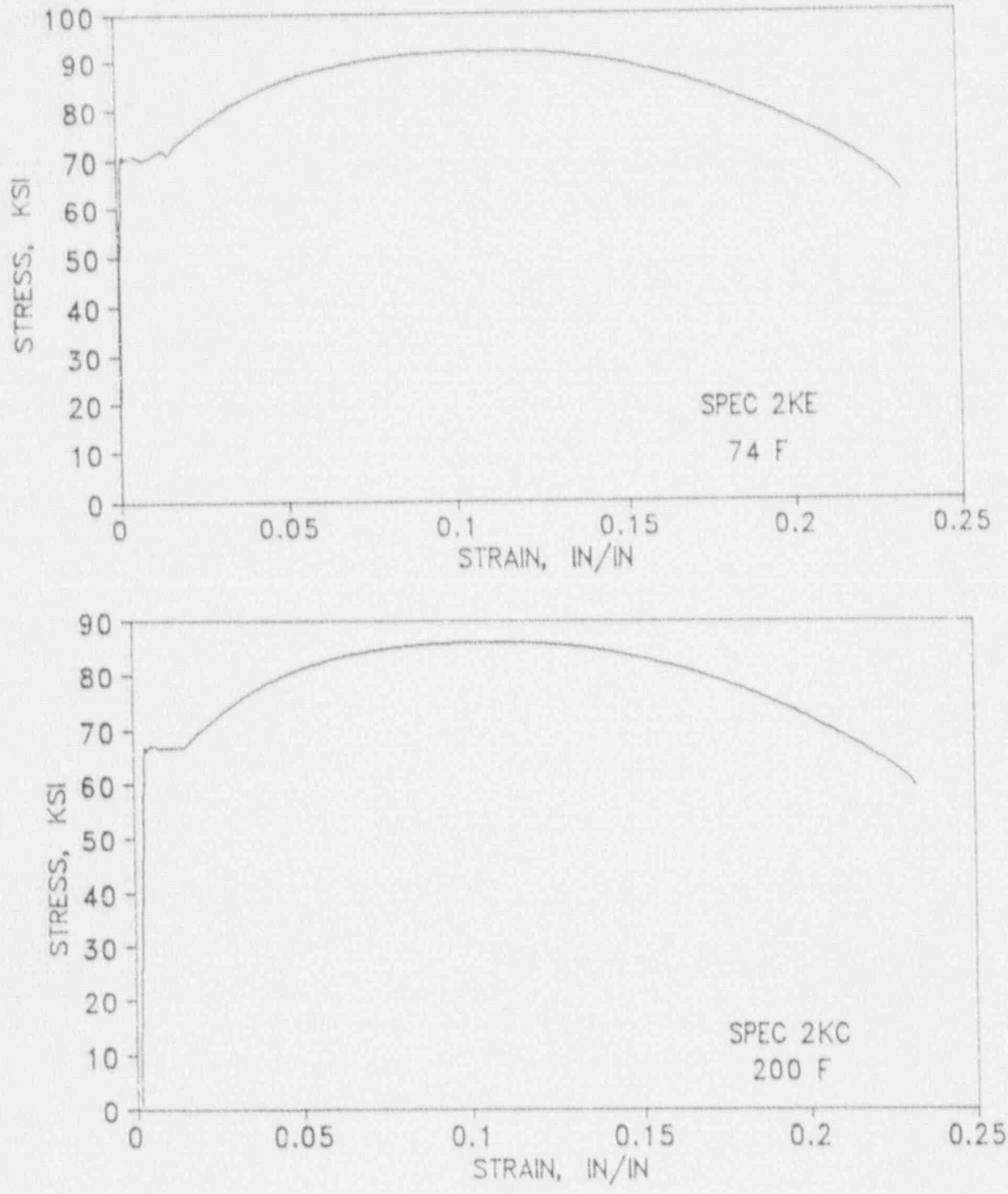

Figure 5-21. Engineering Stress-Strain Curves for the San Onofre Unit 3 Reactor Vessel Shell Plate C-6802-1 Tension Specimens 2KE and 2KC

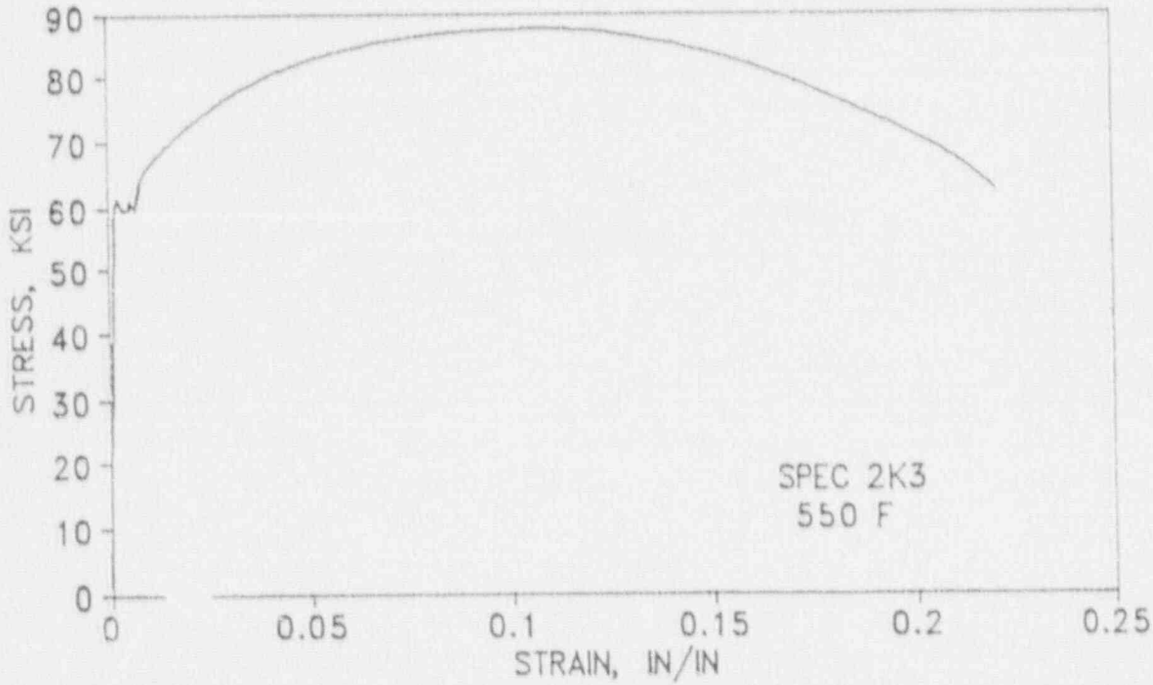

Figure 5-22. Engineering Stress-Strain Curve for the San Onofre Unit 3 Reactor Vessel Shell Plate C-6802-1 Tension Specimen 2K3

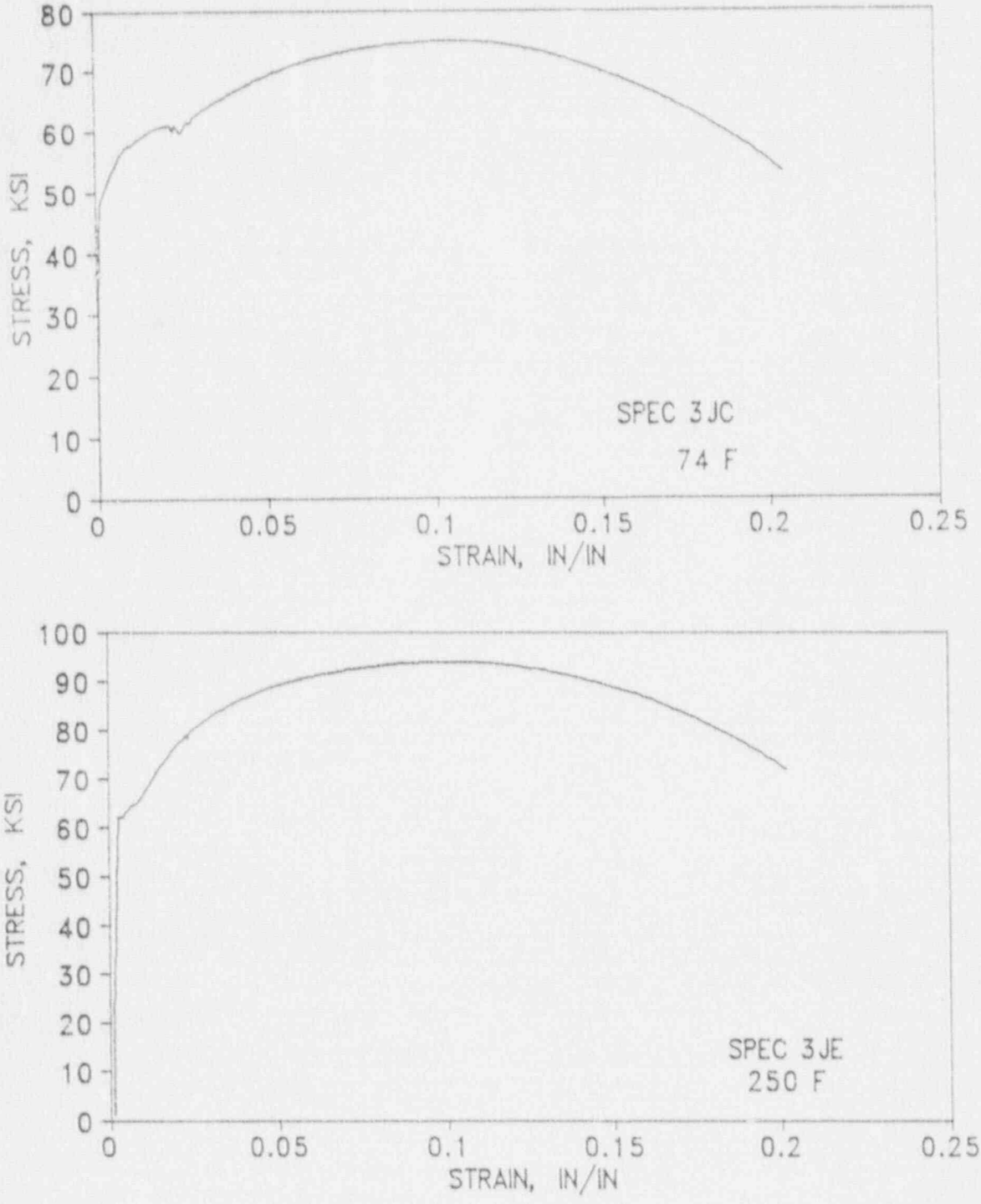

Figure 5-23. Engineering Stress-Strain Curves for the San Onofre Unit 3 Reactor Vessel Weld Metal Tension Specimens 3JC and 3JE

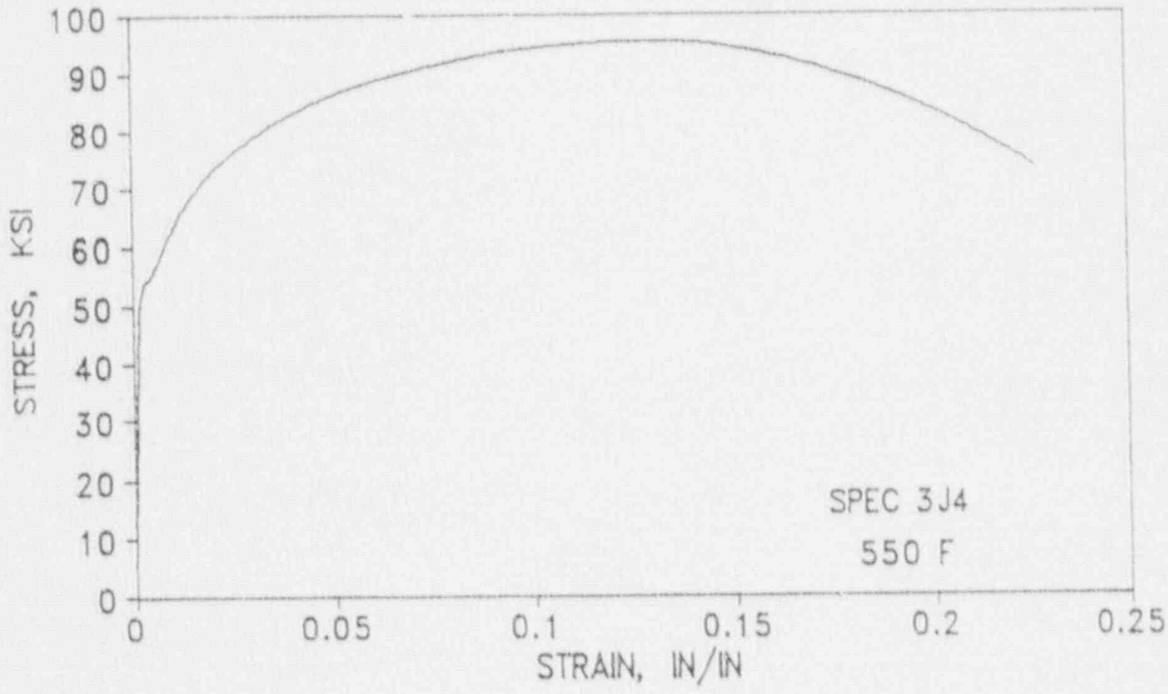

Figure 5-24. Engineering Stress-Strain Curve for the San Onofre Unit 3 Reactor Vessel Weld Metal Tension Specimen 3J4

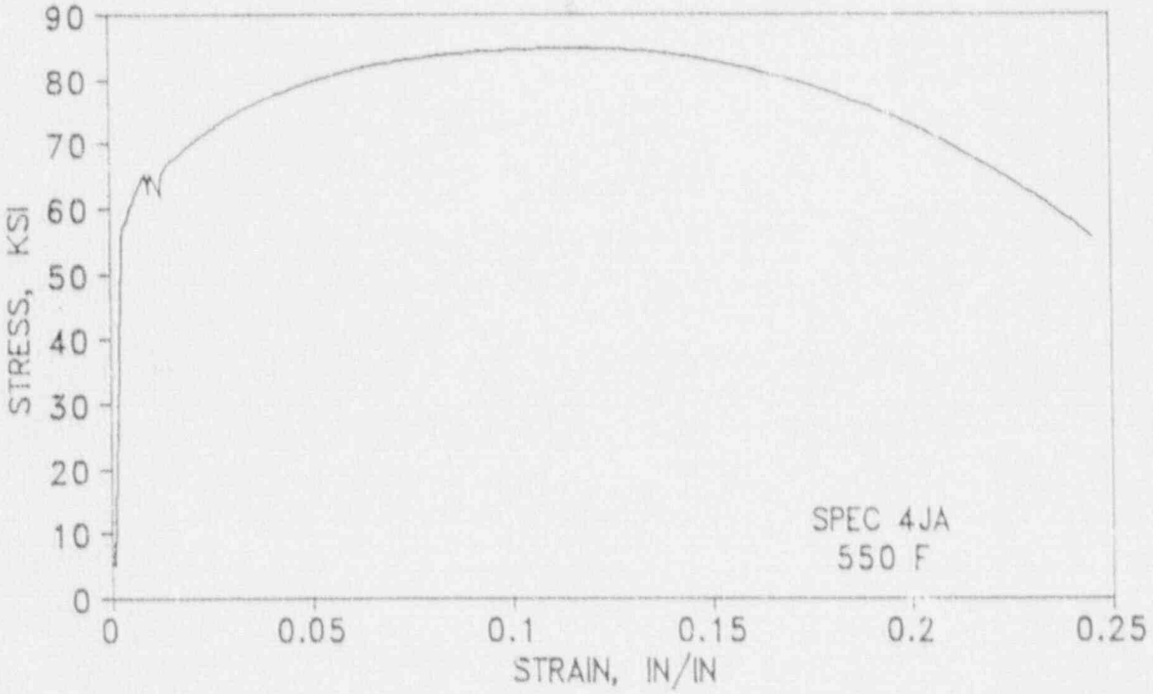

Figure 5-25. Engineering Stress-Strain Curve for the San Onofre Unit 3 Reactor Vessel HAZ Metal Tension Specimen 4JA

SECTION 6.0
RADIATION ANALYSIS AND NEUTRON DOSIMETRY

6.1 Introduction

Knowledge of the neutron environment within the reactor pressure vessel and surveillance capsule geometry is required as an integral part of LWR reactor pressure vessel surveillance programs for two reasons. First, in order to interpret the neutron radiation-induced material property changes observed in the test specimens, the neutron environment (energy spectrum, flux, fluence) to which the test specimens were exposed must be known. Second, in order to relate the changes observed in the test specimens to the present and future condition of the reactor vessel, a relationship must be established between the neutron environment at various positions within the reactor vessel and that experienced by the test specimens. The former requirement is normally met by employing a combination of rigorous analytical techniques and measurements obtained with passive neutron flux monitors contained in each of the surveillance capsules. The latter information is derived solely from analysis.

The use of fast neutron fluence ($E > 1.0$ MeV) to correlate measured material property changes to the neutron exposure of the material for light water reactor applications has traditionally been accepted for development of damage trend curves as well as for the implementation of trend curve data to assess vessel condition. In recent years, however, it has been suggested that an exposure model that accounts for differences in neutron energy spectra between surveillance capsule locations and positions within the vessel wall could lead to an improvement in the uncertainties associated with damage trend curves as well as to a more accurate evaluation of damage gradients through the pressure vessel wall.

Because of this potential shift away from a threshold fluence toward an energy dependent damage function for data correlation, ASTM Standard Practice E853, "Analysis and Interpretation of Light Water Reactor Surveillance Results," recommends reporting displacements per iron atom (dpa) along with fluence

(E > 1.0 MeV) to provide a data base for future reference. The energy dependent dpa function to be used for this evaluation is specified in ASTM Standard Practice E693, "Characterizing Neutron Exposures in Ferritic Steels in Terms of Displacements per Atom." The application of the dpa parameter to the assessment of embrittlement gradients through the thickness of the pressure vessel wall has already been promulgated in Revision 2 to the Regulatory Guide 1.99, "Radiation Damage to Reactor Vessel Materials."

This section provides the results of the neutron dosimetry evaluations performed in conjunction with the analysis of test specimens contained in the surveillance capsule irradiated at the location attached to the vessel wall at 97° (W-97). Fast neutron exposure parameters in terms of neutron fluence (E > 1.0 MeV), neutron fluence (E > 0.1 Mev), and iron atom displacements (dpa) are established for the capsule irradiation history. The analytical formalism relating the measured capsule exposure to the exposure of the vessel wall is described and used to project the integrated exposure of the vessel itself. Also uncertainties associated with the derived exposure parameters at the surveillance capsule and with the projected exposure of the pressure vessel are provided.

6.2 Discrete Ordinates Analysis

A plan view of the reactor geometry at the core midplane is shown in Figure 4-1. Six irradiation capsules attached to the vessel wall are included in the reactor design to constitute the reactor vessel surveillance program. The capsules are located at azimuthal angles of 83°, 97°, 104°, 263°, 277°, and 284° relative to the core cardinal axes as shown in Figure 4-1.

A view of a surveillance capsule assembly is shown in Figure 4-2. A total of 7 stainless steel specimen containers hold the charpy and tensile monitors. The assembly is positioned axially centered on the core midplane, thus spanning the central part of the active fuel zone.

From a neutron transport standpoint, the surveillance capsule structures are significant. They have a marked effect on both the distribution of neutron flux and the neutron energy spectrum in the water annulus between the core barrel and the reactor vessel. In order to properly determine the neutron environment at the test specimen locations, the capsules themselves must be included in the analytical model.

In performing the fast neutron exposure evaluations for the surveillance capsules and reactor vessel, two transport calculations were carried out. These represent two fuel loading geometries for the San Onofre Unit 3 plant as follows:

1. Cycles 1 through 3: A calculation was performed with a power distribution averaged over these three cycles which all have fresh fuel loaded on the periphery.

2. Cycle 4: A calculation was performed with the power distribution averaged over this single cycle which loaded some burned fuel on the periphery. This cycle was assumed to be typical of future cycles and was used to extrapolate exposures to 32 EFPY.

These calculations were combined to produce average relative neutron energy distributions throughout the reactor geometry as well as to establish relative radial distributions of exposure parameters ($\phi(E > 1.0$ Mev), $\phi(E > 0.1$ Mev), and dpa) through the vessel wall integrated over time. The neutron spectral information was required for the interpretation of neutron dosimetry withdrawn from the surveillance capsule as well as for the determination of exposure parameter ratios; i.e., dpa/$\phi(E > 1.0$ MeV), within the pressure vessel geometry. The relative radial gradient information was required to permit the projection of measured exposure parameters to locations interior to the pressure vessel wall; i.e., the 1/4T, 1/2T, and 3/4T locations. In addition differences between the two geometries in calculated dosimeter reaction rates at the center of the surveillance capsule were used to correct the flux history to provide corrected measured reaction rates.

The transport calculations for the reactor model summarized in Figure 4-2 were carried out in R, θ geometry using the DOT two-dimensional discrete ordinates code[11] and the SAILOR cross-section library[12]. The SAILOR library is a 47 group ENDFB-IV based data set produced specifically for light water reactor applications. In these analyses anisotopic scattering was treated with a P_3 expansion of the cross-sections and the angular discretization was modeled with an S_8 order of angular quadrature.

Selected results from the neutron transport analyses performed for the San Onofre Unit 3 reactor are provided in Tables 6-1 through 6-5. The data listed in these tables establish the means for absolute comparisons of analysis and measurement for the capsule irradiation period and provide the means to correlate dosimetry results with the corresponding neutron exposure of the pressure vessel wall.

In Table 6-1, the calculated exposure parameters [φ (E > 1.0 MeV), ϕ(E > 0.1 MeV), and dpa] are given at the geometric center of the two surveillance capsule positions for both the design basis and the plant specific core power distributions. The plant specific data, based on the adjoint transport analysis, are meant to establish the absolute comparison of measurement with analysis. The design basis data derived from the forward calculation are provided as a point of reference against which plant specific fluence evaluations can be compared. Similar data is given in Table 6-2 for the pressure vessel inner radius. Again, the three pertinent exposure parameters are listed for both the design basis and the cycle 1 plant specific power distributions. It is important to note that the data for the vessel inner radius were taken at the clad/base metal interface; and, thus, represent the maximum exposure levels of the vessel wall itself.

Radial gradient information for neutron flux (E > 1.0 MeV), neutron flux (E > 0.1 MeV), and iron atom displacement rate is given in Tables 6-3, 6-4, and 6-5, respectively. The data, obtained from the forward neutron transport calculation, are presented on a relative basis for each exposure parameter at several azimuthal locations. Exposure parameter distributions within the wall may be obtained by normalizing the calculated or projected exposure at the vessel inner radius to the gradient data given in Tables 6-3 through 6-5.

For example, the neutron flux (E > 1.0 MeV) at the 1/4T position on the 45° azimuth is given by:

$$\phi_{1/4T}(45°) = \phi(221.45, 45°)\ F\ (226.93, 45°)$$

where: $\phi_{1/4T}(45°)$ = Projected neutron flux at the 1/4T position on the 45° azimuth

$\phi\ (221.45,45°)$ = Projected or calculated neutron flux at the vessel inner radius on the 45° azimuth.

F (226.93, 45°) = Relative radial distribution function from Table 6-3.

Similar expressions apply for exposure parameters in terms of ϕ (E > 0.1 MeV) and dpa/sec.

The DOT calculations were carried out for a typical octant of the reactor. For the fuel power distributions calculated for cycles 1 through 4, only negligible differences are noted between the different octants, so the use of a single octant to represent the entire reactor geometry is accurate. The model did, however, include wall surveillance capsules at both 7 degrees and 14 degrees with respect to the cardinal axes and these capsules are not included in all octants. This will result in a small correction to the calculated fluence to the reactor vessel at angles near 7 and 14 degrees for octants without the capsules.

6.3 Neutron Dosimetry

The passive neutron sensors included in the San Onofre Unit 3 surveillance program are listed in Table 6-6. (The sulfur monitor has been omitted because the delay between irradiation and receipt at the laboratory precluded analysis. Also given in Table 6-6 are the primary nuclear reactions and associated nuclear constants that were used in the evaluation of the neutron energy spectrum within the capsule and the subsequent determination of the various exposure parameters of interest [ϕ (E > 1.0 Mev), ϕ (E > 0.1 MeV), dpa].

The relative locations of the neutron sensors within the capsules are shown in Figure 4-1. The sets of bare and cadmium shielded monitors were placed in holes drilled in flux monitor housing blocks at three axial levels within the capsules. The monitors are all located at the same radial distance from the core.

The use of passive monitors such as those listed in Table 6-6 does not yield a direct measure of the energy dependent flux level at the point of interest. Rather, the activation or fission process is a measure of the integrated effect that the time- and energy-dependent neutron flux has on the target material over the course of the irradiation period. An accurate assessment of the average neutron flux level incident on the various monitors may be derived from the activation measurements only if the irradiation parameters are well known. In particular, the following variables are of interest:

- The specific activity of each monitor.
- The operating history of the reactor.
- The energy response of the monitor.
- The neutron energy spectrum at the monitor location.
- The physical characteristics of the monitor.

The specific activity of each of the neutron monitors was determined using established ASTM procedures [13 through 25]. Following sample preparation and weighing, the activity of each monitor was determined by means of a lithium-drifted germanium, Ge(Li), gamma spectrometer. The irradiation history of the San Onofre Unit 3 reactor during cycle 1 was obtained from NUREG-0020, "Licensed Operating Reactors Status Summary Report" for the applicable period.

The irradiation history applicable to capsule W-97 is given in Table 6-7. Measured and saturated reaction product specific activities as well as measured full power reaction rates are listed in Table 6-8. Reaction rate values were derived using the pertinent data from Tables 6-6 and 6-7.

In the analysis of the uranium monitors, it was found that the cadmium cover material had become intimately mixed with the uranium and was recovered as a powder. After counting, the mixture was heated in a furnace to attempt to volatilize the cadmium and enable an accurate uranium weight to be obtained. Unfortunately, the mixture reacted with the crucible and no direct weight could be measured. The uranium was then dissolved and a weight obtained. This weight was used to obtain the specific activities in Table 6-8. However, these values were found to be significantly different when ratioed to the other monitors when compared to data from a similar plant. It was concluded that the uranium weight was not reliable. This conclusion is also supported by the variability in weights and ratio of uranium to remaining (not volatilized) fission products. Unfortunately no "as-built" weights were available. The bare uranium values are presumably more reliable but also were not used because more than 50% of the fissions are estimated to have occurred in the U-235 impurity in the depleted uranium.

It was also found that the initial analysis of the Co-60 was not consistent. It was decided to measure the amount of Co-59 in each of the Co-Al wires and the content was found to average 0.7% which is very different from the specified value of 0.17%. Reaction rates for Co were based on the measured concentration for each wire.

Values of key fast neutron exposure parameters were derived from the measured reaction rates using the FERRET least squares adjustment code [26]. The FERRET approach used the measured reaction rate data and the calculated neutron energy spectrum at the the center of the surveillance capsule as input and proceeded to adjust a priori (calculated) group fluxes to produce a best fit (in a least squares sense) to the reaction rate data. The exposure parameters along with associated uncertainties where then obtained from the adjusted spectra.

In the FERRET evaluations, a log normal least-squares algorithm weights both the a priori values and the measured data in accordance with the assigned uncertainties and correlations. In general, the measured values f are linearly related to the flux ϕ by some response matrix A:

$$f_i^{(s,\alpha)} = \sum_g A_{ig}^{(s)} \phi_g^{(\alpha)}$$

where i indexes the measured values belonging to a single data set s, g designates the energy group and α delineates spectra that may be simultaneously adjusted. For example,

$$R_i = \sum_g \sigma_{ig} \phi_g$$

relates a set of measured reaction rates R_i to a single spectrum ϕ_g by the multigroup cross section σ_{ig}. (In this case, FERRET also adjusts the cross-sections.) The lognormal approach automatically accounts for the physical constraint of positive fluxes, even with the large assigned uncertainties.

In the FERRET analysis of the dosimetry data, the continuous quantities (i.e., fluxes and cross-sections) were approximated in 53 groups. The calculated fluxes from the discrete ordinates analysis were expanded into the FERRET group structure using the SAND-II code [27]. This procedure was carried out by first expanding the a priori spectrum into the SAND-II 620 group structure using a SPLINE interpolation procedure for interpolation in regions where group boundaries do not coincide. The 620-point spectrum was then easily collapsed to the group scheme used in FERRET.

The cross-sections were also collapsed into the 53 energy-group structure using SAND II with calculated spectra (as expanded to 620 groups) as weighting functions. The cross sections were taken from the ENDF/B-V dosimetry file. Uncertainty estimates and 53 x 53 covariance matrices were constructed for each cross section. Correlations between cross sections were neglected due to data and code limitations, but are expected to be unimportant.

For each set of data or a priori values, the inverse of the corresponding relative covariance matrix M is used as a statistical weight. In some cases, as for the cross sections, a multigroup covariance matrix is used. More often, a simple parameterized form is used:

$$M_{gg'} = R_N^2 + R_g R_{g'} P_{gg'}$$

where R_N specifies an overall fractional normalization uncertainty (i.e., complete correlation) for the corresponding set of values. The fractional uncertainties R_g specify additional random uncertainties for group g that are correlated with a correlation matrix:

$$P_{gg'} = (1 - \theta)\ \delta_{gg'} + \theta \exp\left[\frac{-(g-g')^2}{2\gamma^2}\right]$$

The first term specifies purely random uncertainties while the second term describes short-range correlations over a range γ (θ specifies the strength of the latter term).

For the a priori calculated fluxes, a short-range correlation of $\gamma = 6$ groups was used. This choice implies that neighboring groups are strongly correlated when θ is close to 1. Strong long-range correlations (or anticorrelations) were justified based on information presented by R.E. Maerker[28]. Maerker's results are closely duplicated when $\gamma = 6$. For the integral reaction rate covariances, simple normalization and random uncertainties were combined as deduced from experimental uncertainties.

Results of the FERRET evaluation of the capsule W-97 dosimetry are given in Table 6-9. The data summarized in Table 6-9 indicated that the capsule received an integrated exposure of 8.00×10^{18} n/cm^2 (E > 1.0 MeV) with an associated uncertainty of ±11%. Also reported are capsule exposures in terms of fluence (E > 0.1 MeV) and iron atom displacements (dpa). Summaries of the fit of the adjusted spectrum are provided in Table 6-10. In general, excellent results were achieved in the fits of the adjusted spectrum to the individual experimental reaction rates. The adjusted spectrum itself is tabulated in Table 6-11 for the FERRET 53 energy group structure.

A summary of the measured and calculated neutron exposure of capsule W-97 is presented in Table 6-12. The comparison between calculation and measurement indicates that the calculation is biased low by 20-24% for all fast neutron exposure parameters listed. Vessel exposure extrapolations have been normalized to include this bias.

Neutron exposure projections at key locations on the pressure vessel inner radius are given in Table 6-13. Along with the current (4.33 EFPY) exposure derived from the capsule W-97 measurements, projections are also provided for an exposure period of 20 EFPY and to end of vessel design life (32 EFPY). The calculated exposure rates based on the Cycle 4 fuel loading were used to perform projections beyond the end of cycle 4.

In the calculation of exposure gradients for use in the development of heatup and cooldown curves for the San Onofre Unit 3 reactor coolant system, exposure projections to 16 EFPY and 32 EFPY were employed. Data based on both a fluence ($E > 1.0$ MeV) slope and a plant specific dpa slope through the vessel wall are provided in Table 6-14. In order to access RT_{NDT} vs. fluence trend curves, dpa equivalent fast neutron fluence levels for the 1/4T and 3/4T positions were defined by the relations

$$\phi' \text{ (1/4T)} = \phi \text{ (Surface)} \left\{\frac{\text{dpa (1/4T)}}{\text{dpa (Surface)}}\right\}$$

$$\phi' \text{ (3/4T)} = \phi \text{ (Surface)} \left\{\frac{\text{dpa (3/4T)}}{\text{dpa (Surface)}}\right\}$$

Using this approach results in the dpa equivalent fluence values listed in Table 6-14.

In Table 6-15 updated lead factors are listed for each of the San Onofre Unit 3 surveillance capsules. These data may be used as a guide in establishing future withdrawal schedules for the remaining capsules.

TABLE 6-1

CALCULATED FAST NEUTRON EXPOSURE PARAMETERS
AT THE SURVEILLANCE CAPSULE CENTER

CYCLE	IRRADIATION TIME (EFPY)	ϕ (E > 1.0 MeV) (n/cm^2-sec)	ϕ (E > 0.1 MeV) (n/cm^2-sec)	dpa/sec
		7° Capsule		
Cycle 1-3	2.807	5.17×10^{10}	9.58×10^{10}	7.31×10^{-11}
Cycle 4	1.520	3.73×10^{10}	6.87×10^{10}	5.28×10^{-11}
Cycle 1-4	4.328			
Average		4.66×10^{10}	8.63×10^{10}	6.60×10^{-11}
		14° Capsule		
Cycle 1-3	2.807	3.72×10^{10}	6.86×10^{10}	5.29×10^{-11}
Cycle 4	1.520	2.61×10^{10}	4.79×10^{10}	3.73×10^{-11}
Cycle 1-4	4.328			
Average		3.33×10^{10}	6.13×10^{10}	4.74×10^{-11}

TABLE 6-2

CALCULATED FAST NEUTRON EXPOSURE PARAMETERS AT
THE PRESSURE VESSEL CLAD/BASE METAL INTERFACE

	0°	15°	30°	45°
		ϕ(E > 1.0Mev) (n/cm^2-sec)		
Cycle 1-3	4.20×10^{10}	2.66×10^{10}	2.37×10^{10}	1.78×10^{10}
Cycle 4	3.22×10^{10}	1.90×10^{10}	1.61×10^{10}	1.22×10^{10}
Cycle 1-4 Average	3.86×10^{10}	2.39×10^{10}	2.10×10^{10}	1.58×10^{10}
		ϕ(E > 0.1Mev) (n/cm^2-sec)		
Cycle 1-3	9.03×10^{10}	5.82×10^{10}	5.07×10^{10}	3.79×10^{10}
Cycle 4	6.88×10^{10}	4.13×10^{10}	3.43×10^{10}	2.57×10^{10}
Cycle 1-4 Average	8.28×10^{10}	5.23×10^{10}	4.49×10^{10}	3.36×10^{10}
		dpa/sec		
Cycle 1-3	6.20×10^{-11}	3.97×10^{-11}	3.51×10^{-11}	2.66×10^{-11}
Cycle 4	4.75×10^{-11}	2.84×10^{-11}	2.39×10^{-11}	1.82×10^{-11}
Cycle 1-4 Average	5.69×10^{-11}	3.57×10^{-11}	3.11×10^{-11}	2.37×10^{-11}

(a) Radius of clad/base metal interface at 221.45 cm.

TABLE 6-3

RELATIVE RADIAL DISTRIBUTIONS OF NEUTRON FLUX (E > 1.0 MeV)
WITHIN THE PRESSURE VESSEL WALL

Radius (cm)	Fraction of Vessel	0°	15°	30°	45°
221.45(1)	0.000	1.0000	1.0000	1.0000	1.0000
221.73	0.013	0.9825	0.9808	0.9824	0.9821
222.38	0.042	0.9289	0.9240	0.9283	0.9287
223.21	0.080	0.8527	0.8457	0.8517	0.8528
224.13	0.122	0.7667	0.7595	0.7655	0.7678
225.05	0.164	0.6842	0.6779	0.6828	0.6861
225.97	0.206	0.6074	0.6026	0.6062	0.6100
226.93	0.250	0.5345	0.5313	0.5336	0.5376
228.03	0.300	0.4607	0.4589	0.4600	0.4643
229.22	0.355	0.3907	0.3901	0.3899	0.3948
230.41	0.409	0.3302	0.3309	0.3296	0.3345
231.61	0.464	0.2784	0.2801	0.2781	0.2829
232.80	0.518	0.2343	0.2366	0.2341	0.2387
233.99	0.572	0.1967	0.1994	0.1968	0.2011
235.19	0.627	0.1647	0.1678	0.1650	0.1692
236.38	0.681	0.1375	0.1408	0.1381	0.1420
237.57	0.736	0.1145	0.1178	0.1153	0.1190
238.77	0.791	0.0948	0.0982	0.0960	0.0994
239.96	0.845	0.0779	0.0814	0.0794	0.0828
241.15	0.899	0.0631	0.0668	0.0652	0.0686
242.25	0.949	0.0508	0.0548	0.0535	0.0572
243.06	0.986	0.0421	0.0464	0.0456	0.0495
243.36(2)	1.000	0.0384	0.0431	0.0424	0.0464

NOTES: 1) Base Metal Inner Radius
2) Base Metal Outer Radius

TABLE 6-4

RELATIVE RADIAL DISTRIBUTIONS OF NEUTRON FLUX (E > 0.1 MeV)
WITHIN THE PRESSURE VESSEL WALL

Radius (cm)	Fraction of Vessel	0°	15°	30°	45°
221.45[1]	0.000	1.000	1.000	1.000	1.000
221.73	0.013	1.008	1.008	1.008	1.009
222.38	0.042	1.006	1.005	1.005	1.009
223.21	0.080	0.989	0.989	0.988	0.996
224.13	0.122	0.960	0.961	0.959	0.970
225.05	0.164	0.924	0.927	0.923	0.937
225.97	0.206	0.884	0.890	0.884	0.901
226.93	0.250	0.841	0.850	0.841	0.861
228.03	0.300	0.791	0.803	0.792	0.814
229.22	0.355	0.737	0.751	0.739	0.763
230.41	0.409	0.683	0.700	0.686	0.713
231.61	0.464	0.630	0.649	0.635	0.663
232.80	0.518	0.579	0.599	0.585	0.614
233.99	0.572	0.528	0.550	0.536	0.566
235.19	0.627	0.479	0.503	0.489	0.519
236.38	0.681	0.432	0.456	0.444	0.474
237.57	0.736	0.385	0.411	0.400	0.430
238.77	0.791	0.340	0.366	0.357	0.387
239.96	0.845	0.296	0.323	0.315	0.345
241.15	0.899	0.251	0.279	0.274	0.304
242.25	0.949	0.209	0.238	0.235	0.266
243.06	0.986	0.175	0.206	0.206	0.238
243.36[2]	1.000	0.161	0.192	0.193	0.226

NOTES: 1) Base Metal Inner Radius
2) Base Metal Outer Radius

TABLE 6-5

RELATIVE RADIAL DISTRIBUTIONS OF IRON DISPLACEMENT RATE (dpa)
WITHIN THE PRESSURE VESSEL WALL

Radius (cm)	Fraction of Vessel	0°	15°	30°	45°
221.45[1]	0.000	1.000	1.000	1.000	1.000
221.45	0.000	1.000	1.000	1.000	1.000
221.73	0.013	0.986	0.985	0.986	0.986
222.38	0.042	0.942	0.938	0.941	0.941
223.21	0.080	0.879	0.874	0.877	0.879
224.13	0.122	0.808	0.803	0.805	0.808
225.05	0.164	0.738	0.735	0.736	0.740
225.97	0.206	0.673	0.672	0.671	0.676
226.93	0.250	0.611	0.611	0.609	0.614
228.03	0.300	0.546	0.548	0.544	0.551
229.22	0.355	0.483	0.487	0.482	0.489
230.41	0.409	0.427	0.433	0.426	0.434
231.61	0.464	0.377	0.384	0.377	0.386
232.80	0.518	0.333	0.341	0.333	0.342
233.99	0.572	0.293	0.302	0.294	0.304
235.19	0.627	0.258	0.267	0.260	0.269
236.38	0.681	0.226	0.236	0.228	0.238
237.57	0.736	0.196	0.207	0.200	0.210
238.77	0.791	0.170	0.180	0.174	0.184
239.96	0.845	0.145	0.156	0.151	0.161
241.15	0.899	0.121	0.133	0.129	0.139
242.25	0.949	0.100	0.112	0.109	0.120
243.06	0.986	0.0835	0.0960	0.0946	0.106
243.36[2]	1.000	0.0764	0.0896	0.0885	0.100

NOTES: 1) Base Metal Inner Radius
2) Base Metal Outer Radius

TABLE 6-6

NUCLEAR PARAMETERS FOR NEUTRON FLUX MONITORS

Monitor Material	Reaction of Interest	Target Weight Fraction	Response Range	Product Half-Life	Fission Yield (%)
Copper	$Cu^{63}(n,\alpha)Co^{60}$	0.6917	E > 5 MeV	5.272 yrs	
Titanium	$Ti^{46}(n,p)Sc^{46}$	0.0778	E > 4 MeV	83.85 days	
Iron	$Fe^{54}(n,p)Mn^{54}$	0.0582	E > 2 MeV	312.2 days	
Nickel	$Ni^{58}(n,p)Co^{58}$	0.6830	E > 2 MeV	70.90 days	
Uranium-238*	$U^{238}(n,f)Cs^{137}$	1.0	E > 1 MeV	30.17 yrs	5.99
Uranium-238	$U^{238}(n,f)Cs^{137}$	1.0	E > 1 MeV	30.12 yrs	5.99
Cobalt-Aluminum*	$Co^{59}(n,\partial)Co^{60}$	0.0070**	0.4ev>E> 0.015 MeV	5.272 yrs	
Cobalt-Aluminum	$Co^{59}(n,\partial)Co^{60}$	0.0070**	E > 0.015 MeV	5.272 yrs	

*Denotes that monitor is cadmium shielded.

**Average value of 6 measurements. Measured cobalt concentration value for each wire was used to get activity per unit mass of cobalt.

TABLE 6-7

IRRADIATION HISTORY OF NEUTRON SENSORS
CONTAINED IN CAPSULE W-97

Irradiation Period	P_j (MW_t)	Irradiation Period	P_j (MW_t)	Irradiation Period	P_j (MW_t)
9 /1983	118958	12 /1985	0	3 /1988	2505525
10 /1983	728980	1 /1986	1137179	4 /1988	2323149
11 /1983	1049800	2 /1986	951789	5 /1988	0
12 /1983	1651300	3 /1986	1060286	6 /1988	0
1 /1984	415741	4 /1986	2313945	7 /1988	0
2 /1984	0	5 /1986	2503081	8 /1988	517640
3 /1984	1415800	6 /1986	2422034	9 /1988	2435963
4 /1984	2185194	7 /1986	2129940	10 /1988	2477912
5 /1984	1157057	8 /1986	2221739	11 /1988	2433112
6 /1984	755354	9 /1986	2001976	12 /1988	2469278
7 /1984	638154	10 /1986	610986	1 /1989	2300423
8 /1984	1643144	11 /1986	2032603	2 /1989	2238355
9 /1984	2405823	12 /1986	1873034	3 /1989	2509434
10 /1984	2169606	1 /1987	100514	4 /1989	1454279
11 /1984	0	2 /1987	0	5 /1989	2516439
12 /1984	1961635	3 /1987	1431146	6 /1989	2252528
1 /1985	2106963	4 /1987	2438732	7 /1989	1783842
2 /1985	0	5 /1987	2459096	8 /1989	2480029
3 /1985	752146	6 /1987	2043680	9 /1989	2424722
4 /1985	1798082	7 /1987	2468870	10 /1989	2465612
5 /1985	2340249	8 /1987	2505525	11 /1989	2420731
6 /1985	1583225	9 /1987	2431401	12 /1989	2492573

NOTE: Reference Power = 3390 MW_t

TABLE 6-8

MEASURED SENSOR ACTIVITIES AND REACTION RATES

Monitor and Axial Location	Measured Activity (dis/sec-gm)	Saturated Activity (dis/sec-gm)	Reaction Rate (RPS/NUCLEUS)
Cu-63 (n,α) Co-60			
Top	2.13×10^5	5.89×10^5	
Middle	2.45×10^5	6.78×10^5	
Bottom	2.11×10^5	5.84×10^5	
Average	2.23×10^5	6.17×10^5	9.41×10^{-17}
Fe-54(n,p) Mn-54			
Top	2.01×10^6	4.78×10^6	
Middle	2.00×10^6	4.75×10^6	
Bottom	1.86×10^6	4.42×10^6	
Average	1.96×10^6	4.65×10^6	7.43×10^{-15}
Ni-58 (n,p) Co-58			
Top	4.83×10^6	7.11×10^7	
Middle	4.61×10^6	6.79×10^7	
Bottom	4.37×10^6	6.44×10^7	
Average	4.60×10^6	6.78×10^7	9.68×10^{-15}
Ti-46 (n,p) Sc-46			
Top	1.49×10^5	1.52×10^6	
Middle	1.41×10^5	1.44×10^6	
Bottom	1.32×10^5	1.35×10^6	
Average	1.41×10^5	1.44×10^6	1.38×10^{-15}

TABLE 6-8

MEASURED SENSOR ACTIVITIES AND REACTION RATES - cont'd

Monitor and Axial Location	Measured Activity (dis/sec-gm)	Saturated Activity (dis/sec-gm)	Reaction Rate (RPS/NUCLEUS)
U-238 (n,f) Cs-137 (Cd)			
Top	5.36×10^{5}	5.85×10^{6}	
Middle	4.47×10^{5}	4.88×10^{6}	
Bottom	4.96×10^{5}	5.41×10^{6}	
Average	4.93×10^{5}	5.38×10^{6}	3.55×10^{-14}
U-238 (n,f) Cs-137 (Bare)			
Top	8.60×10^{5}	9.40×10^{6}	
Middle	7.74×10^{5}	8.45×10^{6}	
Bottom	6.73×10^{5}	7.35×10^{6}	
Average	7.69×10^{5}	8.40×10^{6}	5.54×10^{-14}
Co-59 (n,γ) Co-60			
Top	1.42×10^{8}	3.93×10^{8}	
Middle	1.42×10^{8}	3.93×10^{8}	
Bottom	1.02×10^{8}	2.82×10^{8}	
Average	1.29×10^{8}	3.56×10^{8}	4.88×10^{-12}
Co-59 (n,γ) Co-60 (Cd)			
Top	1.70×10^{7}	4.70×10^{7}	
Middle	1.84×10^{7}	5.09×10^{7}	
Bottom	1.57×10^{7}	4.34×10^{7}	
Average	1.70×10^{7}	4.71×10^{7}	6.68×10^{-13}

TABLE 6-9

SUMMARY OF NEUTRON DOSIMETRY RESULTS

	TIME AVERAGED EXPOSURE RATES	
ϕ (E > 1.0 MeV) (n/cm^2-sec)	5.86×10^{10}	± 11%
ϕ (E > 0.1 MeV) (n/cm^2-sec)	1.14×10^{11}	± 18%
dpa/sec	8.52×10^{-11}	± 11%
ϕ (E < 0.414 eV) (n/cm^2-sec)	1.47×10^{11}	± 23%
	INTEGRATED CAPSULE EXPOSURE	
Φ (E > 1.0 MeV) (n/cm^2)	8.00×10^{18}	± 11%
Φ (E > 0.1 MeV) (n/cm^2)	1.56×10^{19}	± 18%
dpa	1.16×10^{-2}	± 11%
Φ (E < 0.414 eV) (n/cm^2)	2.01×10^{19}	± 23%

NOTE: Total Irradiation Time = 4.33 EFPY

TABLE 6-10

COMPARISON OF MEASURED AND FERRET CALCULATED
REACTION RATES AT THE SURVEILLANCE CAPSULE CENTER

Reaction	Measured	Adjusted Calculation	C/M
Cu-63 (n,α) Co-60	9.41×10^{-17}	9.48×10^{-17}	1.01
Fe-54 (n,p) Mn-54	7.43×10^{-15}	7.47×10^{-15}	1.00
Ni-58 (n,p) Co-58 (Cd)	9.68×10^{-15}	9.54×10^{-15}	0.99
Ti-46 (n,p) Sc-46	1.38×10^{-15}	1.40×10^{-15}	1.01
Co-59 (n,γ) Co-60 (Cd)	6.69×10^{-13}	6.61×10^{-13}	0.99
Co-59 (n,γ) Co-60	4.88×10^{-12}	4.56×10^{-12}	0.93

TABLE 6-11

ADJUSTED NEUTRON ENERGY SPECTRUM AT

THE SURVEILLANCE CAPSULE CENTER

Group	Energy (Mev)	Adjusted Flux (n/cm^2-sec)	Group	Energy (Mev)	Adjusted Flux (n/cm^2-sec)
1	1.73×10^{1}	9.00×10^{6}	28	9.12×10^{-3}	3.20×10^{9}
2	1.49×10^{1}	2.15×10^{7}	29	5.53×10^{-3}	4.19×10^{9}
3	1.35×10^{1}	9.46×10^{7}	30	3.36×10^{-3}	1.33×10^{9}
4	1.16×10^{1}	2.34×10^{8}	31	2.84×10^{-3}	1.30×10^{9}
5	1.00×10^{1}	5.51×10^{3}	32	2.40×10^{-3}	1.30×10^{9}
6	8.61×10^{0}	9.78×10^{8}	33	2.04×10^{-3}	3.78×10^{9}
7	7.41×10^{0}	2.43×10^{9}	34	1.23×10^{-3}	3.62×10^{9}
8	6.07×10^{0}	3.45×10^{9}	35	7.49×10^{-4}	3.52×10^{9}
9	4.97×10^{0}	6.15×10^{9}	36	4.54×10^{-4}	3.52×10^{9}
10	3.68×10^{0}	5.95×10^{9}	37	2.75×10^{-4}	3.94×10^{9}
11	2.87×10^{0}	9.86×10^{9}	38	1.67×10^{-4}	5.30×10^{9}
12	2.23×10^{0}	9.21×10^{9}	39	1.01×10^{-4}	4.29×10^{9}
13	1.74×10^{0}	9.27×10^{9}	40	6.14×10^{-5}	4.14×10^{9}
14	1.35×10^{0}	7.05×10^{9}	41	3.73×10^{-5}	3.84×10^{9}
15	1.11×10^{0}	9.75×10^{9}	42	2.26×10^{-5}	3.53×10^{9}
16	8.21×10^{-1}	8.99×10^{9}	43	1.37×10^{-5}	3.28×10^{9}
17	6.39×10^{-1}	8.07×10^{9}	44	8.32×10^{-6}	3.01×10^{9}
18	4.98×10^{-1}	5.84×10^{9}	45	5.04×10^{-6}	2.68×10^{9}
19	3.88×10^{-1}	6.68×10^{9}	46	3.06×10^{-6}	2.43×10^{9}
20	3.02×10^{-1}	9.85×10^{9}	47	1.86×10^{-6}	2.18×10^{9}
21	1.83×10^{-1}	8.38×10^{9}	48	1.13×10^{-6}	1.62×10^{9}
22	1.11×10^{-1}	6.87×10^{9}	49	6.83×10^{-7}	1.66×10^{9}
23	6.74×10^{-2}	4.75×10^{9}	50	4.14×10^{-7}	4.12×10^{9}
24	4.09×10^{-2}	2.68×10^{9}	51	2.51×10^{-7}	1.17×10^{10}
25	2.55×10^{-2}	3.66×10^{9}	52	1.52×10^{-7}	2.54×10^{10}
26	1.99×10^{-2}	1.73×10^{9}	53	9.24×10^{-8}	1.06×10^{11}
27	1.50×10^{-2}	2.17×10^{9}			

NOTE: Tabulated energy levels represent the upper energy of each group.

TABLE 6-12

COMPARISON OF CALCULATED AND MEASURED
EXPOSURE LEVELS FOR CAPSULE W-97

	Calculated	Measured	C/M
$\Phi(E > 1.0\ MeV)\ \{n/cm^2\}$	6.36×10^{18}	8.00×10^{18}	0.80
$\Phi(E > 0.1\ MeV)\ \{n/cm^2\}$	1.18×10^{19}	1.56×10^{19}	0.76
dpa	9.01×10^{-3}	1.16×10^{-2}	0.78

TABLE 6-13

NEUTRON EXPOSURE PROJECTIONS AT KEY LOCATIONS
ON THE PRESSURE VESSEL CLAD/BASE METAL INTERFACE FOR SAN ONOFRE UNIT 3

	AZIMUTHAL ANGLE			
	0°(a)	15°	30°	45°
4.33 EFPY				
Φ(E>1.0 MeV) (n/cm^2)	6.63×10^{18}	4.11×10^{18}	3.61×10^{18}	2.72×10^{18}
Φ(E>0.1 MeV) (n/cm^2)	1.49×10^{19}	9.44×10^{18}	8.11×10^{18}	6.07×10^{18}
dpa	0.0100	0.00628	0.00547	0.00416
20.0 EFPY				
Φ(E>1.0 MeV) (n/cm^2)	2.66×10^{19}	1.59×10^{19}	1.36×10^{19}	1.03×10^{19}
Φ(E>0.1 MeV) (n/cm^2)	5.99×10^{19}	3.64×10^{19}	3.05×10^{19}	2.29×10^{19}
dpa	0.0463	0.0290	0.0253	0.0192
32.0 EFPY				
Φ(E>1.0 MeV) (n/cm^2)	4.20×10^{19}	2.50×10^{19}	2.13×10^{19}	1.61×10^{19}
Φ(E>0.1 MeV) (n/cm^2)	9.44×10^{19}	5.71×10^{19}	4.77×10^{19}	3.57×10^{19}
dpa	0.0634	0.0382	0.0324	0.0246

(a) Maximum point on the pressure vessel

TABLE 6-14

NEUTRON EXPOSURE VALUES FOR USE IN THE GENERATION OF HEATUP/COOLDOWN CURVES

20 EFPY

	NEUTRON FLUENCE (E > 1.0 MeV) SLOPE (n/cm^2)			dpa SLOPE (equivalent n/cm^2)		
	Surface	1/4 T	3/4 T	Surface	1/4 T	3/4 T
0°	2.66E+19	1.42E+19	2.91E+18	2.66E+19	1.63E+19	5.02E+18
15°	1.59E+19	8.46E+18	1.79E+18	1.59E+19	9.73E+18	3.18E+18
30°	1.36E+19	7.27E+18	1.50E+18	1.36E+19	8.30E+18	2.64E+18
45°	1.03E+19	5.53E+18	1.17E+18	1.03E+19	6.31E+18	2.09E+18

32 EFPY

	NEUTRON FLUENCE (E > 1.0 MeV) SLOPE (n/cm^2)			dpa SLOPE (equivalent n/cm^2)		
	Surface	1/4 T	3/4 T	Surface	1/4 T	3/4 T
0°	4.20E+19	2.24E+19	4.58E+18	4.20E+19	2.56E+19	7.91E+18
15°	2.50E+19	1.33E+19	2.81E+18	2.50E+19	1.53E+19	4.99E+18
30°	2.13E+19	1.14E+19	2.35E+18	2.13E+19	1.30E+19	4.13E+18
45°	1.61E+19	8.64E+18	1.83E+18	1.61E+19	9.87E+18	3.26E+18

(a) Maximum point on the pressure vessel

TABLE 6-15

UPDATED LEAD FACTORS FOR SAN ONOFRE UNIT 3
SURVEILLANCE CAPSULES

Capsule	Lead Factor[a]
83°	1.21
97	1.21
104	0.86
263	1.21
277	1.21
284	0.86

(a) Plant specific evaluation for fuel cycles 1 through 4. If future fuel loading patterns similar to Cycle 4 are used, the lead factors for capsules at 83°, 263°, and 277° will decrease towards an asymptotic value of 1.16 and the capsules at 104° and 284° will decrease towards 0.81.

SECTION 7.0

SURVEILLANCE CAPSULE REMOVAL SCHEDULE

The following removal schedule meets ASTM E185-82 and is recommended for future capsules to be removed from the San Onofre Unit 3 reactor vessel:

Capsule Location (deg.)	Capsule Lead Factor	Removal EFPY (b)	Estimated Fluence (n/cm^2)
97.0	1.21	4.33 (a)	0.8×10^{19} (actual)
83.0	1.21	6.0	1.0×10^{19}
263.0	1.21	15.0	2.4×10^{19}
277.0	1.21	32.0	5.1×10^{19}
104.0	0.86	Standby	- - - -
284.0	0.86	Standby	- - - -

(a) Plant Specific Evaluation

(b) Effective full power years from plant startup.

SECTION 8.0
REFERENCES

1. Combustion Engineering Report No. S-NLM-002, "Program for Irradiation Surveillance of San Onofre Reactor Vessel Materials San Onofre Nuclear Generating Station, Units 2 and 3", October 30, 1974

2. Combustion Engineering Report No. TR-S-MCM-004, "Southern California Edison San Onofre Unit 3, Evaluation of Baseline Specimens, Reactor Vessel Materials Irradiation Surveillance Program", November 30, 1979

3. Code of Federal Regulations, 10CFR50, Appendix G, "Fracture Toughness Requirements", and Appendix H, "Reactor Vessel Material Surveillance Program Requirements," U.S. Nuclear Regulatory Commission, Washington, D.C.

4. ASTM E185-82, "Standard Practice for Light-Water Cooled Nuclear Power Reactor Vessels, E706 (IF)."

5. ASTM E23-88, "Standard Test Methods for Notched Bar Impact Testing of Metallic Materials."

6. ASTM A370-89, "Standard Test Methods and Definitions for Mechanical Testing of Steel Products."

7. ASTM E8-89, "Standard Test Methods of Tension Testing of Metallic Materials."

8. ASTM E21-79 (1988), "Standard Practice for Elevated Temperature Tension Tests of Metallic Materials."

9. ASTM E83-85, "Standard Practice for Verification and Classification of Extensometers."

10. Regulatory Guide 1.99, Proposed Revision 2, "Radiation Damage to Reactor Vessel Materials", U.S. Nuclear Regulatory Commission, February, 1986.

11. R. G. Soltesz, R. K. Disney, J. Jedruch, and S. L. Ziegler, "Nuclear Rocket Shielding Methods, Modification, Updating and Input Data Preparation. Vol. 5--Two-Dimensional Discrete Ordinates Transport Technique", WANL-PR(LL)-034, Vol. 5, August 1970.

12. "ORNL RSCI Data Library Collection DLC-76 SAILOR Coupled Self-Shielded, 47 Neutron, 20 Gamma-Ray, P3, Cross Section Library for Light Water Reactors".

13. ASTM Designation E482-82, "Standard Guide for Application of Neutron Transport Methods for Reactor Vessel Surveillance", in ASTM Standards, Section 12, American Society for Testing and Materials, Philadelphia, PA, 1984.

14. ASTM Designation E560-77, "Standard Recommended Practice for Extrapolating Reactor Vessel Surveillance Dosimetry Results", in ASTM Standards, Section 12, American Society for Testing and Materials, Philadelphia, PA, 1984.

15. ASTM Designation E693-79, "Standard Practice for Characterizing Neutron Exposures in Ferritic Steels in Terms of Displacements per Atom (dpa)", in ASTM Standards, Section 12, American Society for Testing and Materials, Philadelphia, PA, 1984.

16. ASTM Designation E706-81a, "Standard Master Matrix for Light-Water Reactor Pressure Vessel Surveillance Standard", in ASTM Standards, Section 12, American Society for Testing and Materials, Philadelphia, PA, 1984.

17. ASTM Designation E853-84, "Standard Practice for Analysis and Interpretation of Light-Water Reactor Surveillance Results", in ASTM Standards, Section 12, American Society for Testing and Materials, Philadelphia, PA, 1984.

18. ASTM Designation E261-77, "Standard Method for Determining Neutron Flux, Fluence, and Spectra by Radioactivation Techniques", in ASTM Standards, Section 12, American Society for Testing and Materials, Philadelphia, PA, 1984.

19. ASTM Designation E262-77, "Standard Method for Measuring Thermal Neutron Flux by Radioactivation Techniques", in ASTM Standards, Section 12, American Society for Testing and Materials, Philadelphia, PA, 1984.

20. ASTM Designation E263-82, "Standard Method for Determining Fast-Neutron Flux Density by Radioactivation of Iron", in ASTM Standards, Section 12, American Society for Testing and Materials, Philadelphia, PA, 1984.

21. ASTM Designation E264-82, "Standard Method for Determining Fast-Neutron Flux Density by Radioactivation of Nickel", in ASTM Standards, Section 12, American Society for Testing and Materials, Philadelphia, PA, 1984.

22. ASTM Designation E481-78, "Standard Method for Measuring Neutron-Flux Density by Radioactivation of Cobalt and Silver", in ASTM Standards, Section 12, American Society for Testing and Materials, Philadelphia, PA, 1984.

23. ASTM Designation E523-82, "Standard Method for Determining Fast-Neutron Flux Density by Radioactivation of Copper", in ASTM Standards, Section 12, American Society for Testing and Materials, Philadelphia, PA, 1984.

24. ASTM Designation E704-84, "Standard Method for Measuring Reaction Rates by Radioactivation of Uranium-238", in ASTM Standards, Section 12, American Society for Testing and Materials, Philadelphia, PA, 1984.

25. ASTM Designation E1005-84, "Standard Method for Application and Analysis of Radiometric Monitors for Reactor Vessel Surveillance", in ASTM Standards, Section 12, American Society for Testing and Materials, Philadelphia, PA, 1984.

26. F. A. Schmittroth, FERRET Data Analysis Code, HEDL-TME 79-40, Hanford Engineering Development Laboratory, Richland, WA, September 1979.

27. W. N. McElroy, S. Berg and T. Crocket, A Computer-Automated Iterative Method of Neutron Flux Spectra Determined by Foil Activation, AFWL-TR-7-41, Vol. I-IV, Air Force Weapons Laboratory, Kirkland AFB, NM, July 1967.

28. EPRI-NP-2188, "Development and Demonstration of an Advanced Methodology for LWR Dosimetry Applications", R. E. Maerker, et al., 1981.

APPENDIX A

Load-Time Records for Charpy Impact Tests

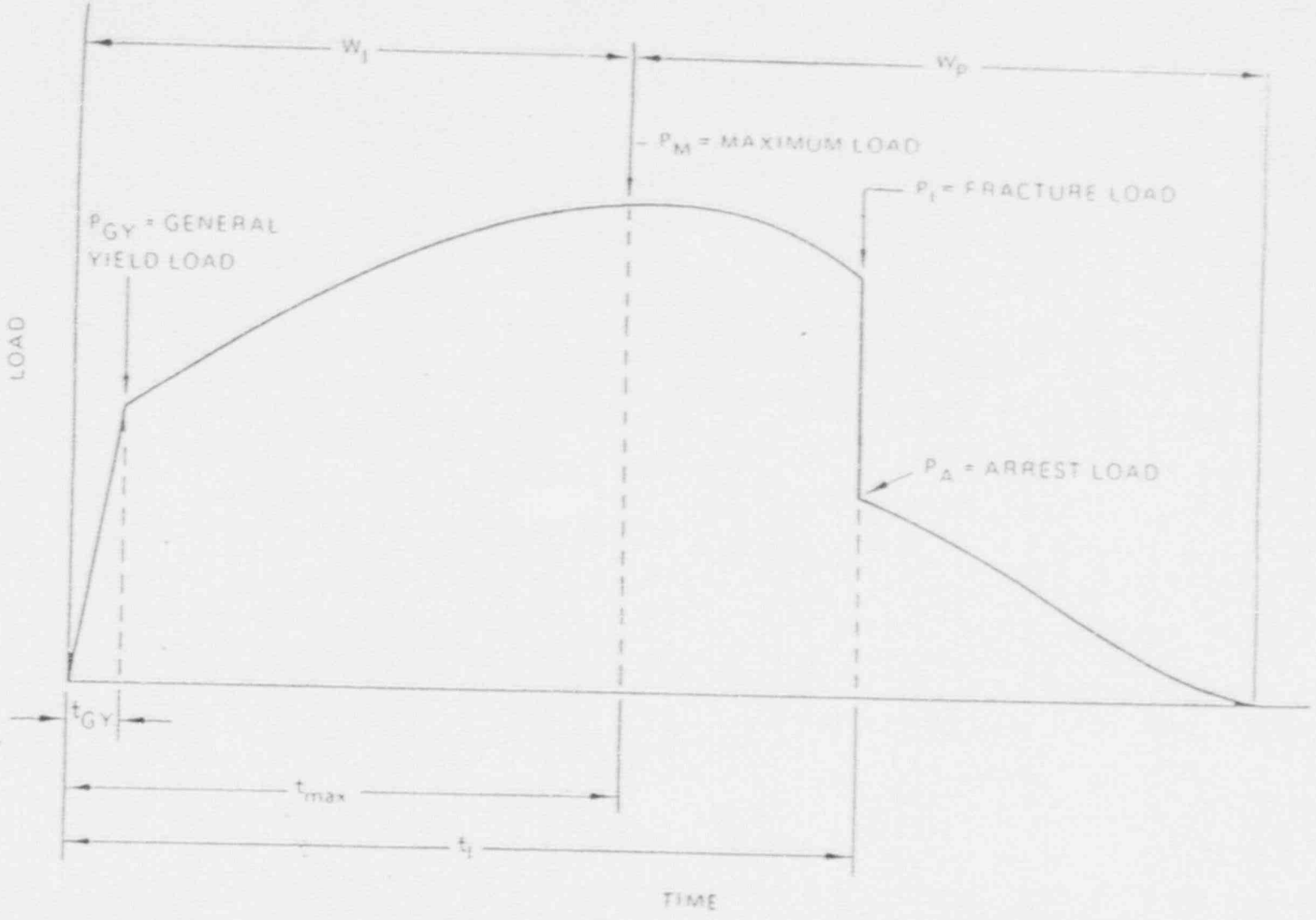

Figure A-1. Idealized load-time record for an instrumented Charpy impact test.

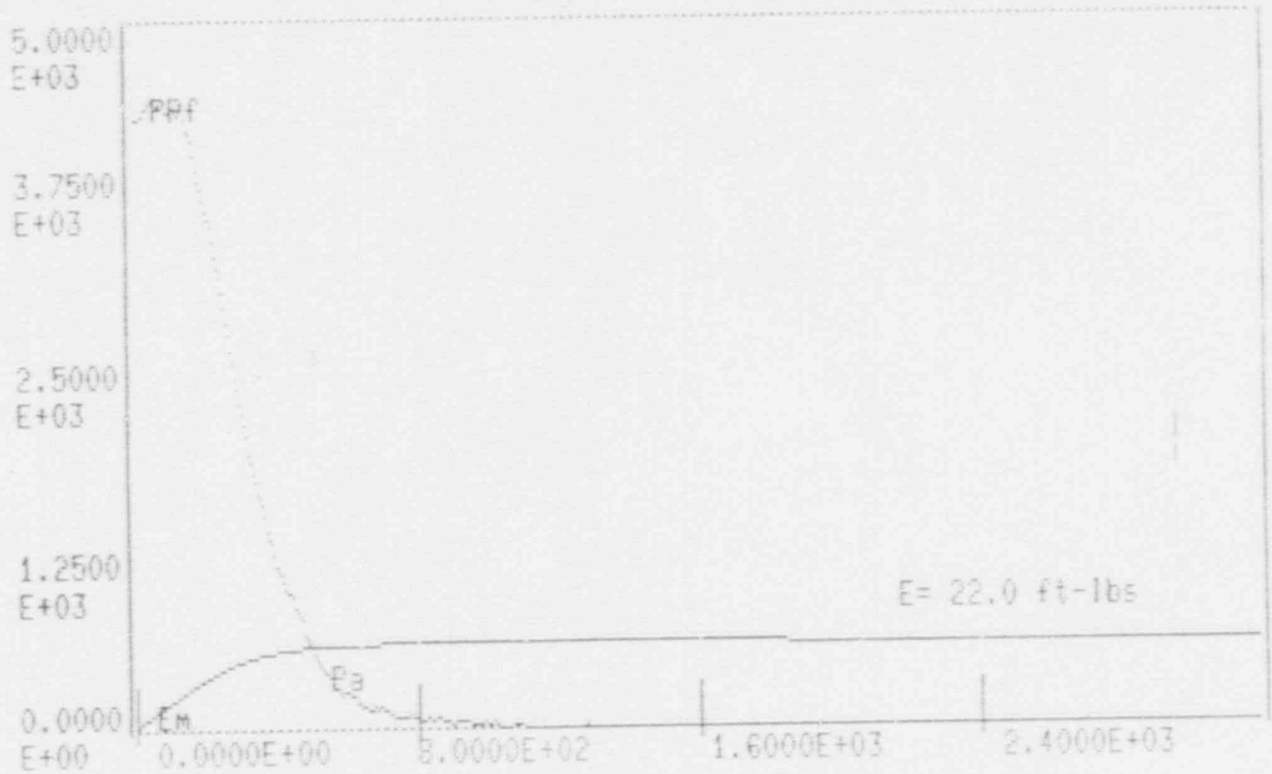

Figure A-2. Charpy impact test load-time record for Specimen 153.

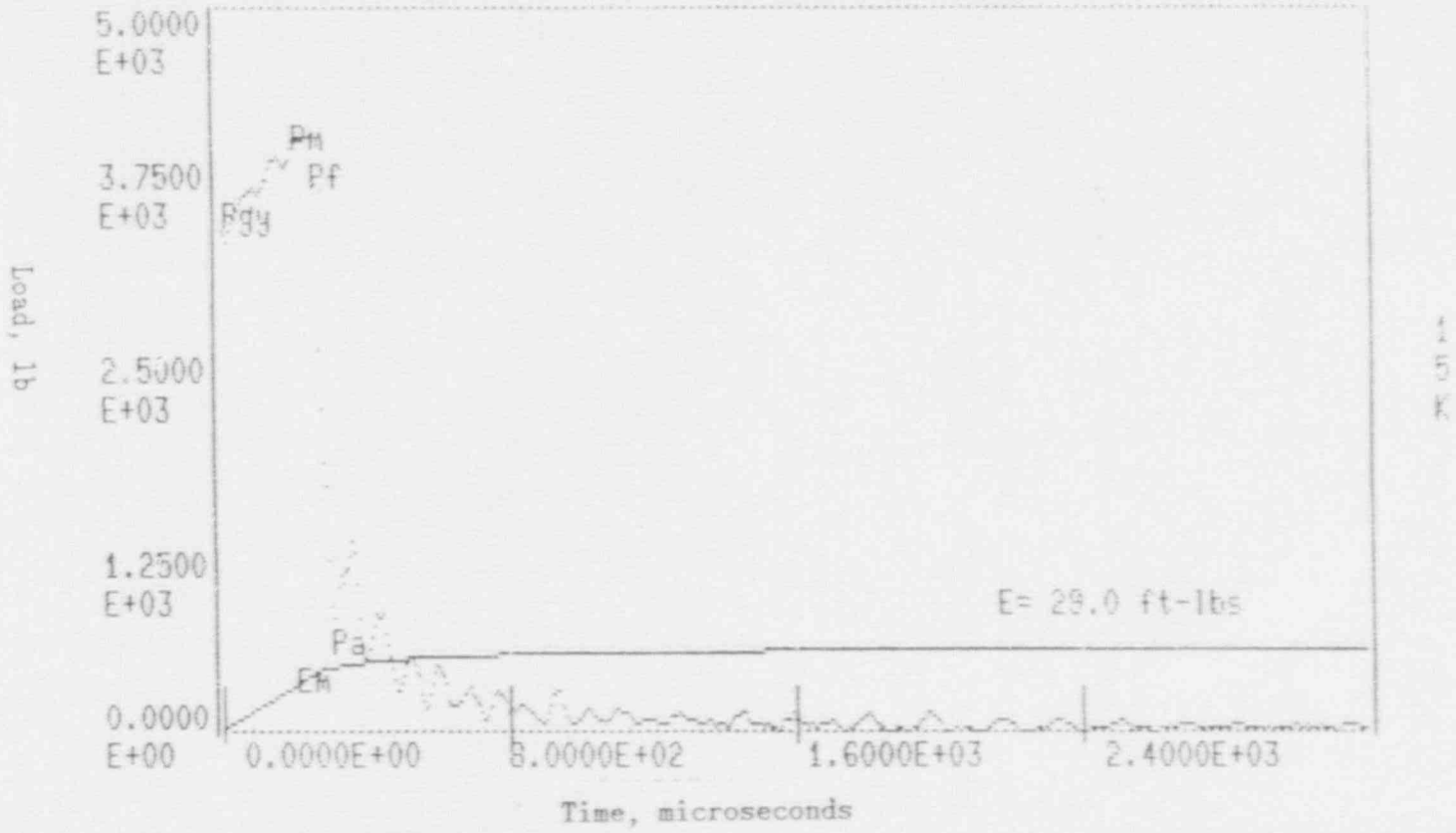

Figure A-3. Charpy impact test load-time record for Specimen 15K.

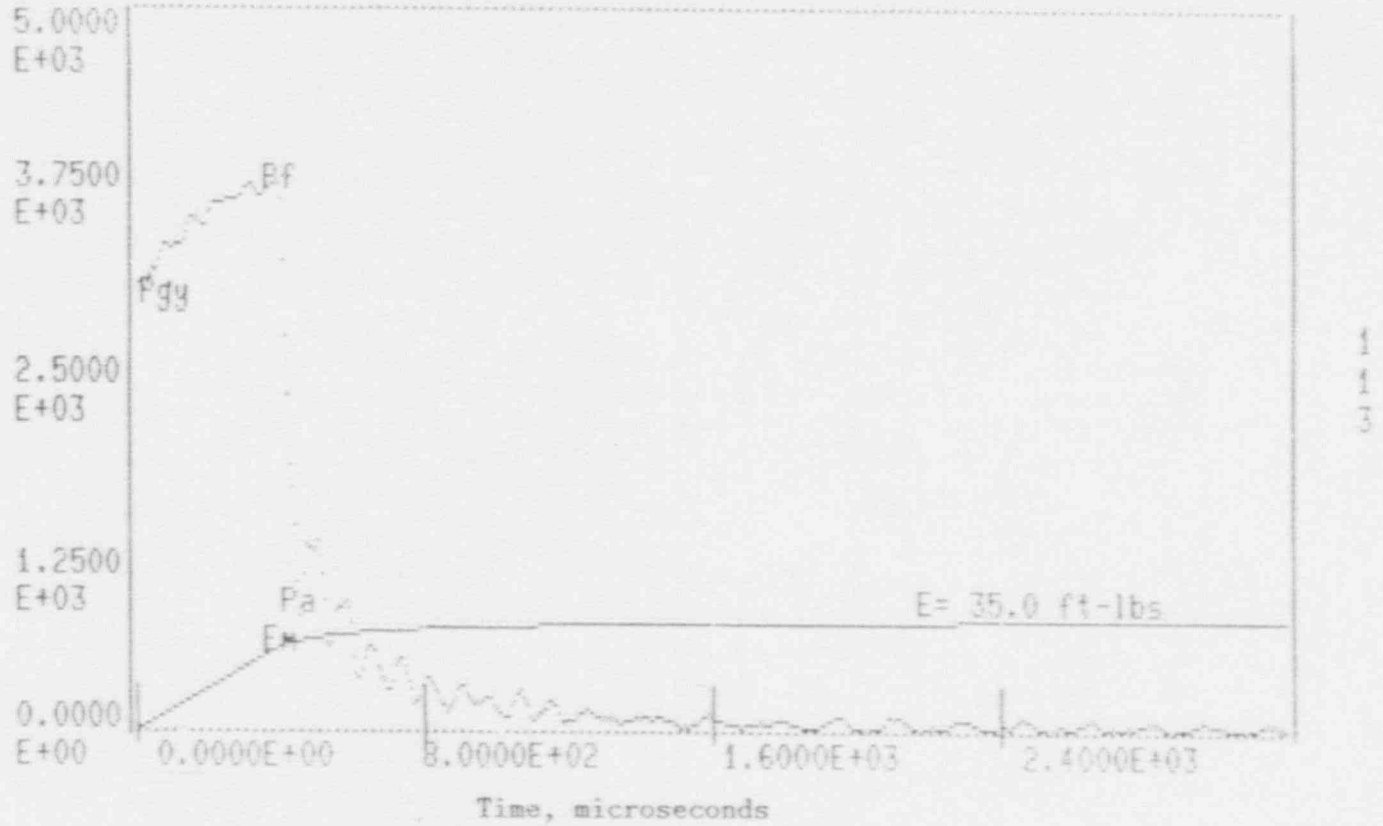

Figure A-4. Charpy impact test load-time record for Specimen 113.

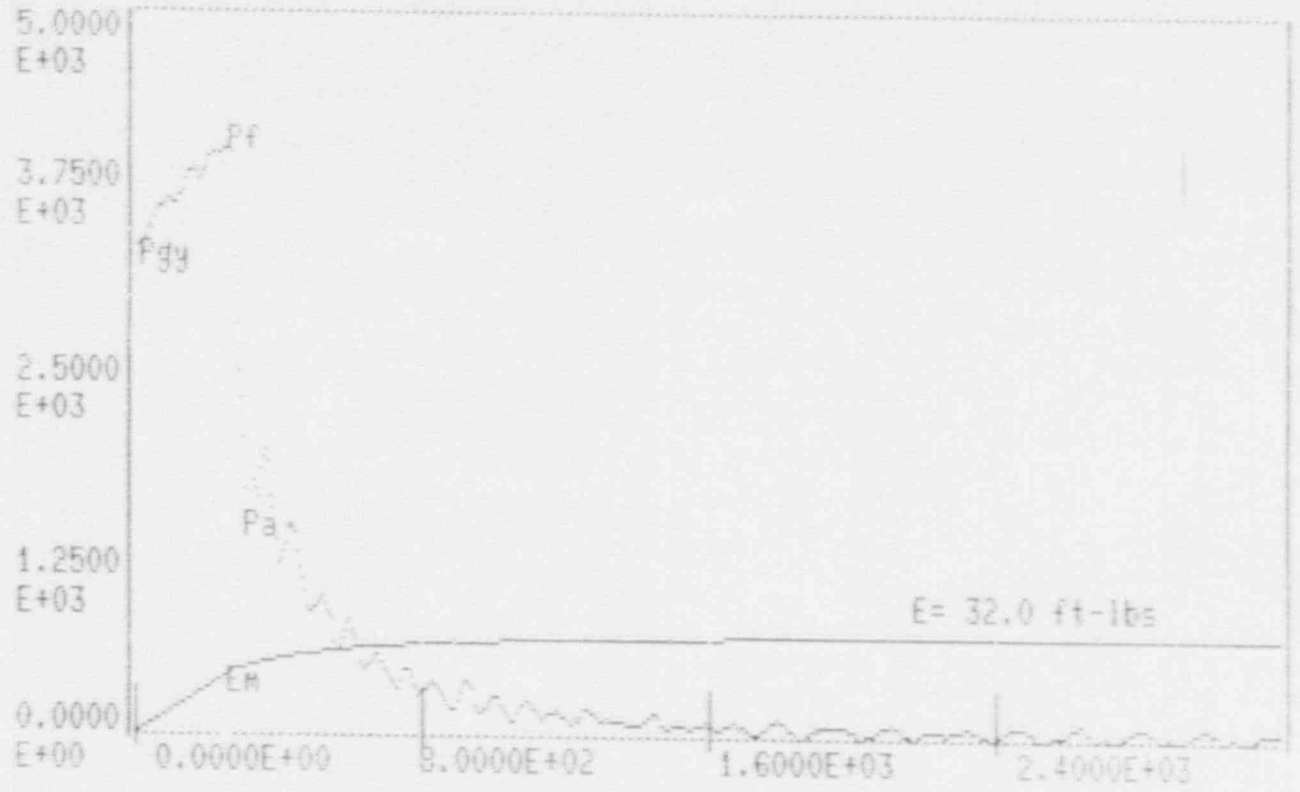

Figure A-5. Charpy impact test load-time record for Specimen 14Y.

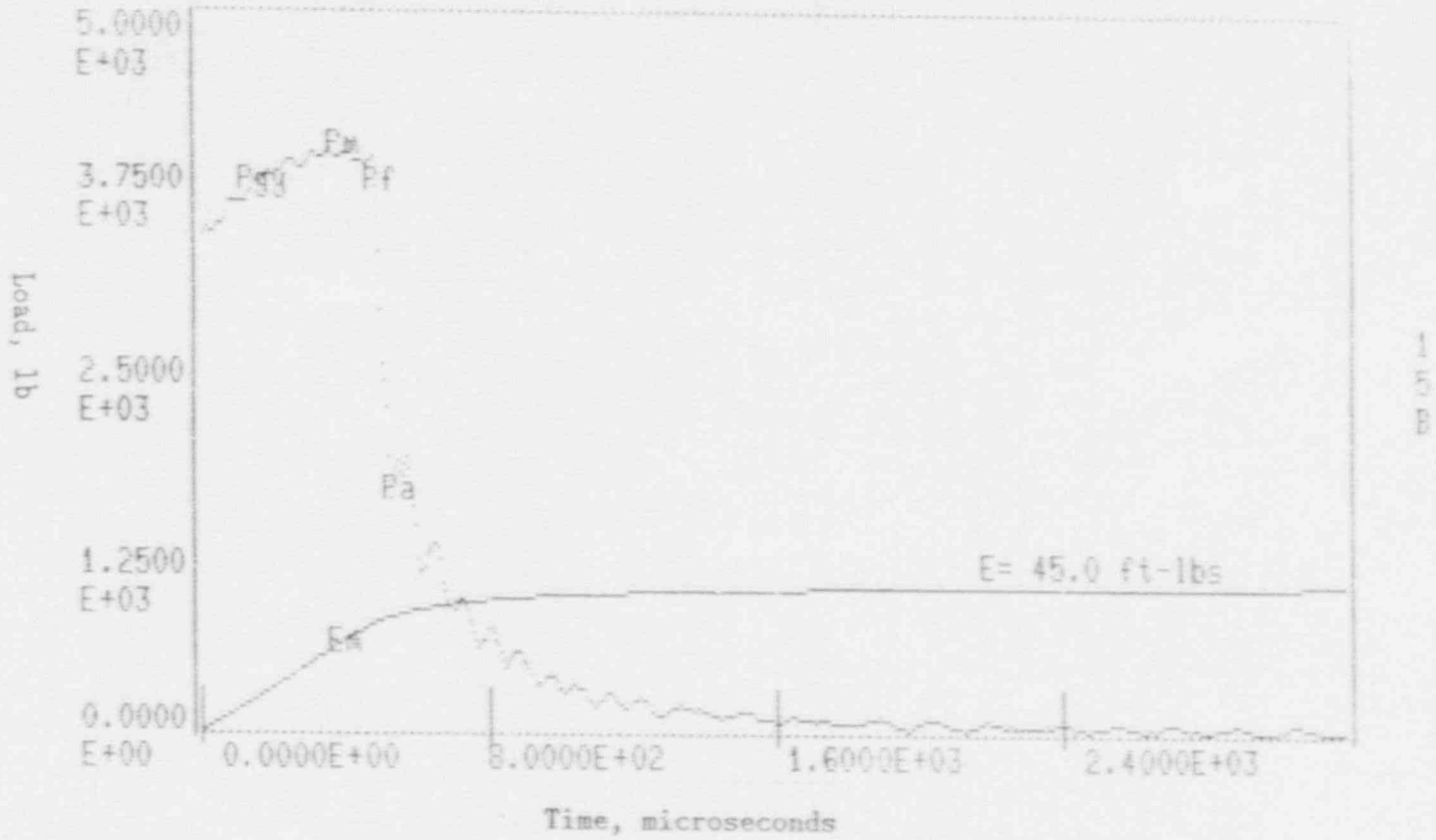

Figure A-6. Charpy impact test load-time record for Specimen 15B.

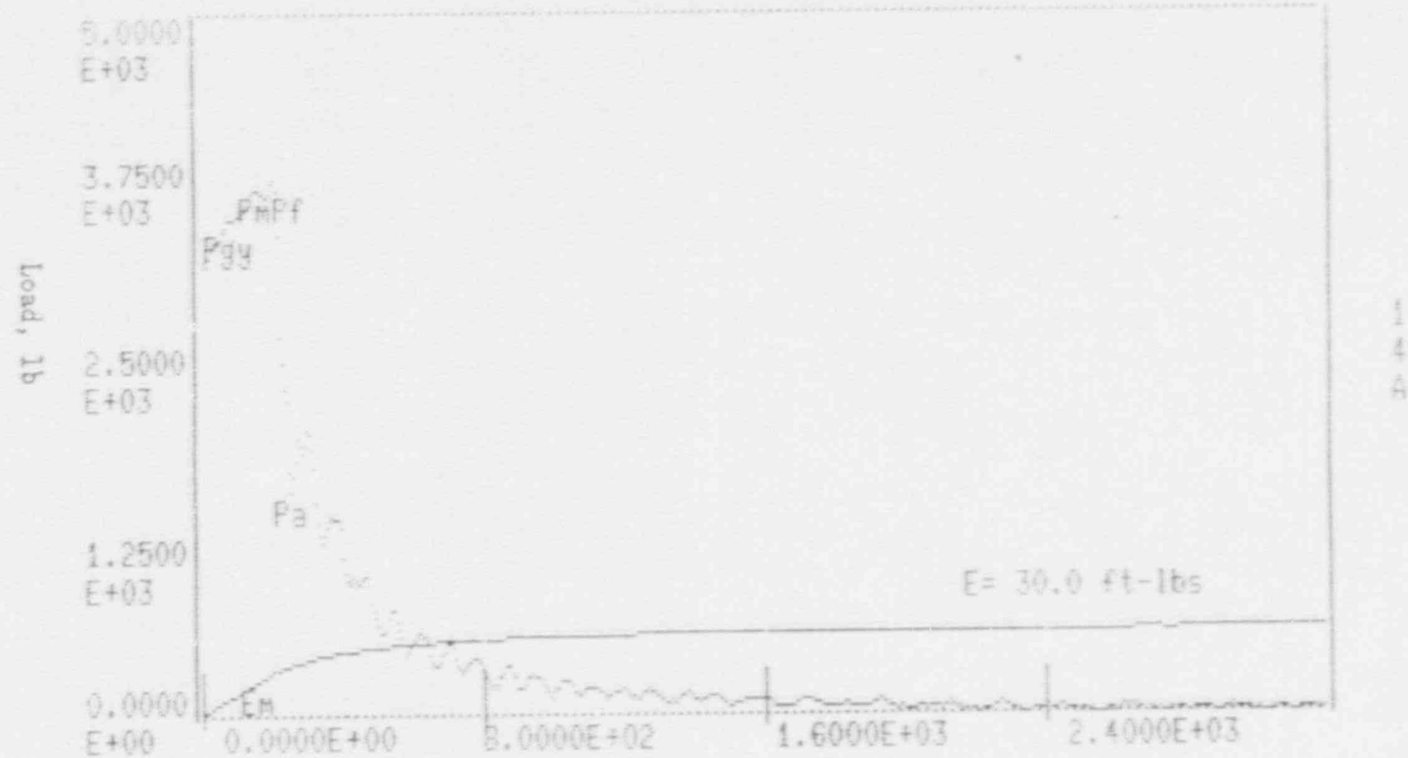

Figure A-7. Charpy impact test load-time record for Specimen 14A.

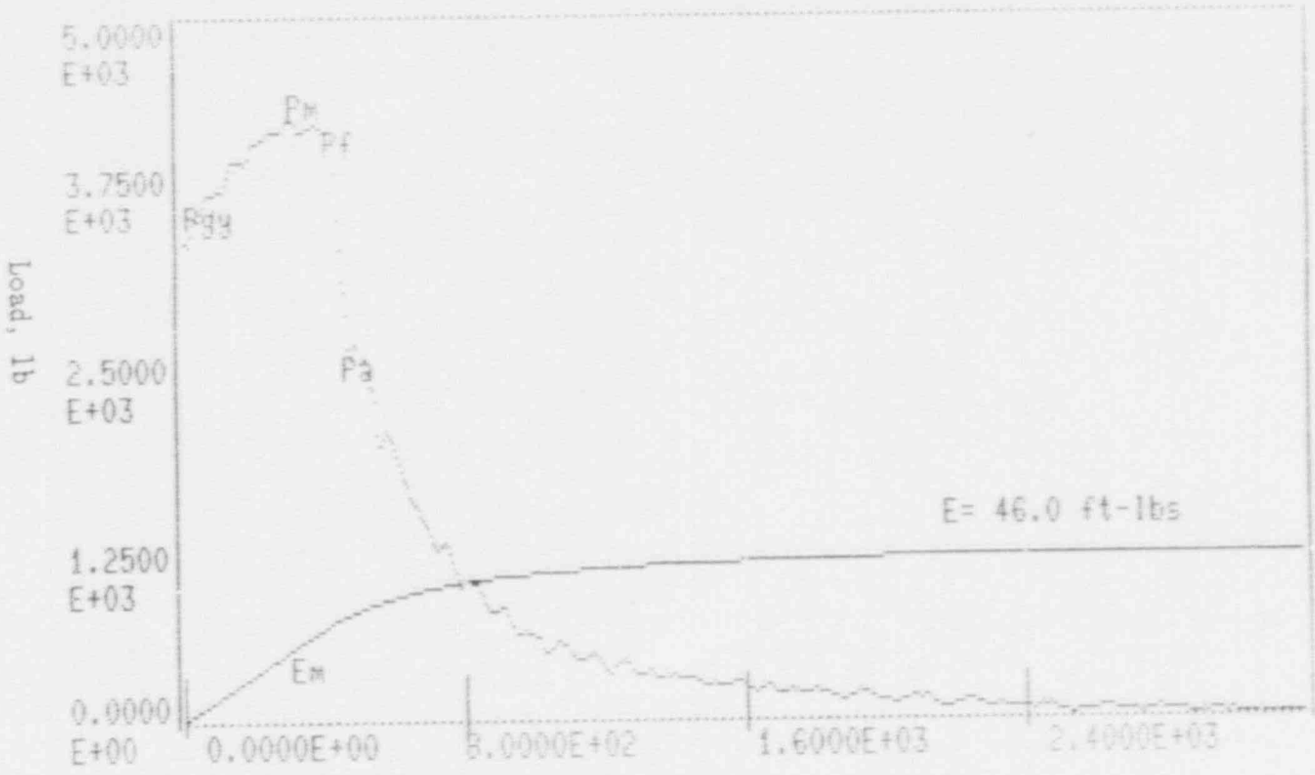

Figure A-8. Charpy impact test load-time record for Specimen 14E.

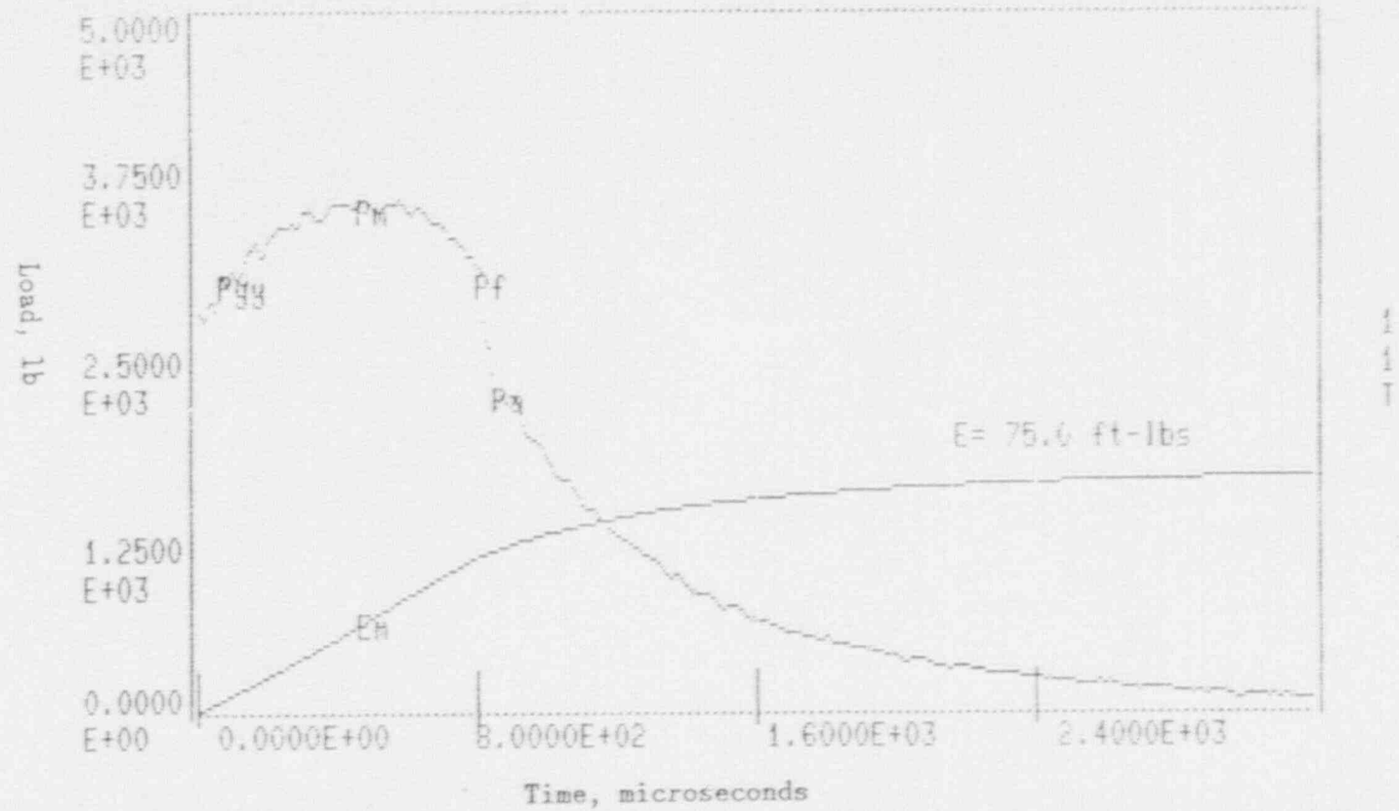

Figure A-9. Charpy impact test load-time record for Specimen 11T.

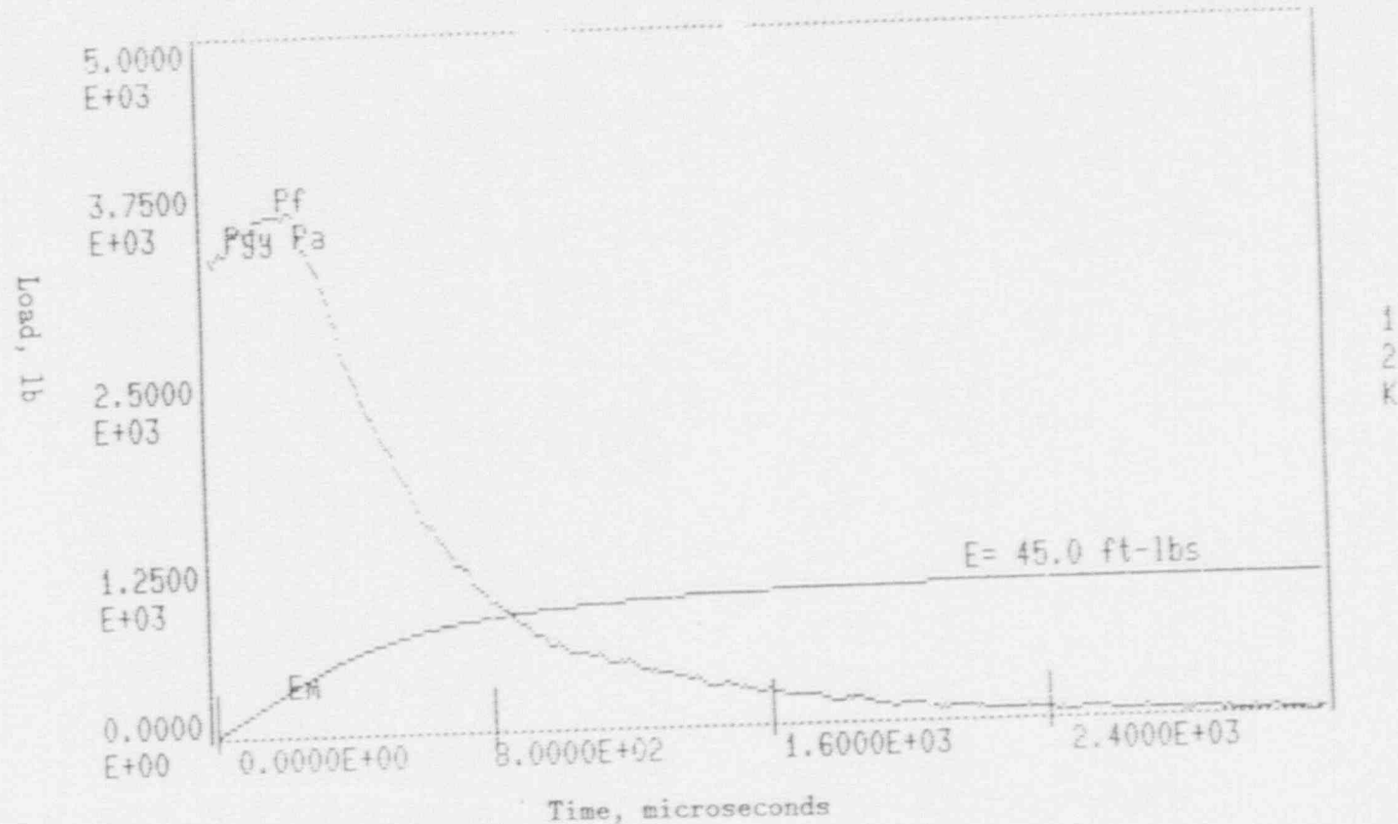

Figure A-10. Charpy impact test load-time record for Specimen 12K.

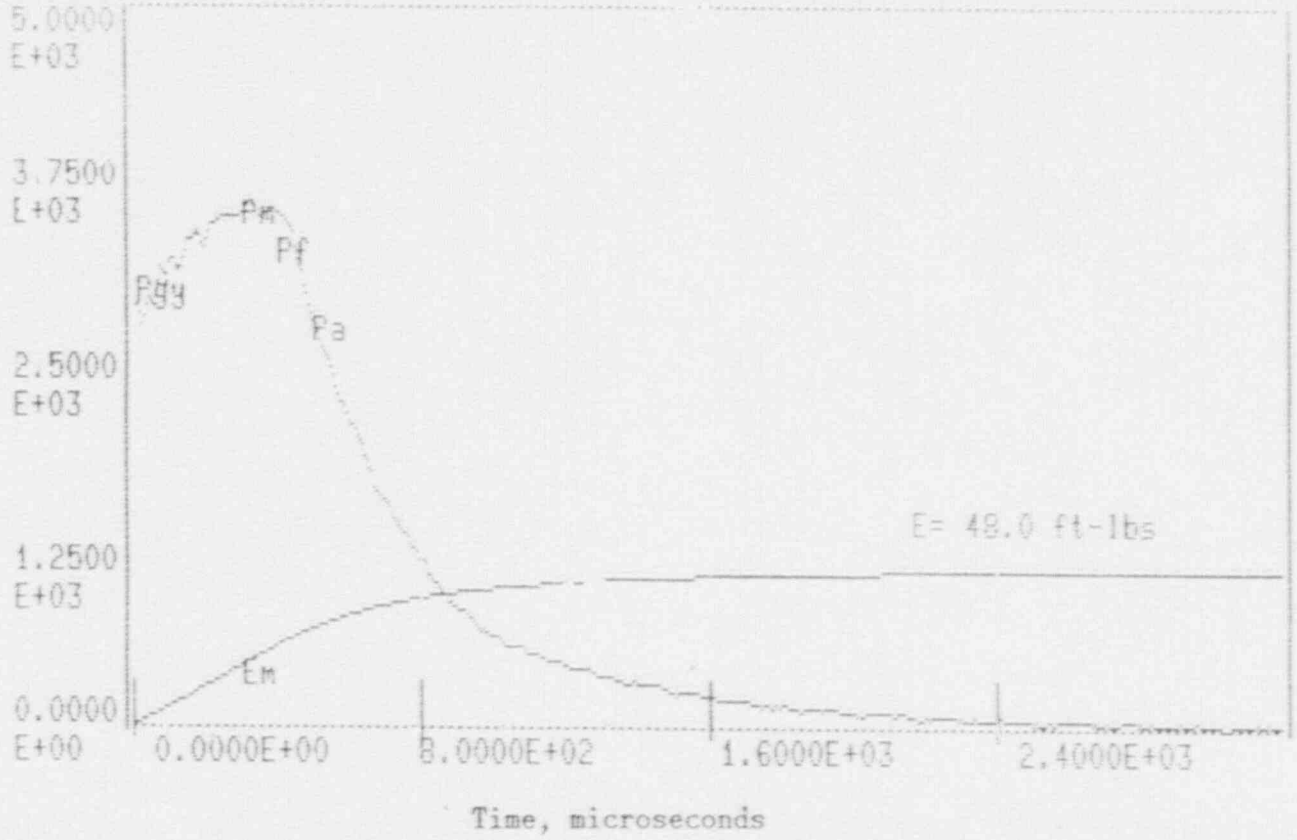

Figure A-11. Charpy impact test load-time record for Specimen 12L.

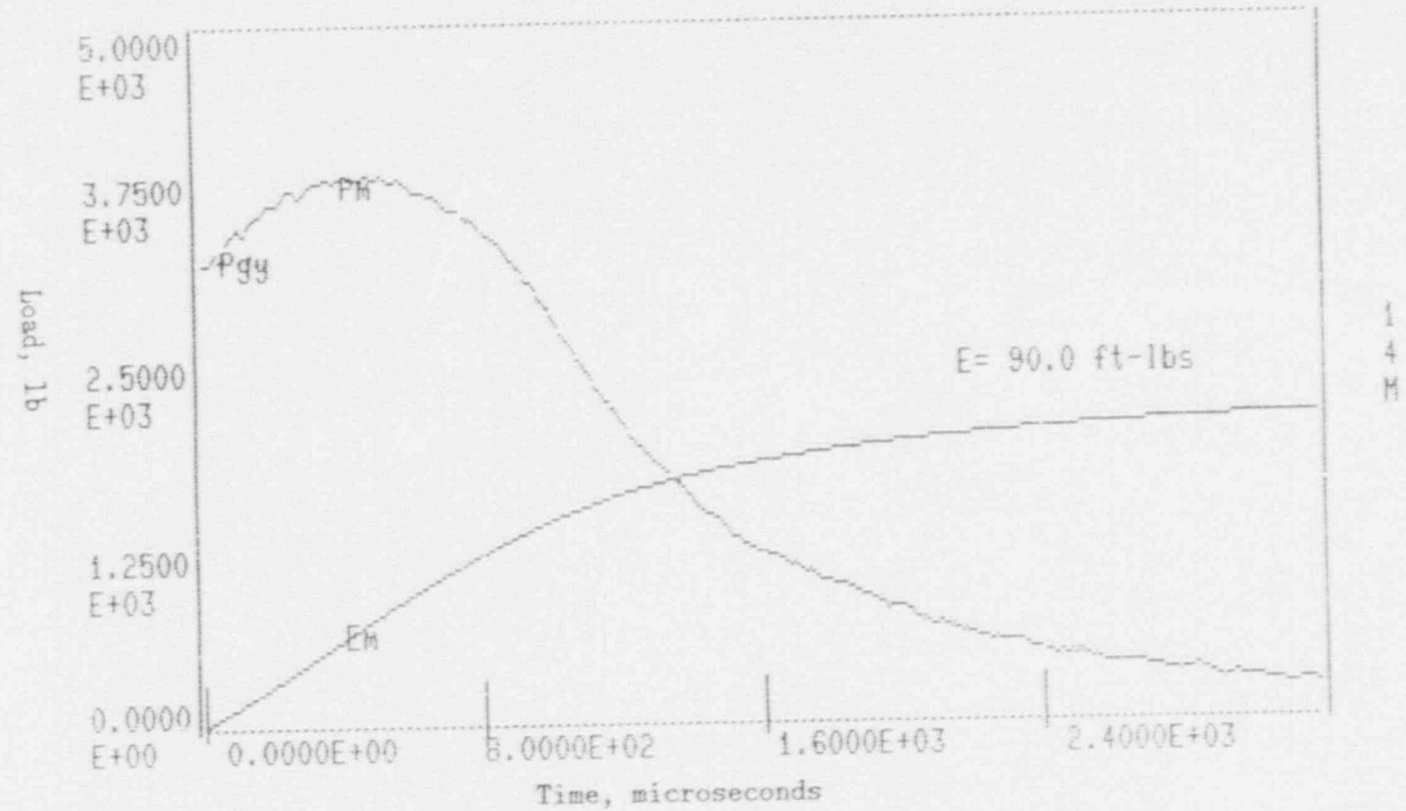

Figure A-12. Charpy impact test load-time record for Specimen 14M.

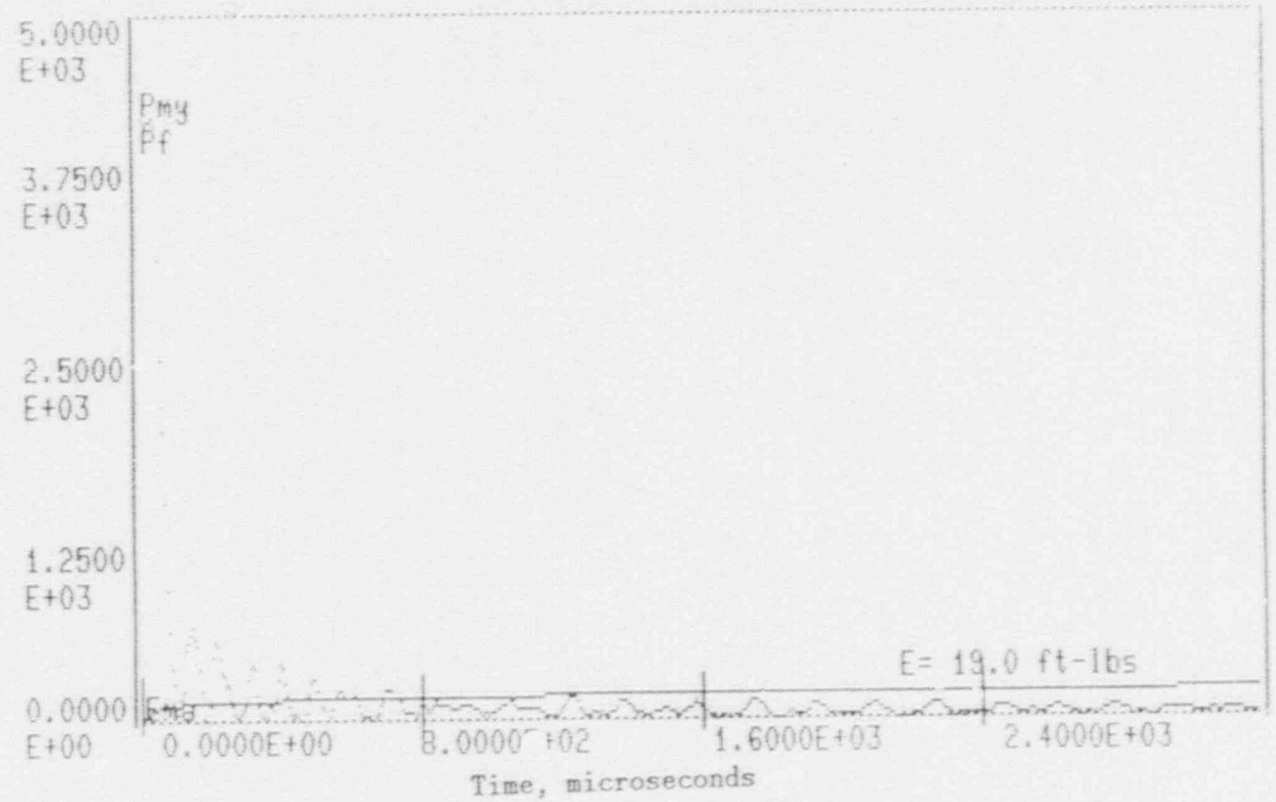

Figure A-13. Charpy impact test load-time record for Specimen 25U.

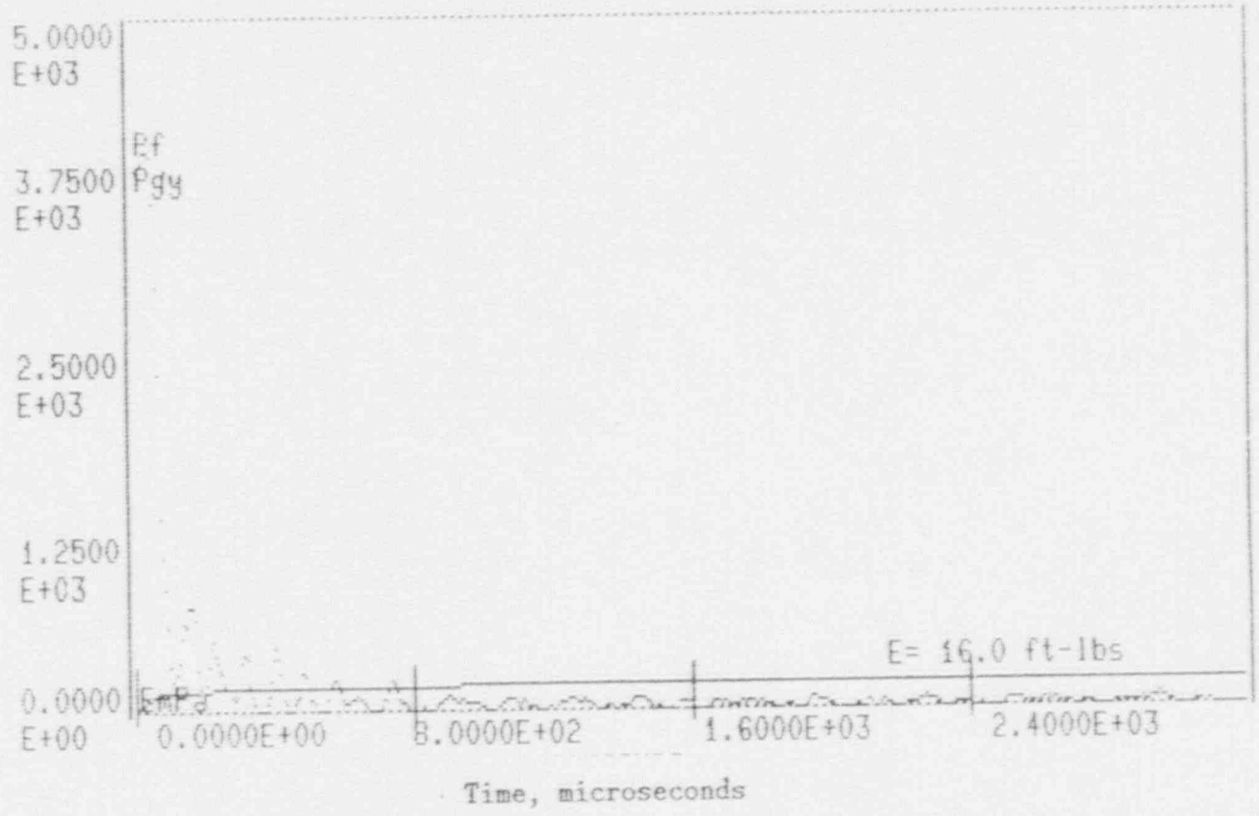

Figure A-14. Charpy impact test load-time record for Specimen 23K.

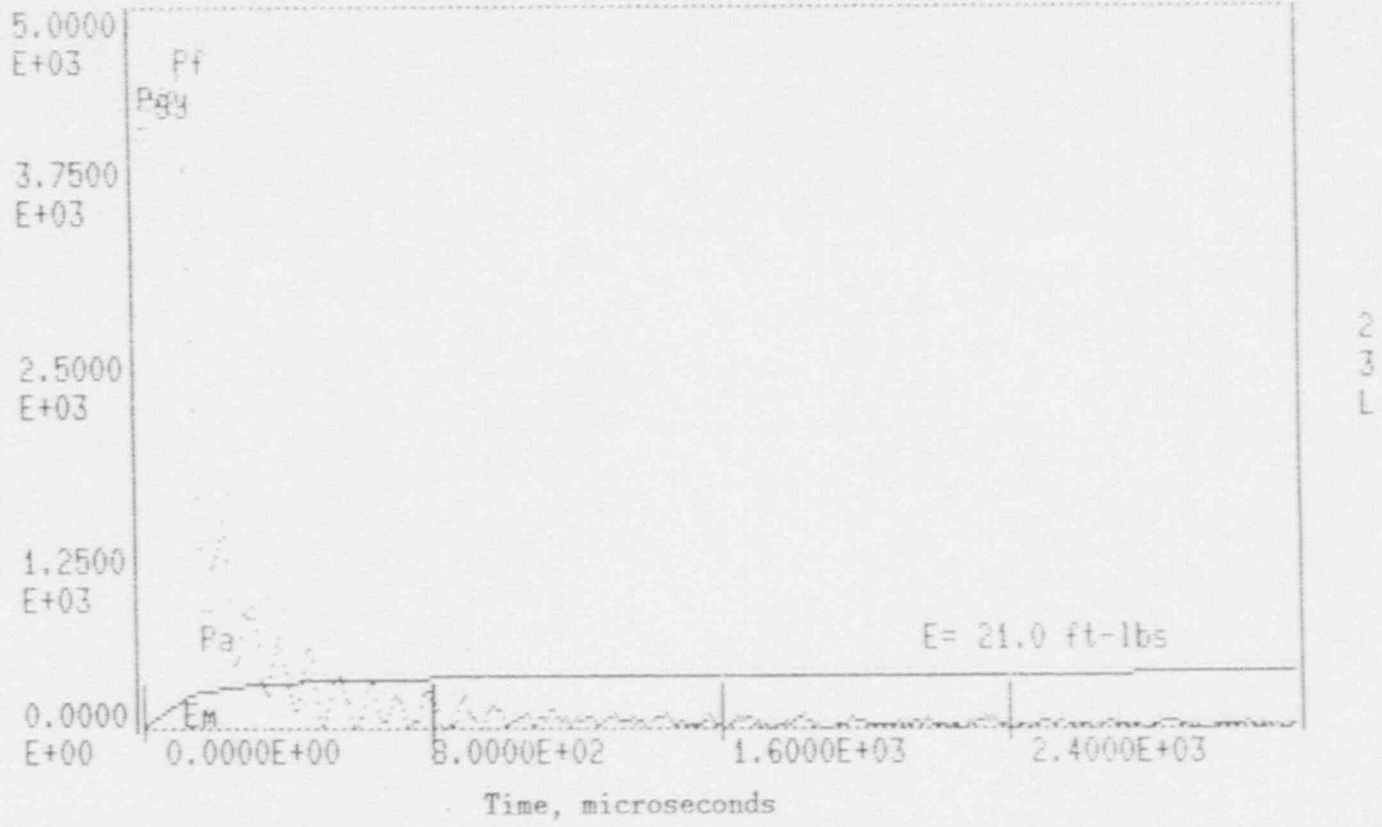

Figure A-15. Charpy impact test load-time record for Specimen 23L.

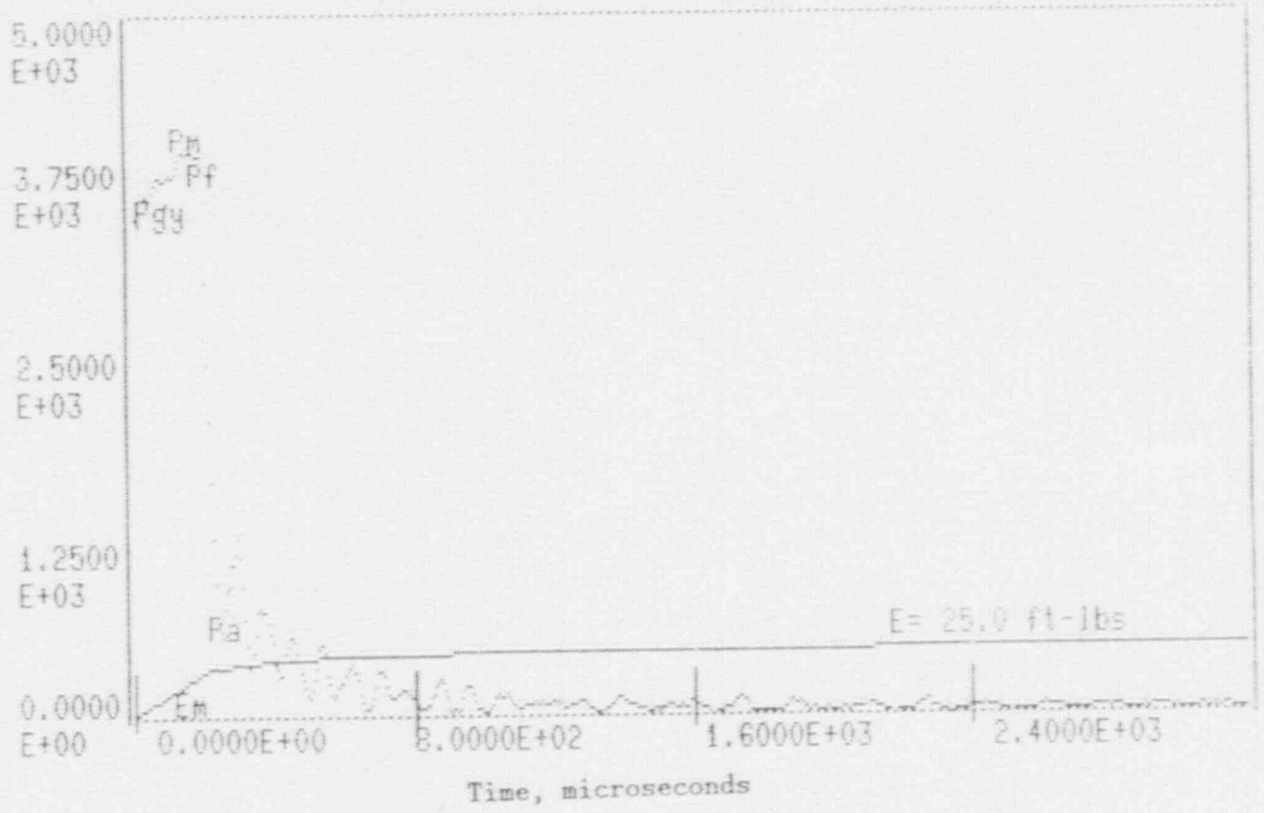

Figure A-16. Charpy impact test load-time record for Specimen 22B.

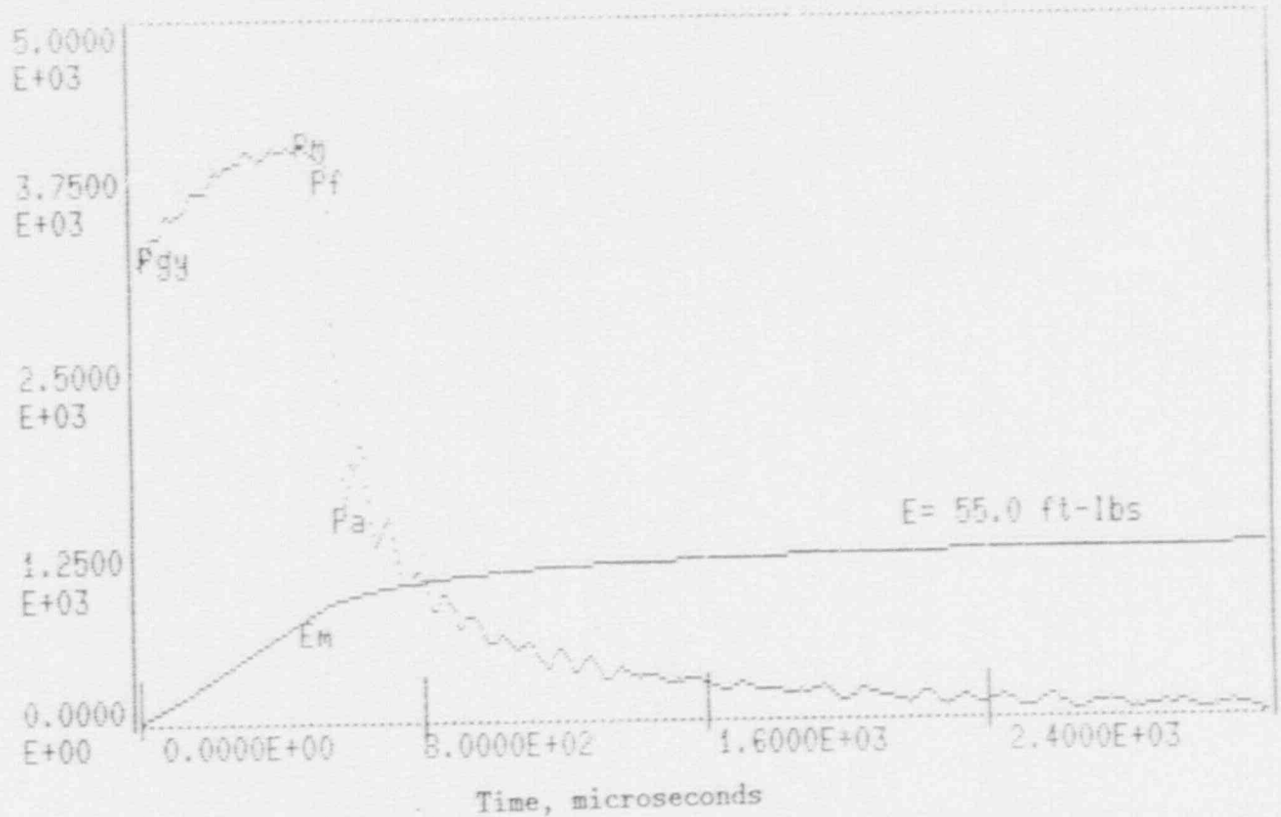

Figure A-17. Charpy impact test load-time record for Specimen 25J.

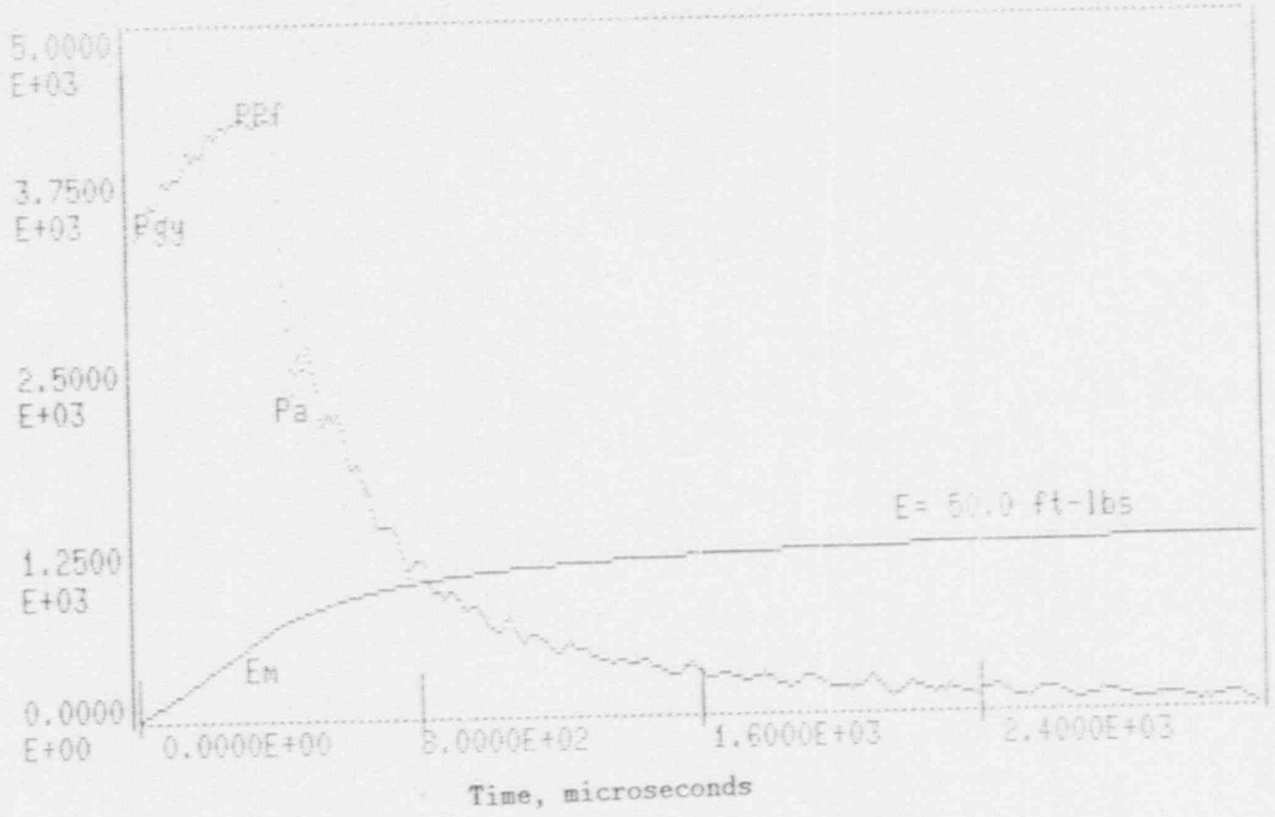

Figure A-18. Charpy impact test load-time record for Specimen 25L.

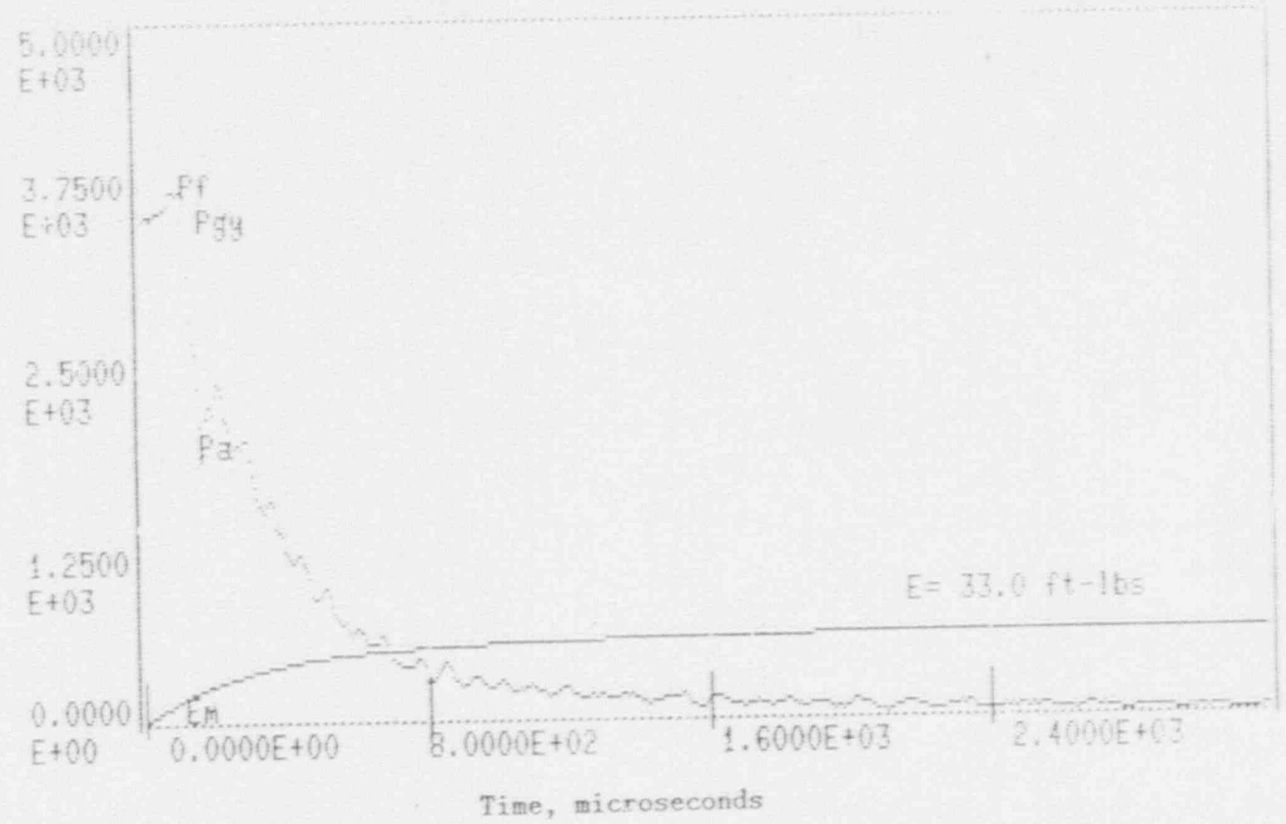

Figure A-19. Charpy impact test load-time record for Specimen 247.

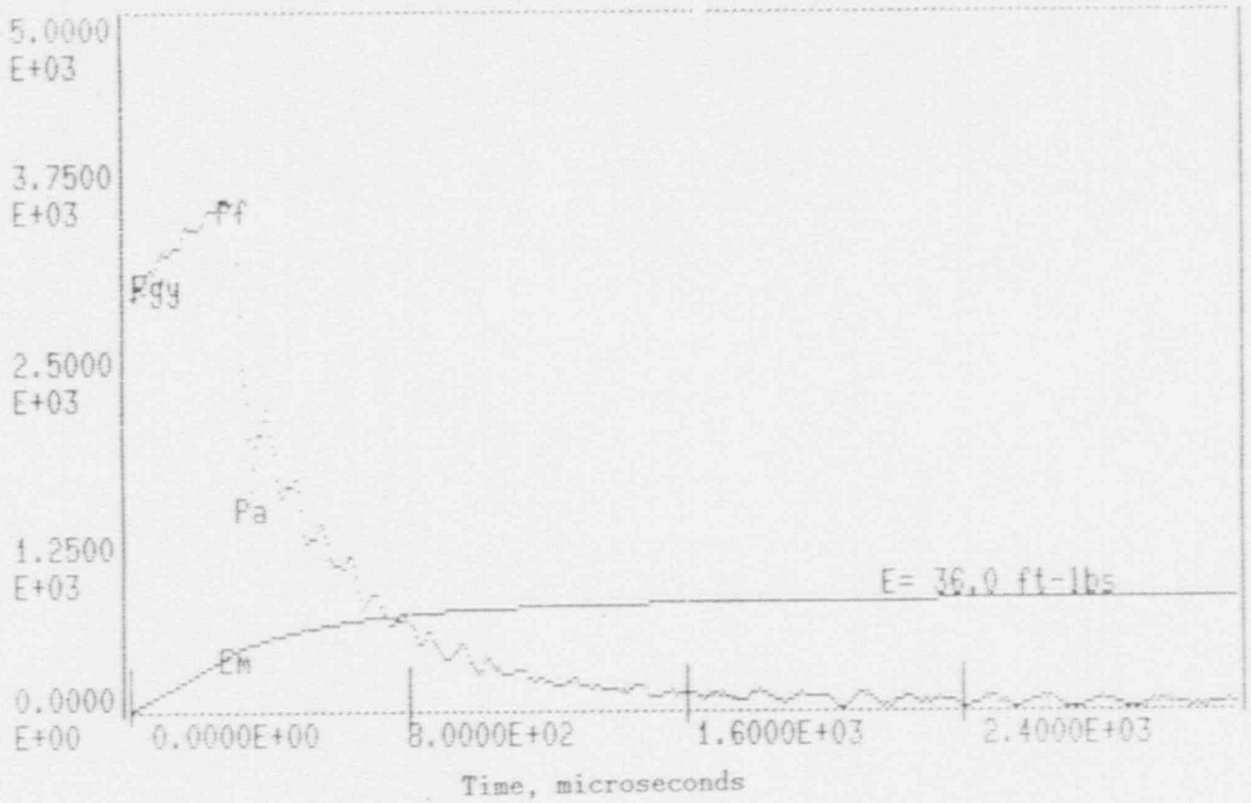

Figure A-20. Charpy impact test load-time record for Specimen 223.

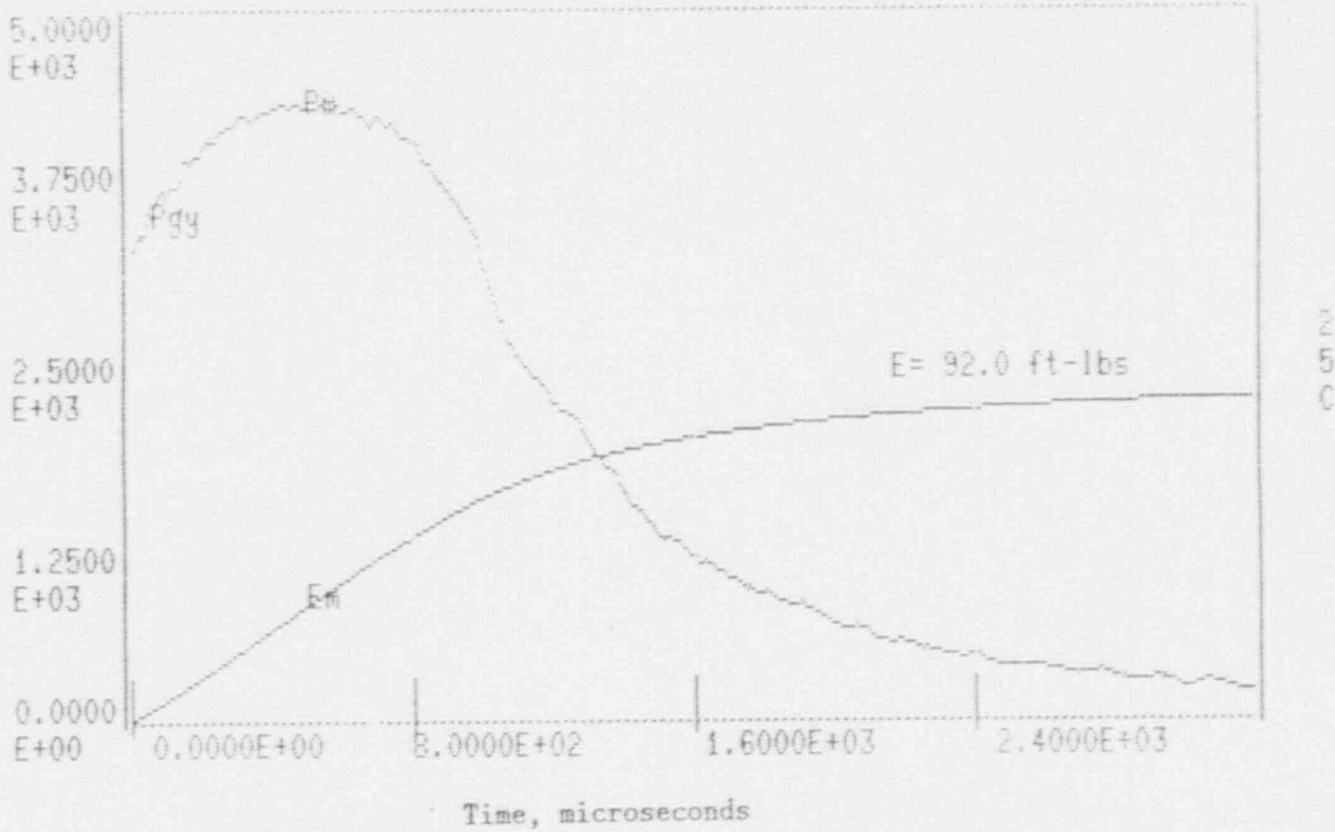

Figure A-21. Charpy impact test load-time record for Specimen 25C.

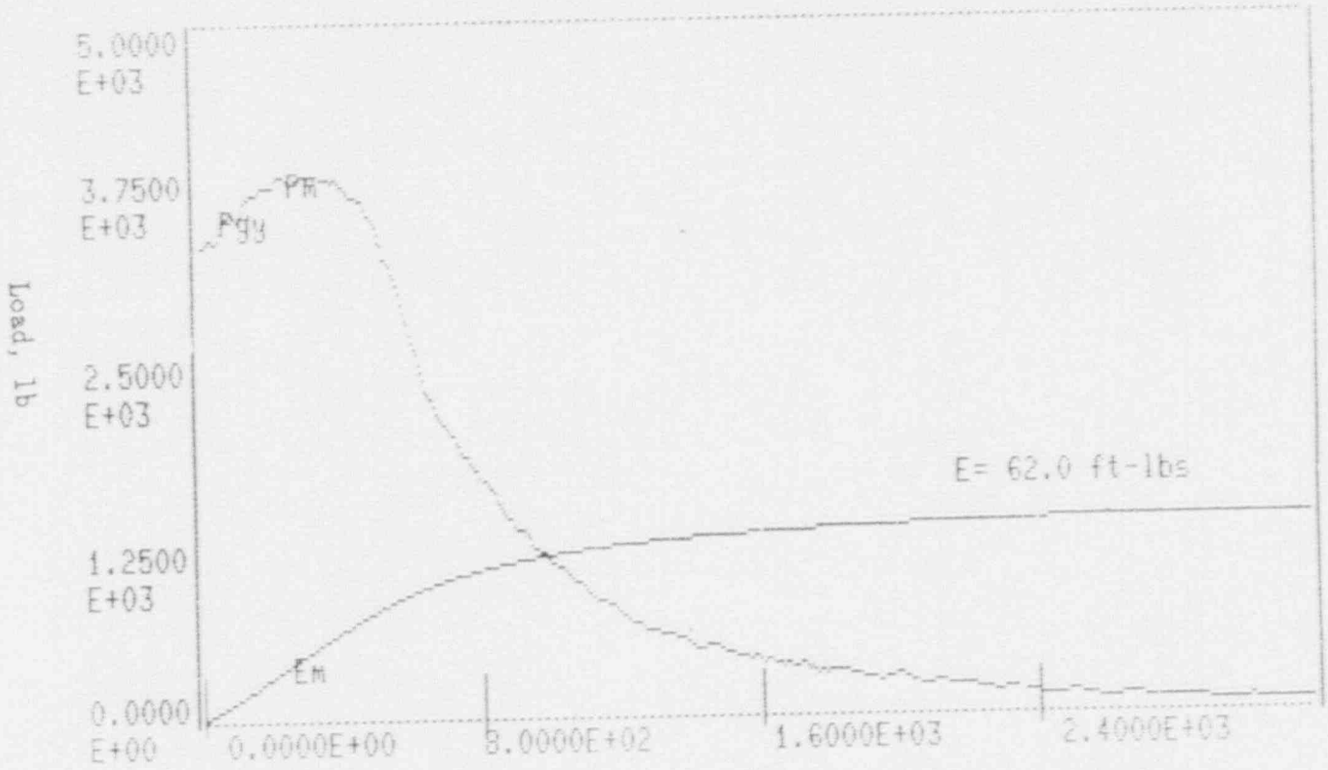

Figure A-22. Charpy impact test load-time record for Specimen 245.

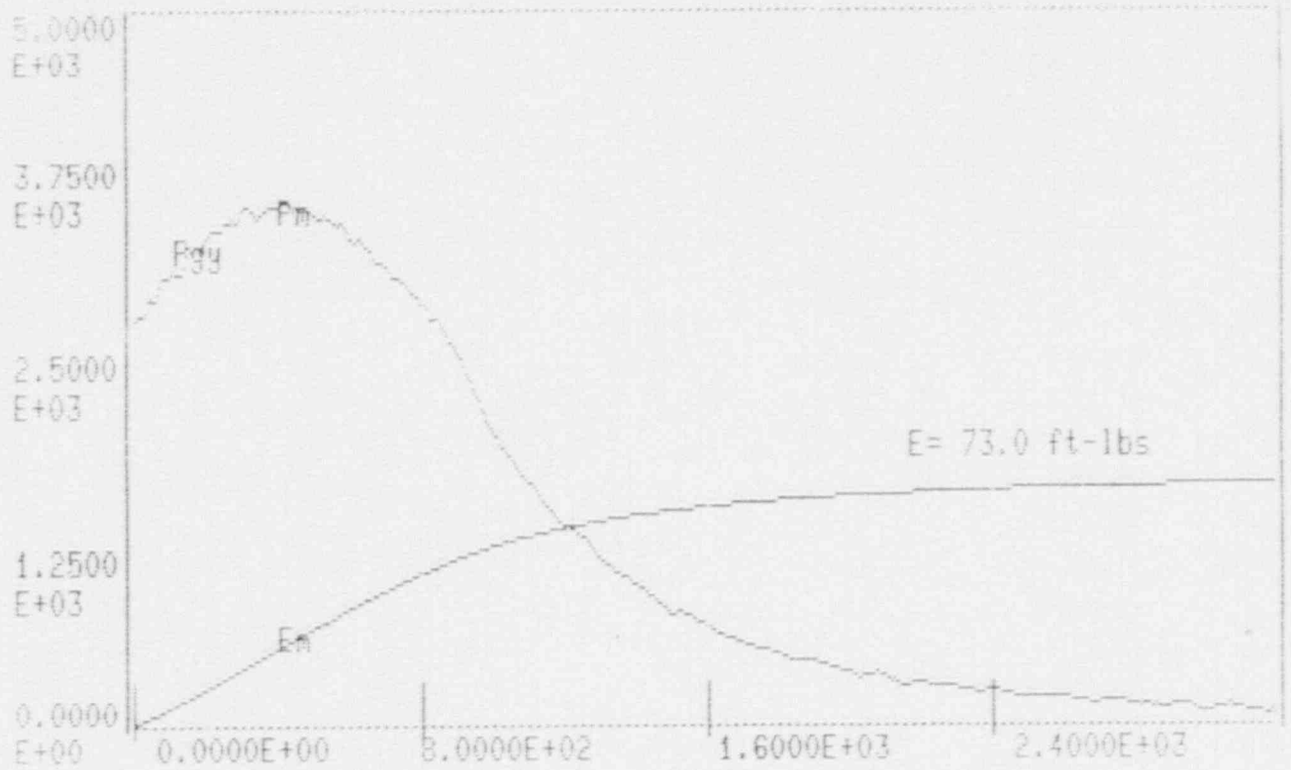

Figure A-23. Charpy impact test load-time record for Specimen 23M.

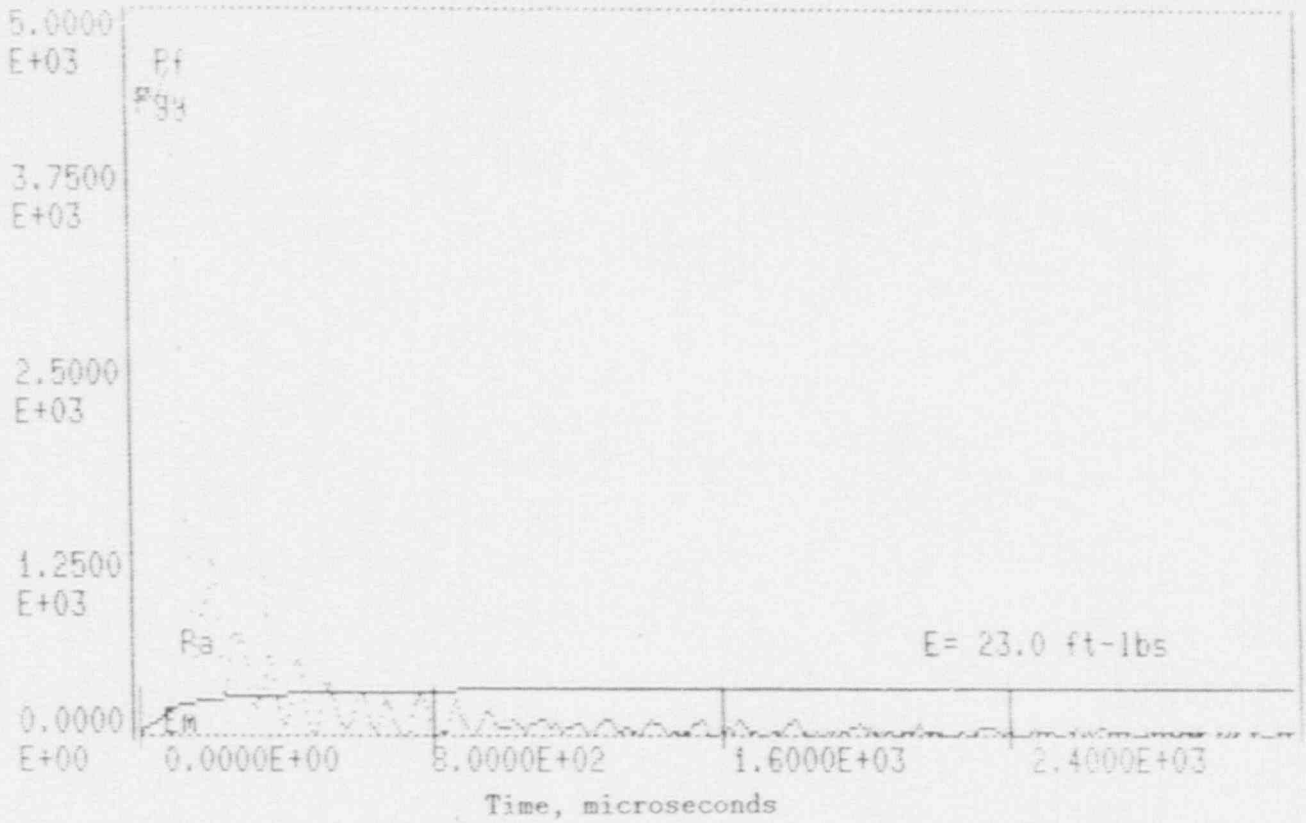

Figure A-24. Charpy impact test load-time record for Specimen 363.

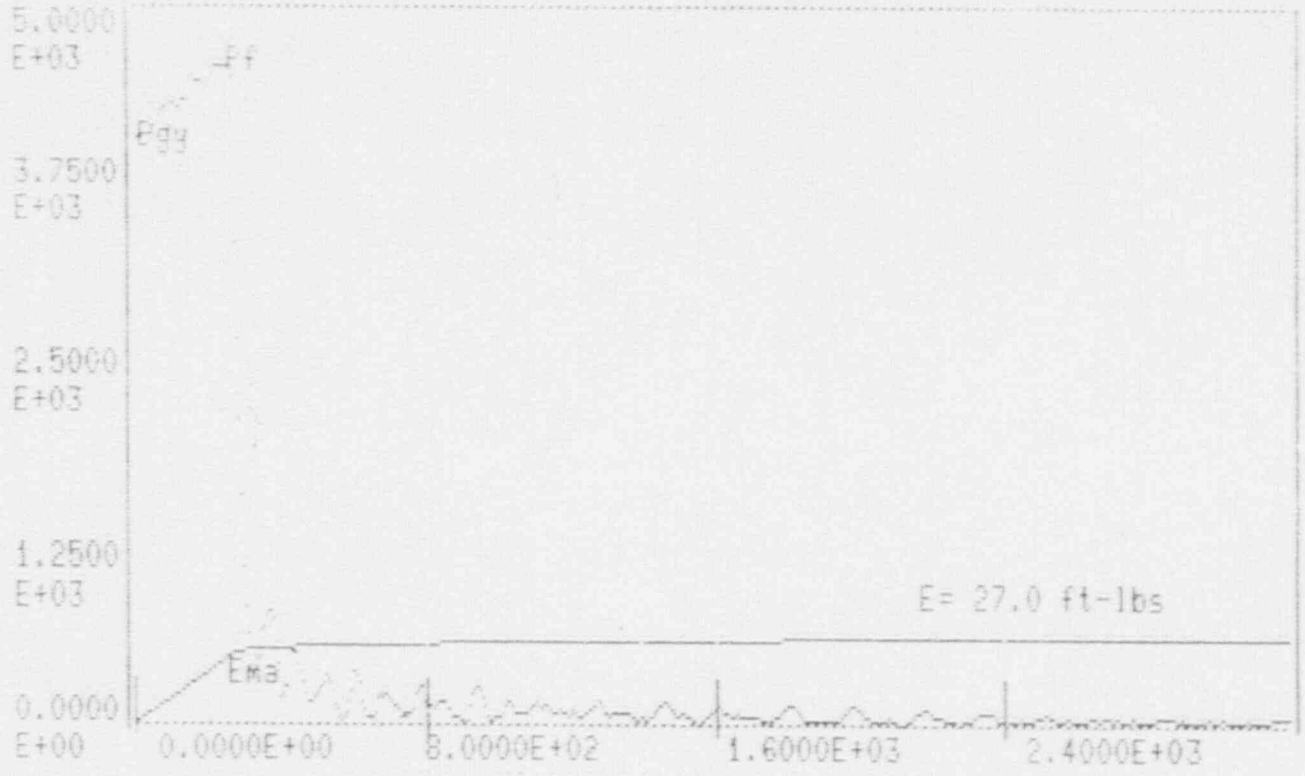

Figure A-25. Charpy impact test load-time record for Specimen 33L.

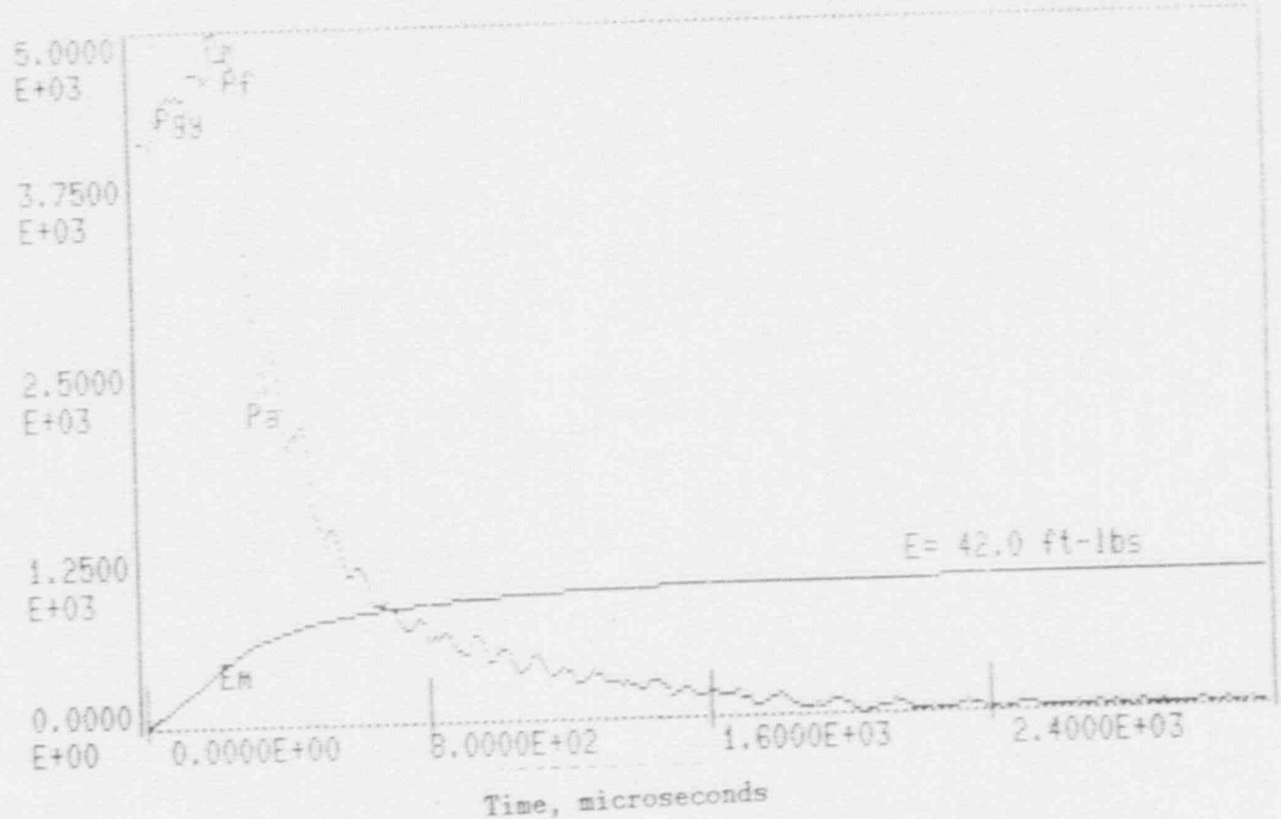

Figure A-26. Charpy impact test load-time record for Specimen 37B.

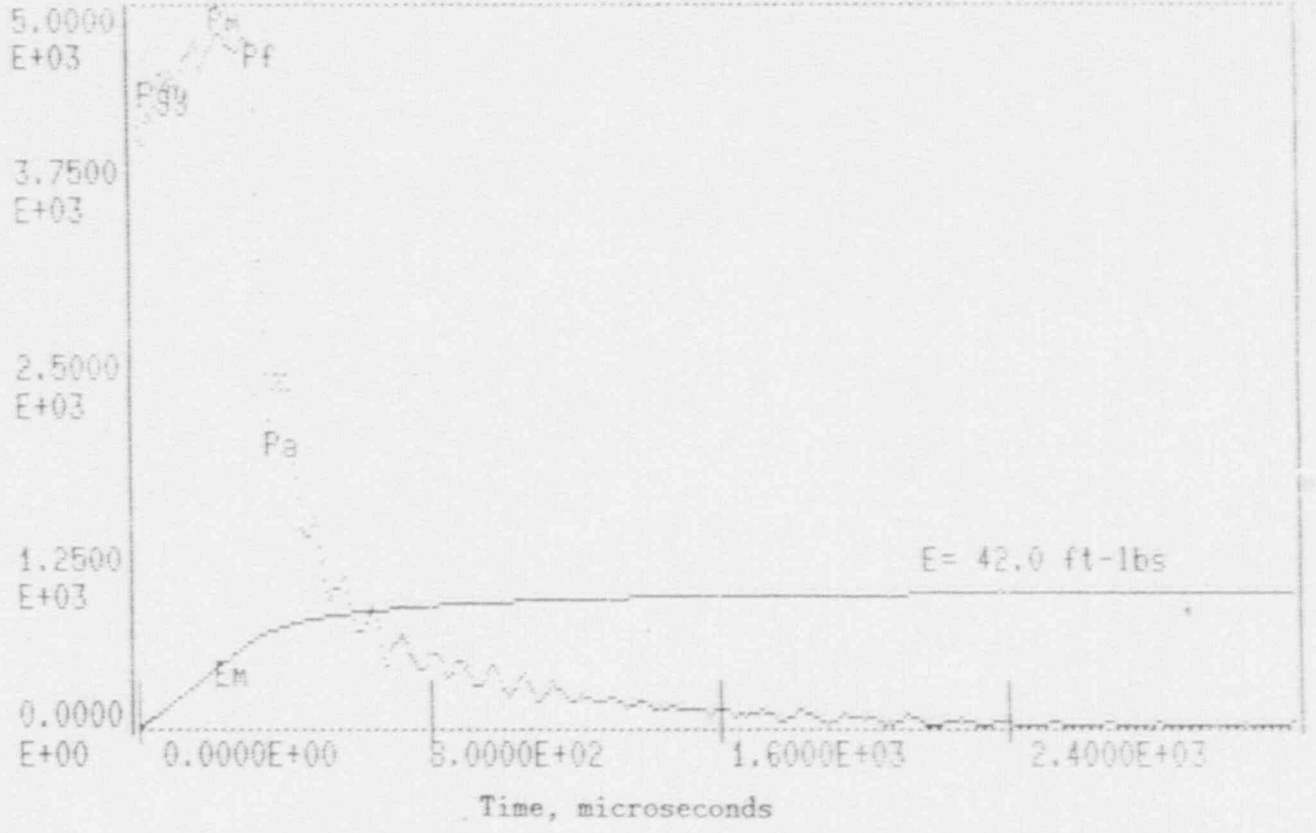

Figure A-27. Charpy impact test load-time record for Specimen 367.

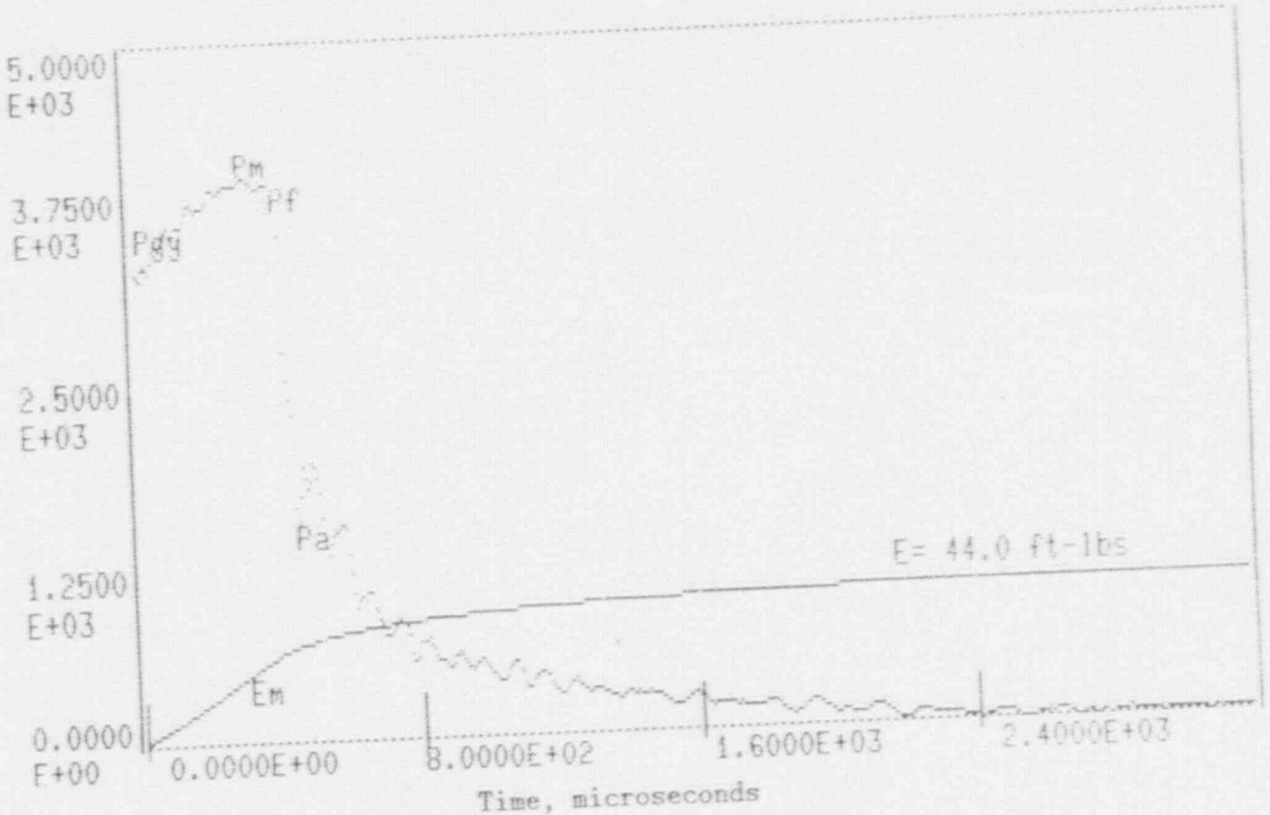

Figure A-28. Charpy impact test load-time record for Specimen 331.

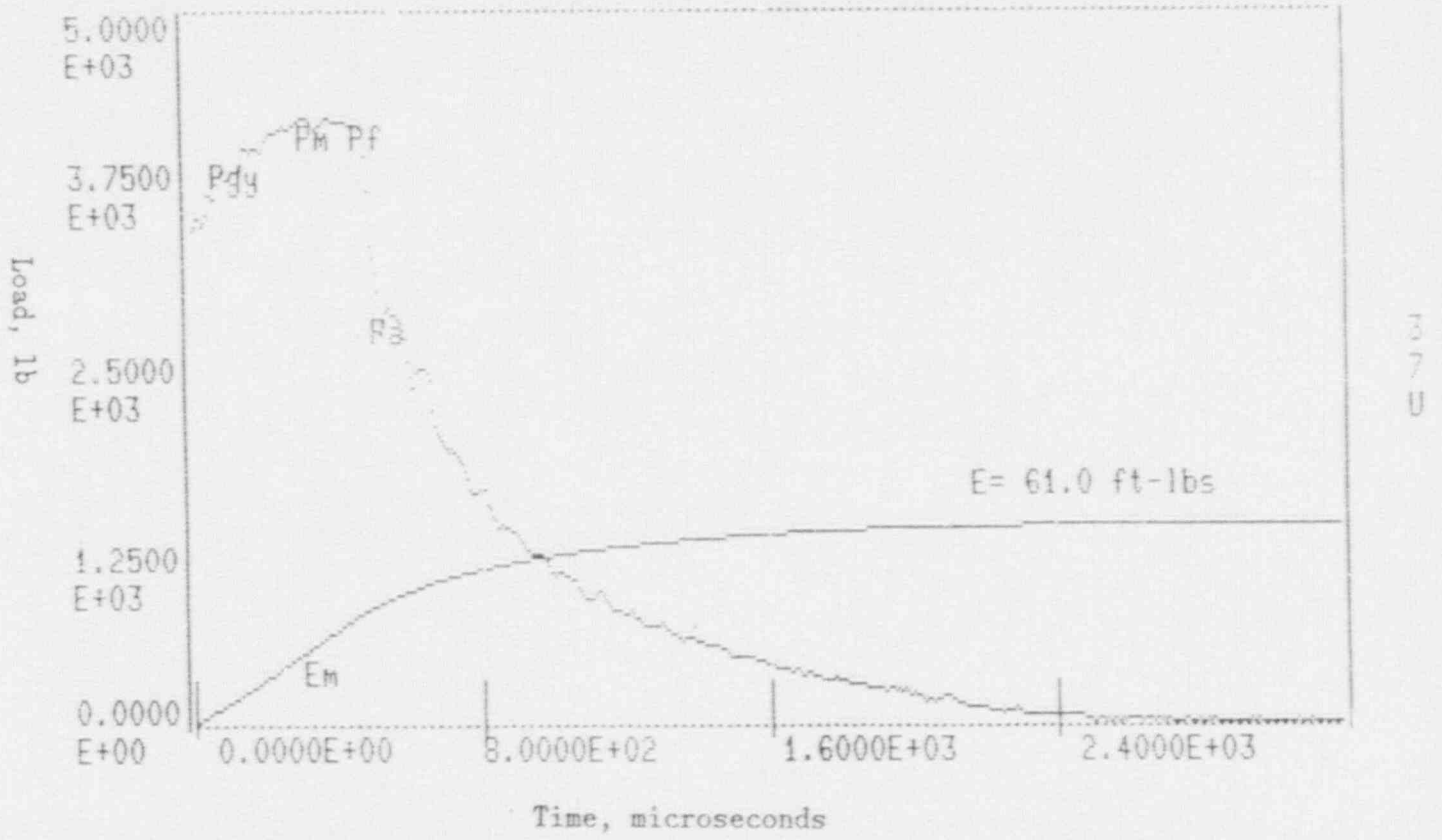

Figure A-29. Charpy impact test load-time record for Specimen 37U.

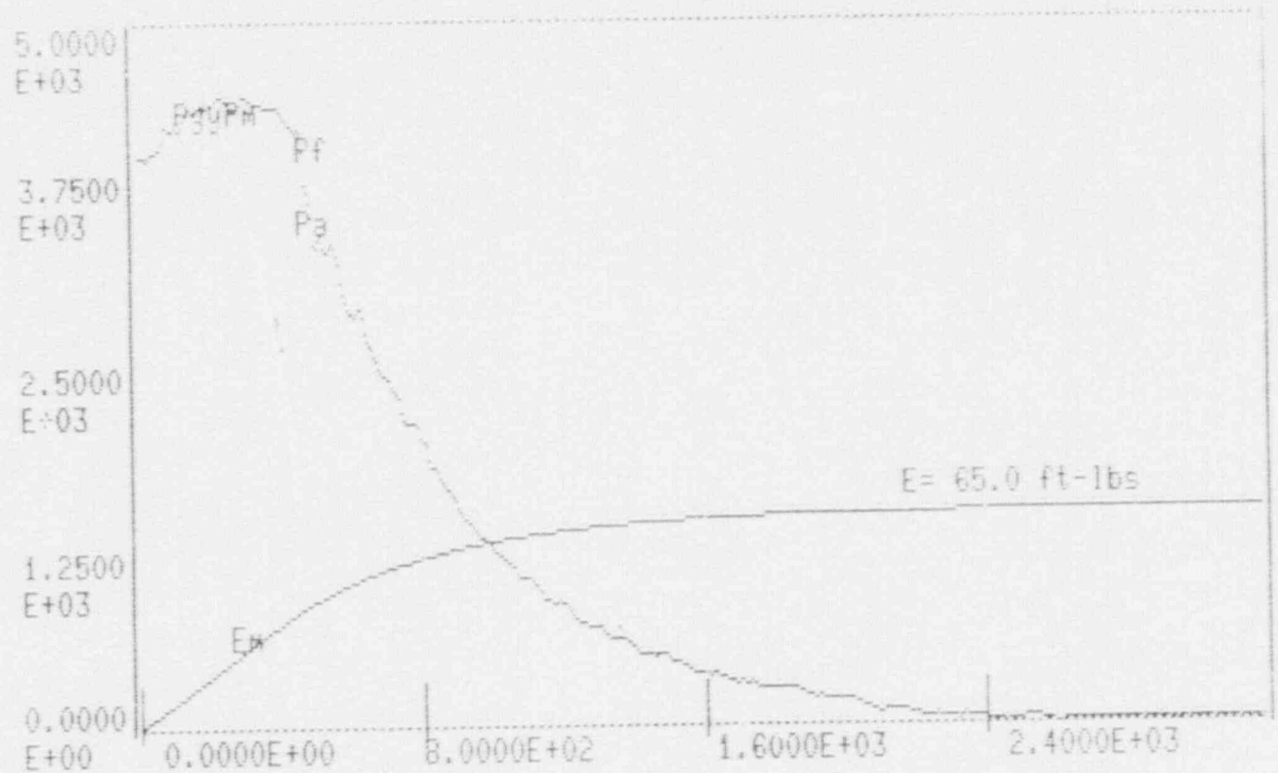

Figure A-30. Charpy impact test load-time record for Specimen 371.

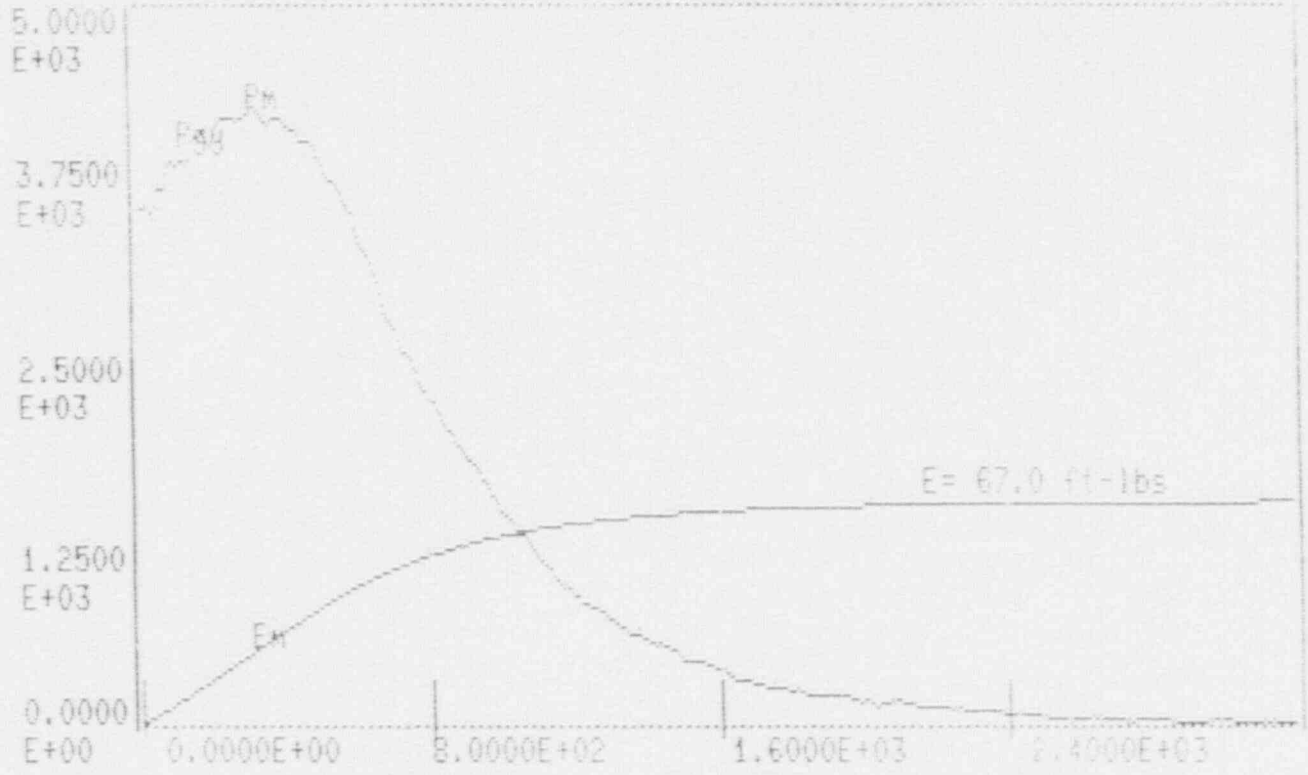

Figure A-31. Charpy impact test load-time record for Specimen 365.

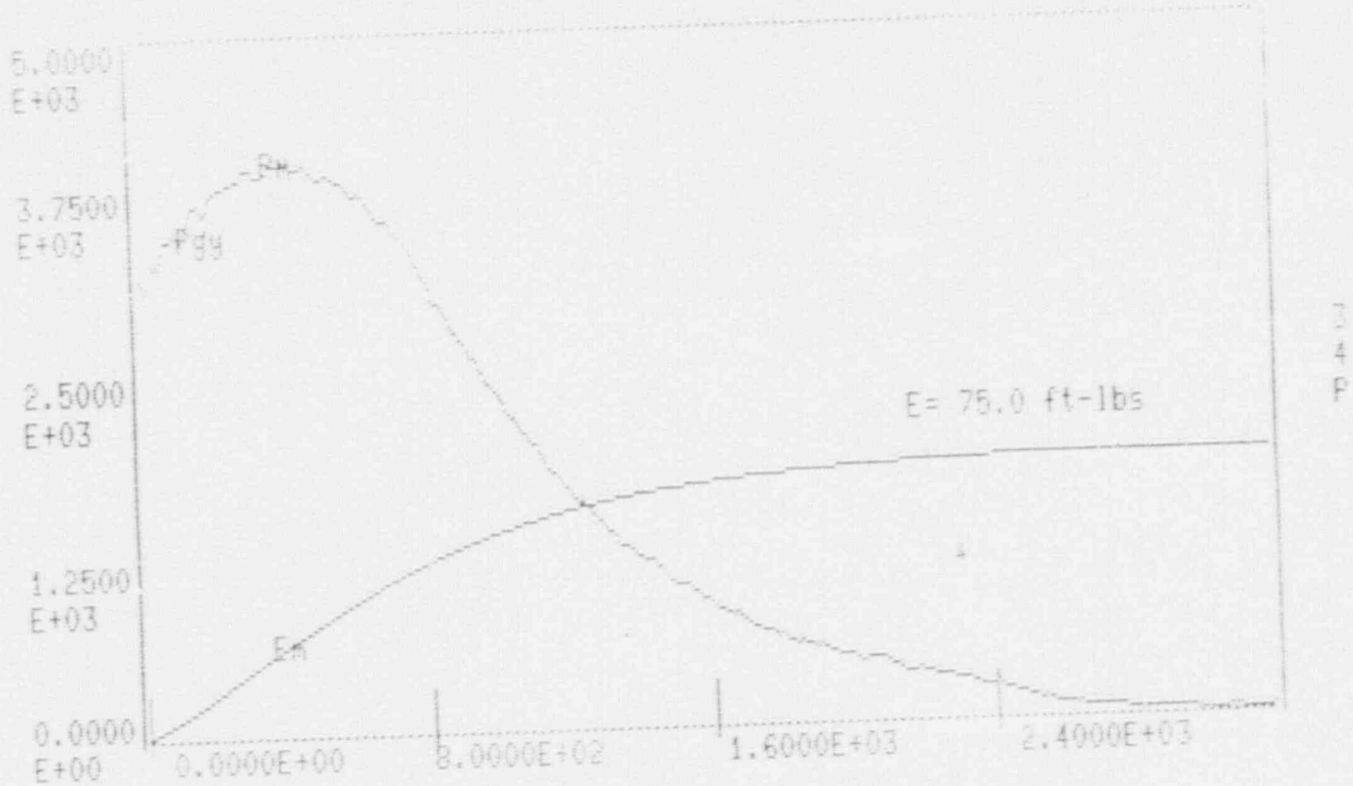

Figure A-32. Charpy impact test load-time record for Specimen 34P.

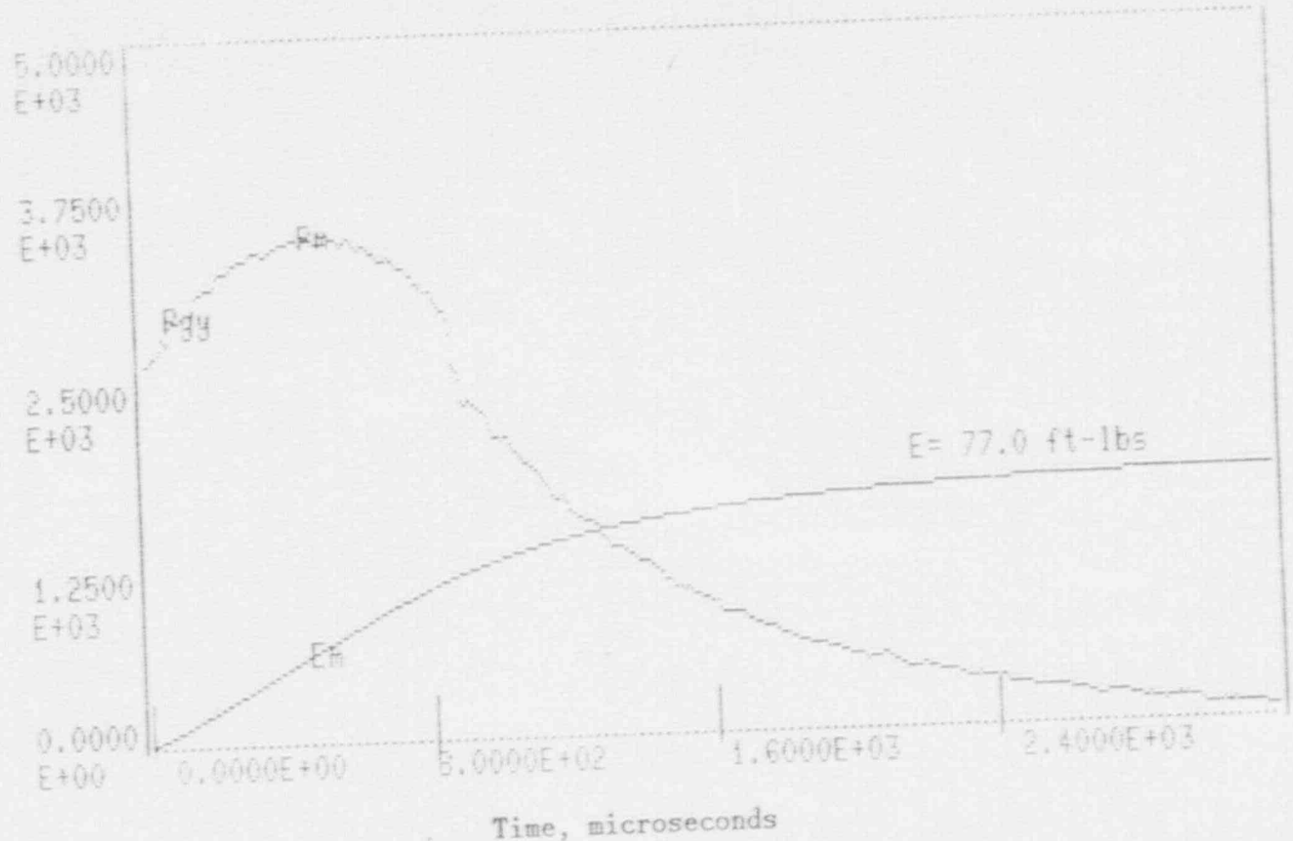

Figure A-33. Charpy impact test load-time record for Specimen 33D.

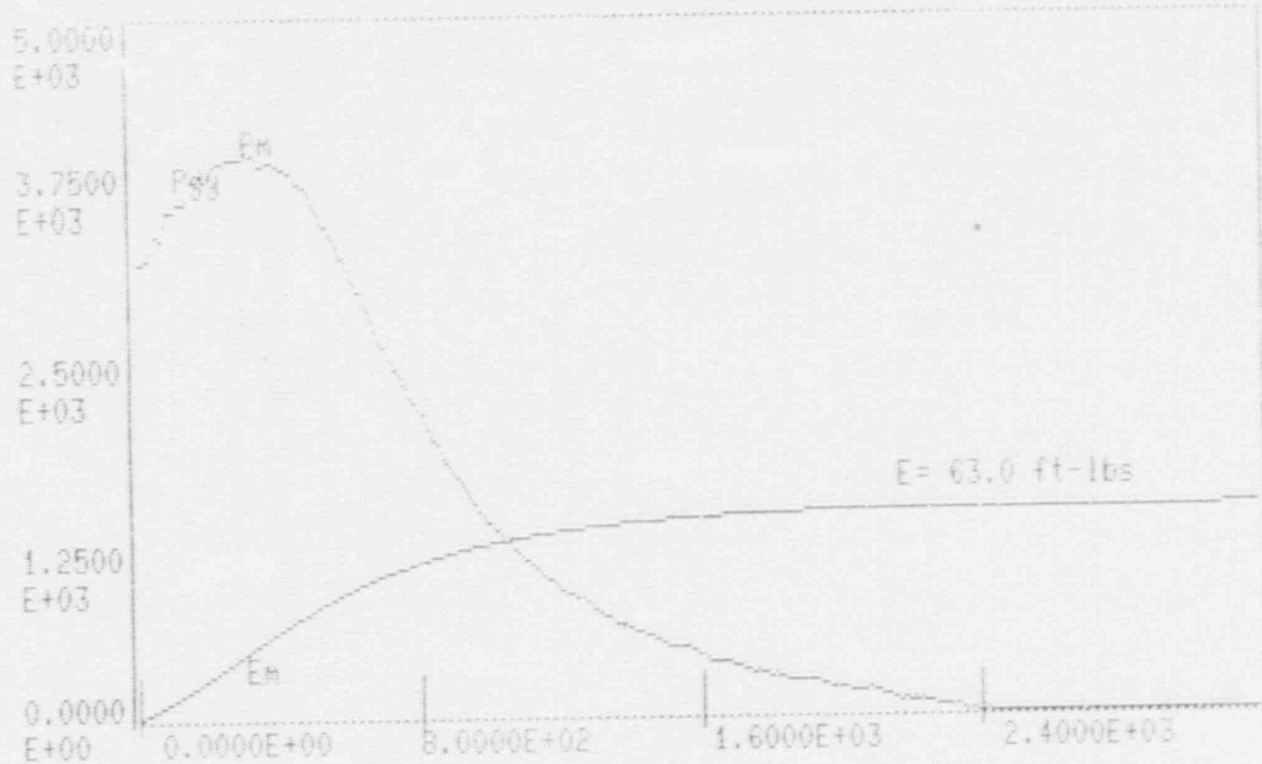

Figure A-34. Charpy impact test load-time record for Specimen 377.

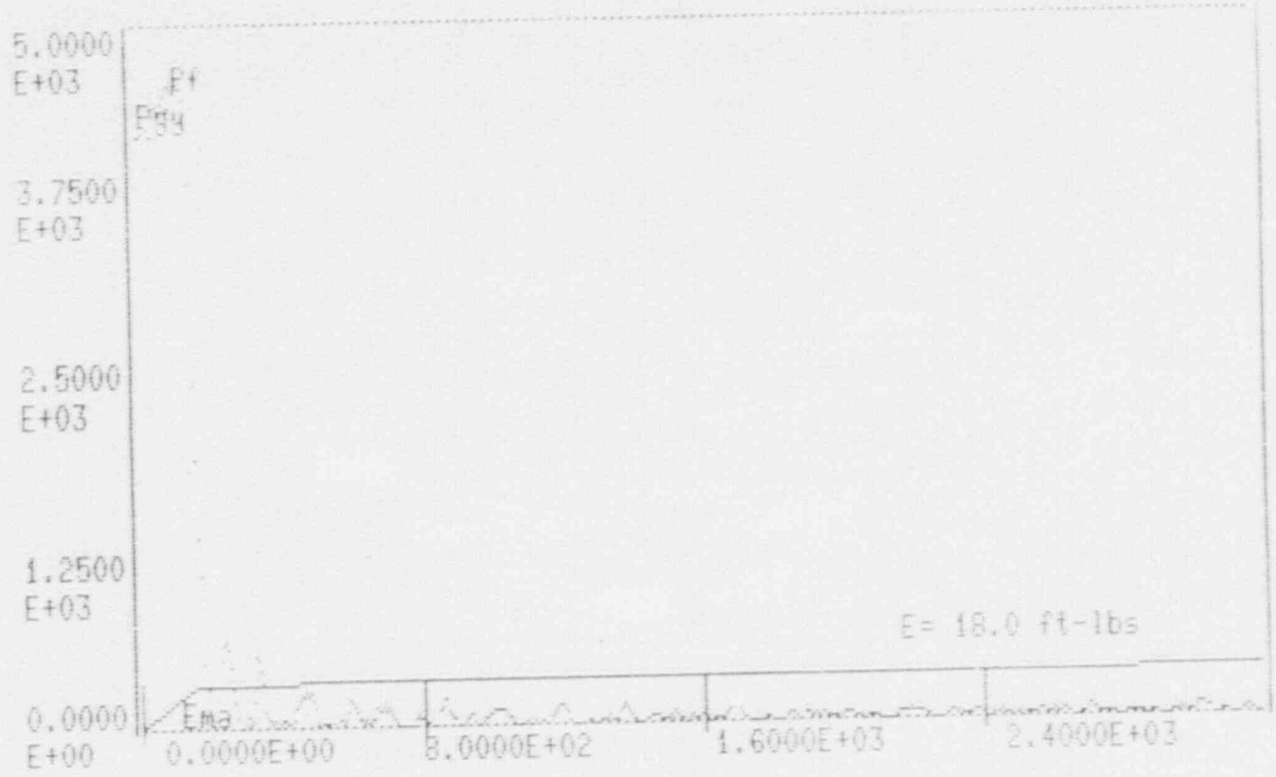

Figure A-35. Charpy impact test load-time record for Specimen 42L.

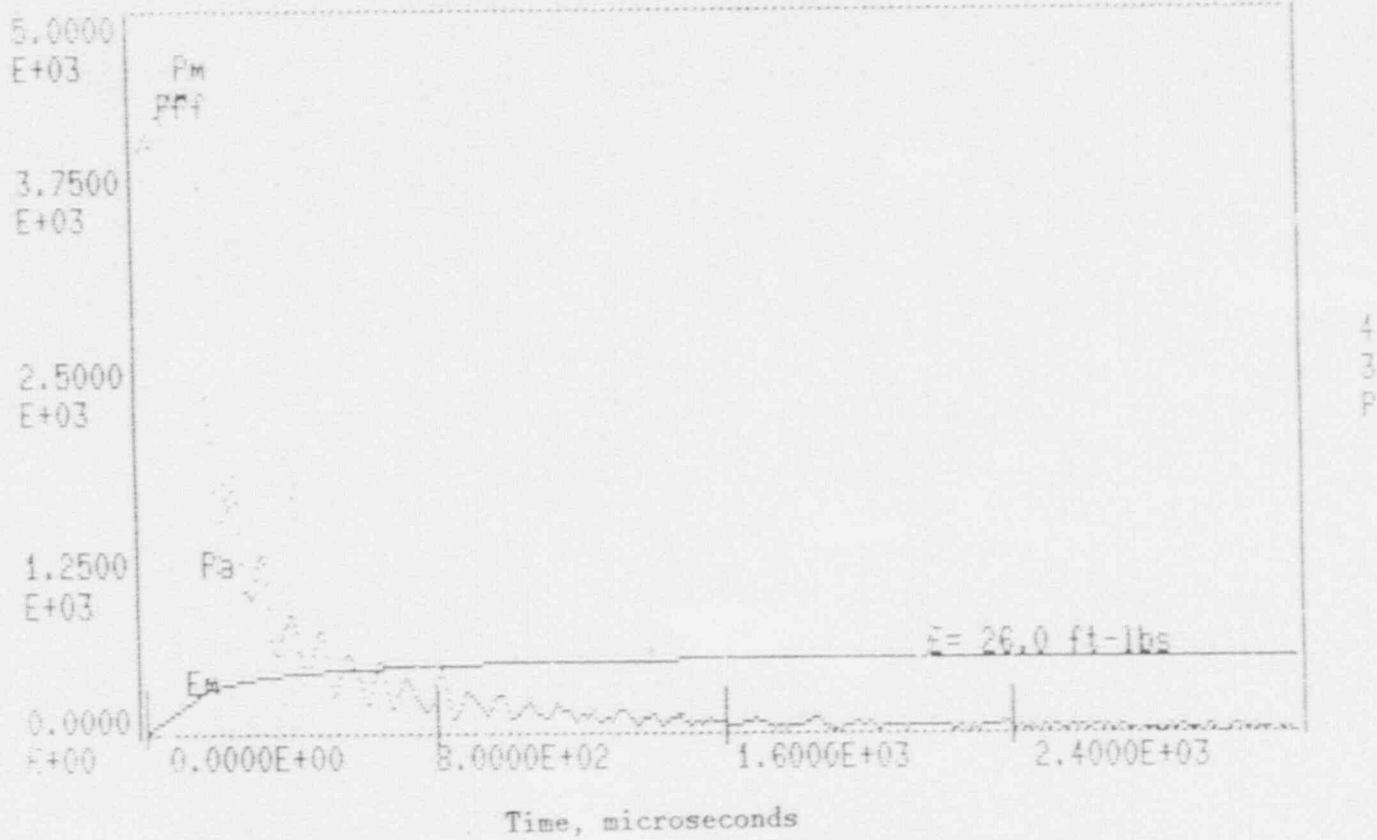

Figure A-36. Charpy impact test load-time record for Specimen 43P.

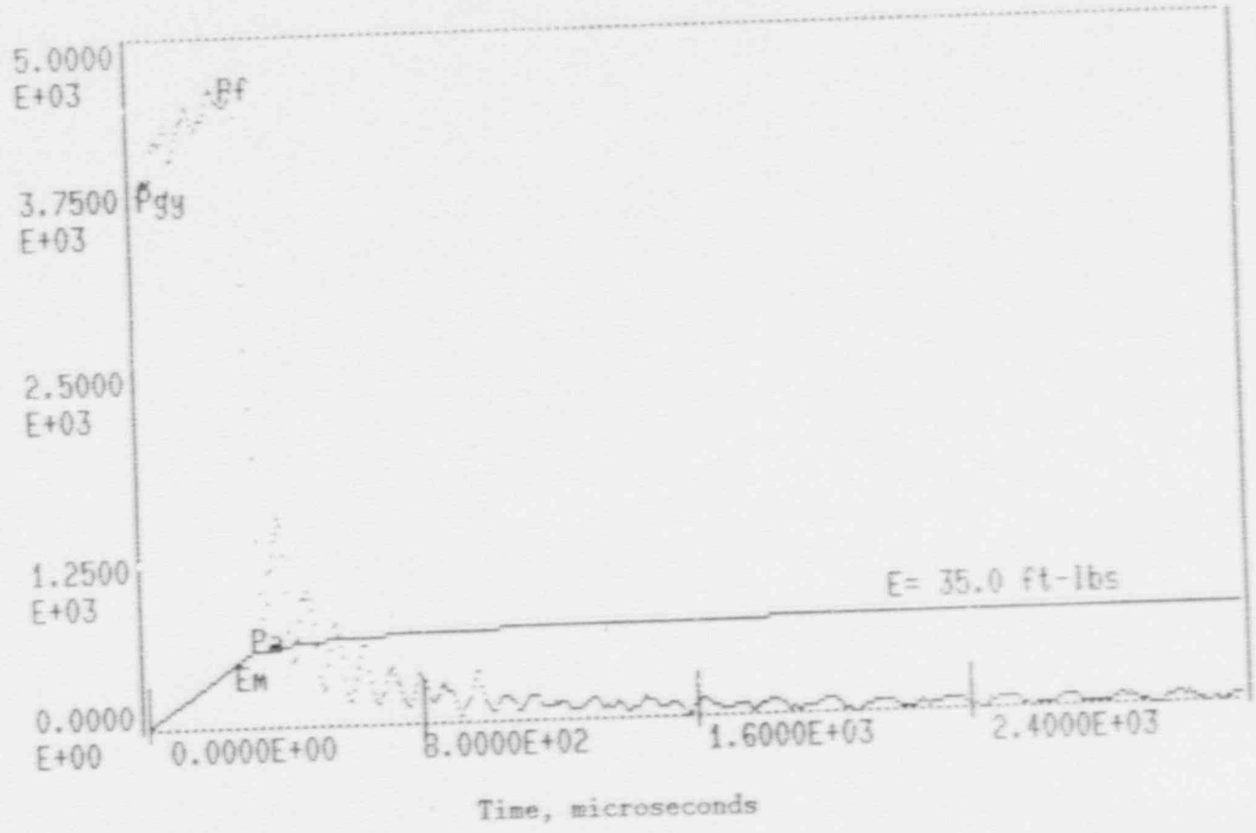

Figure A-37. Charpy impact test load-time record for Specimen 464.

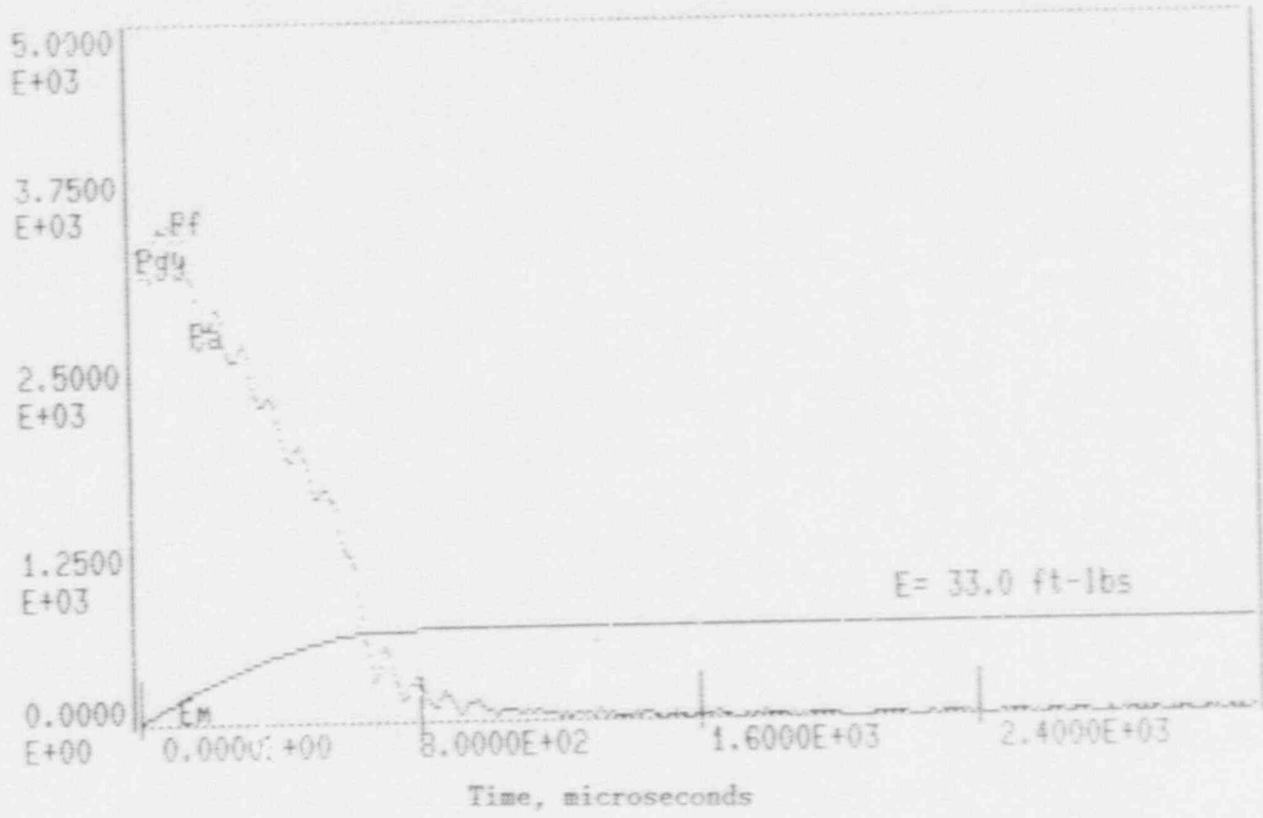

Figure A-38. Charpy impact test load-time record for Specimen 41C.

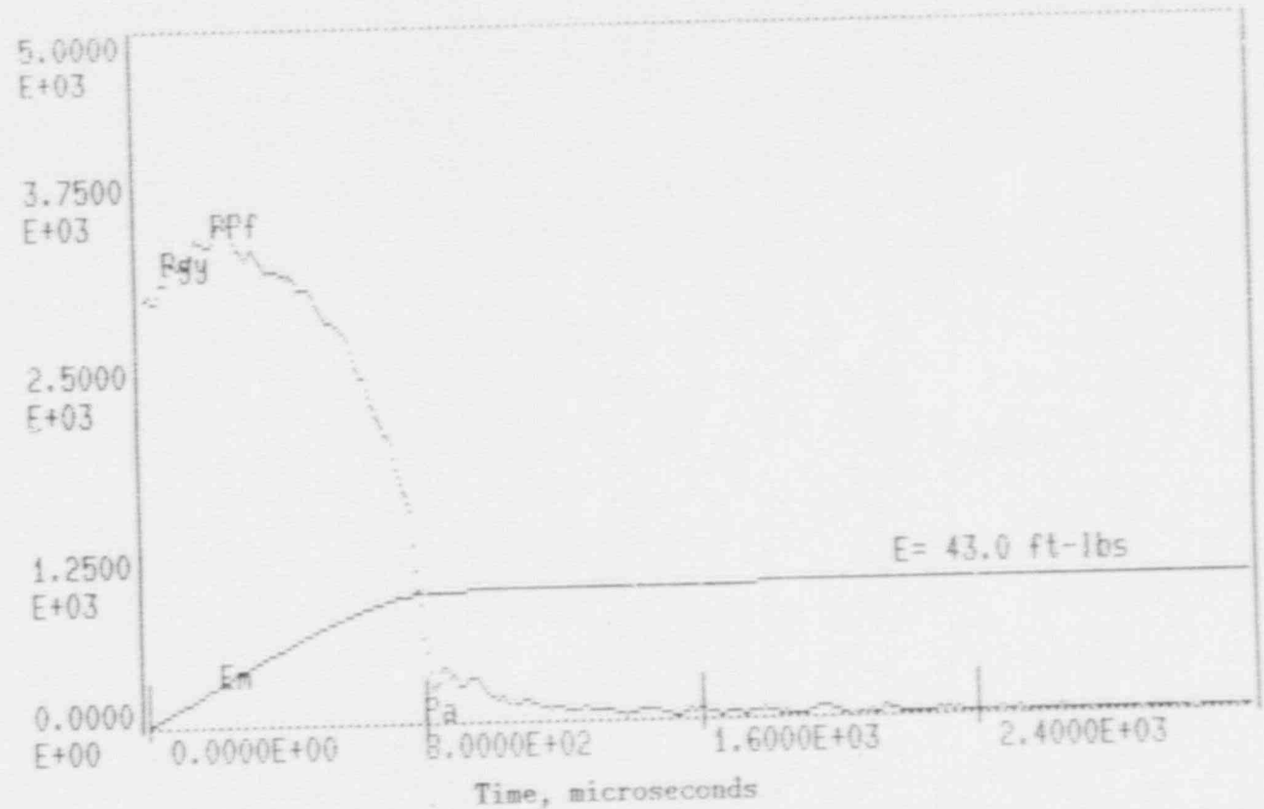

Figure A-39. Charpy impact test load-time record for Specimen 47E.

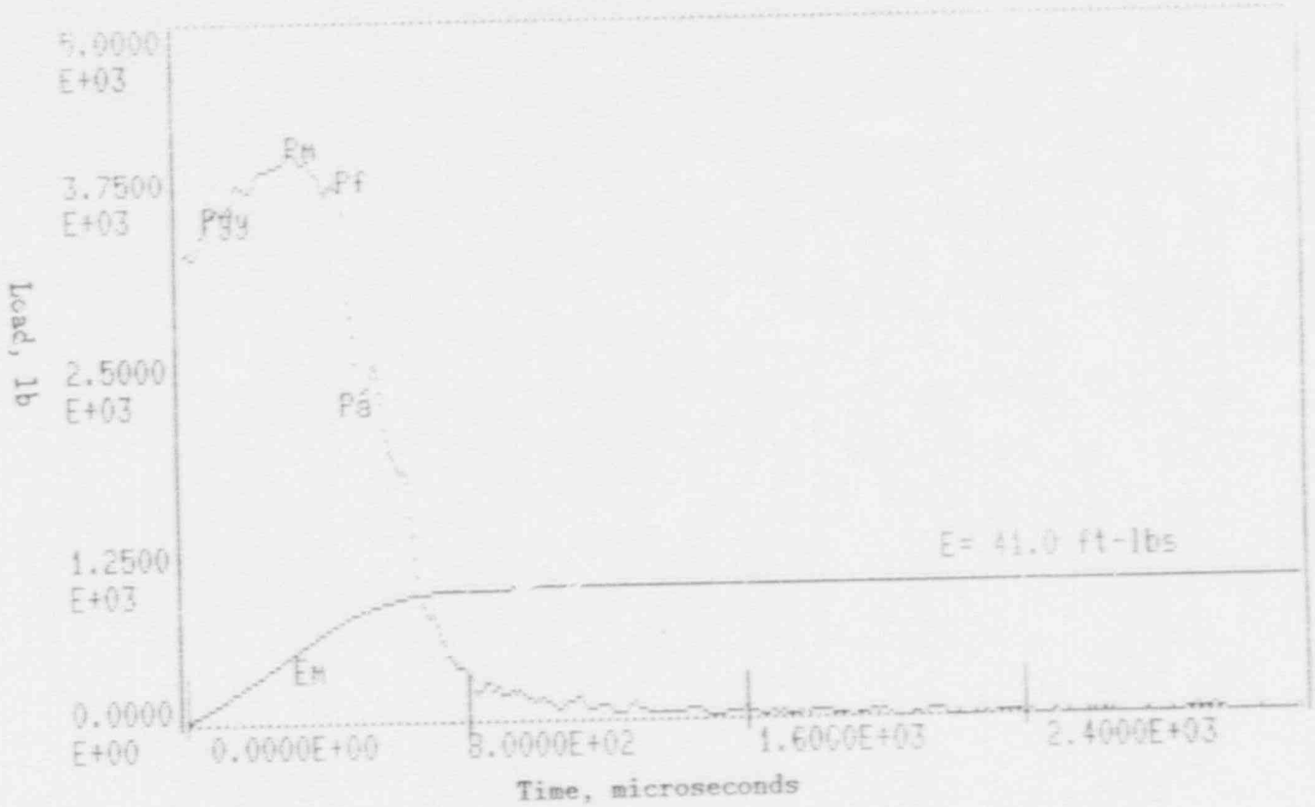

Figure A-40. Charpy impact test load-time record for Specimen 46T.

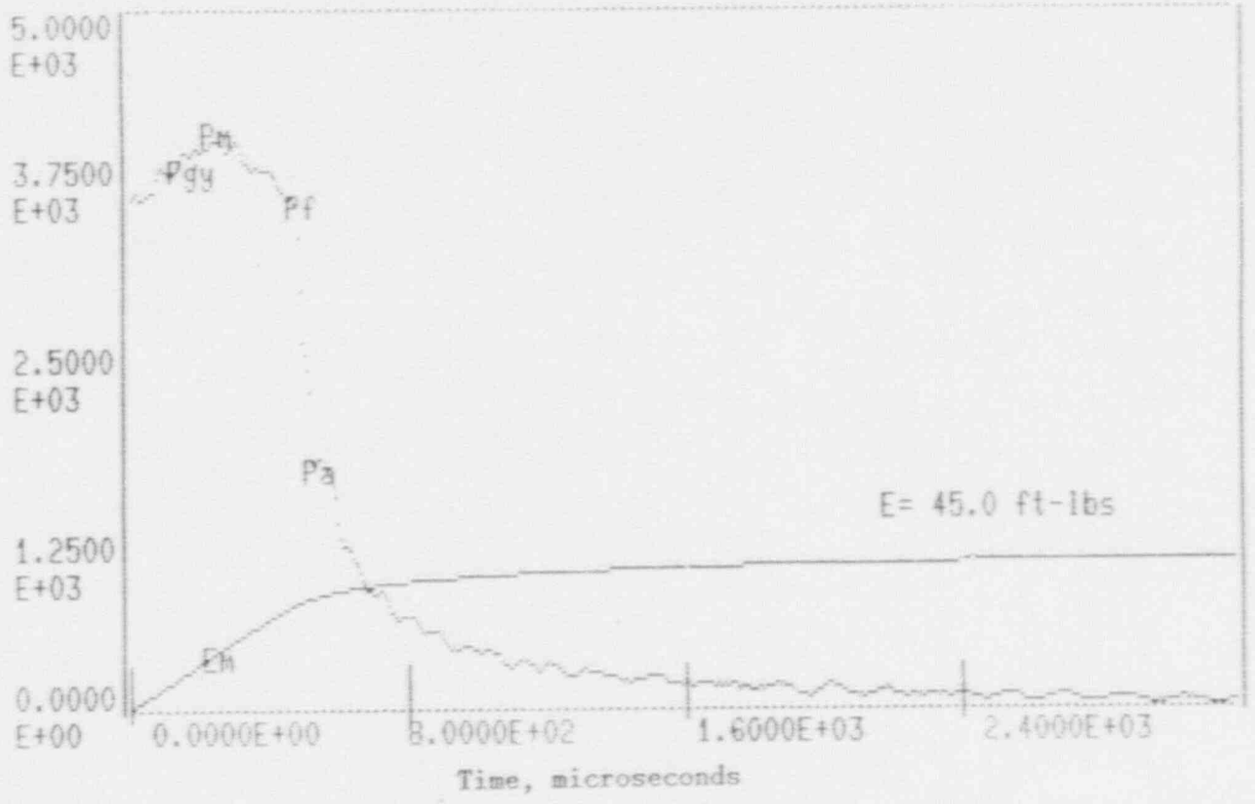

Figure A-41. Charpy impact test load-time record for Specimen 45M.

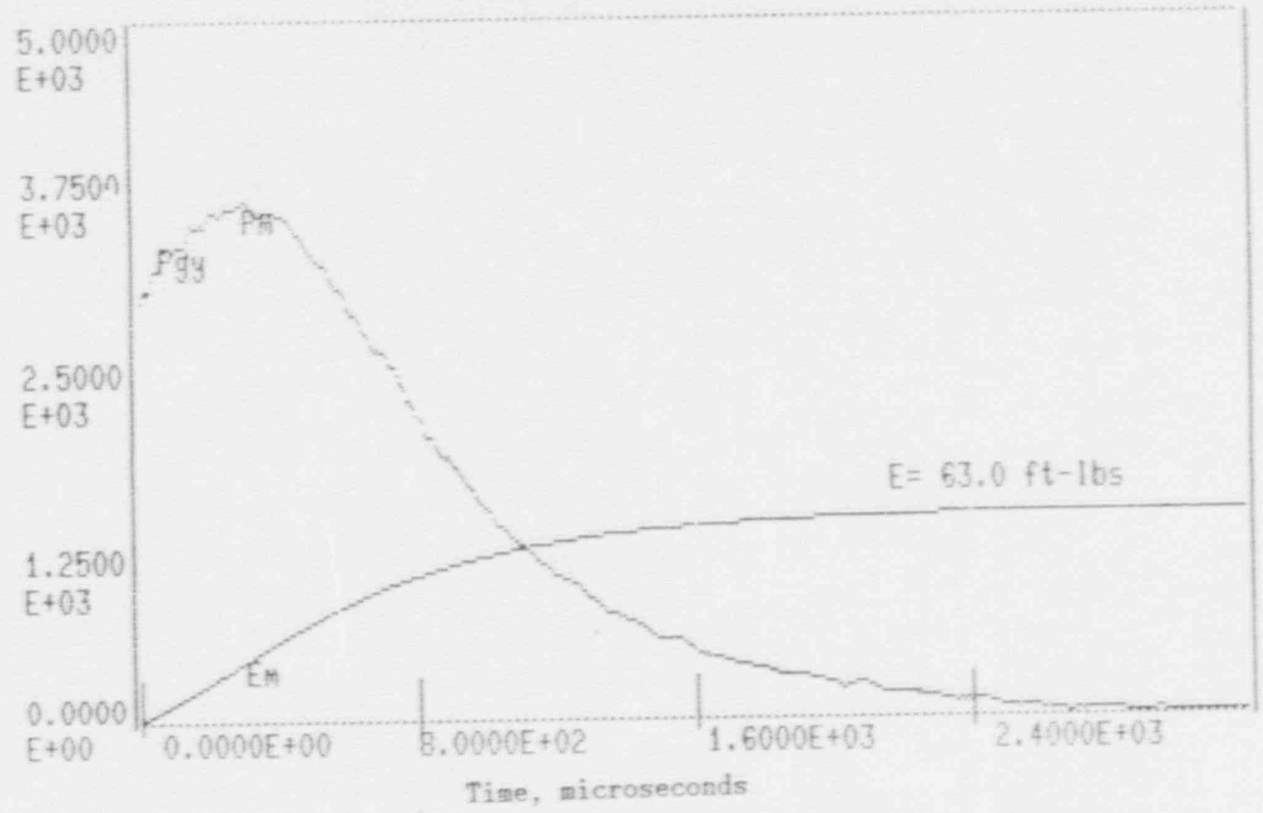

Figure A-41. Charpy impact test load-time record for Specimen 437.

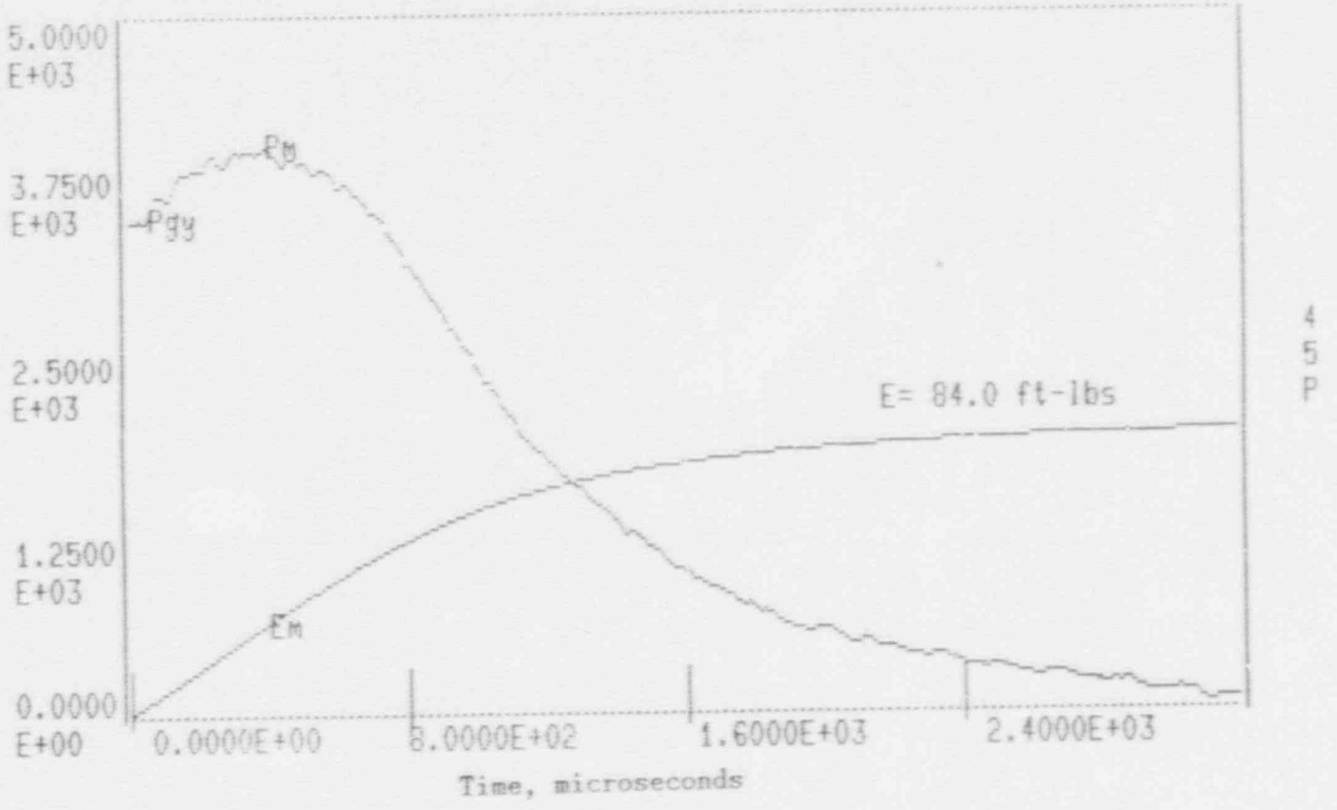

Figure A-43. Charpy impact test load-time record for Specimen 45P.

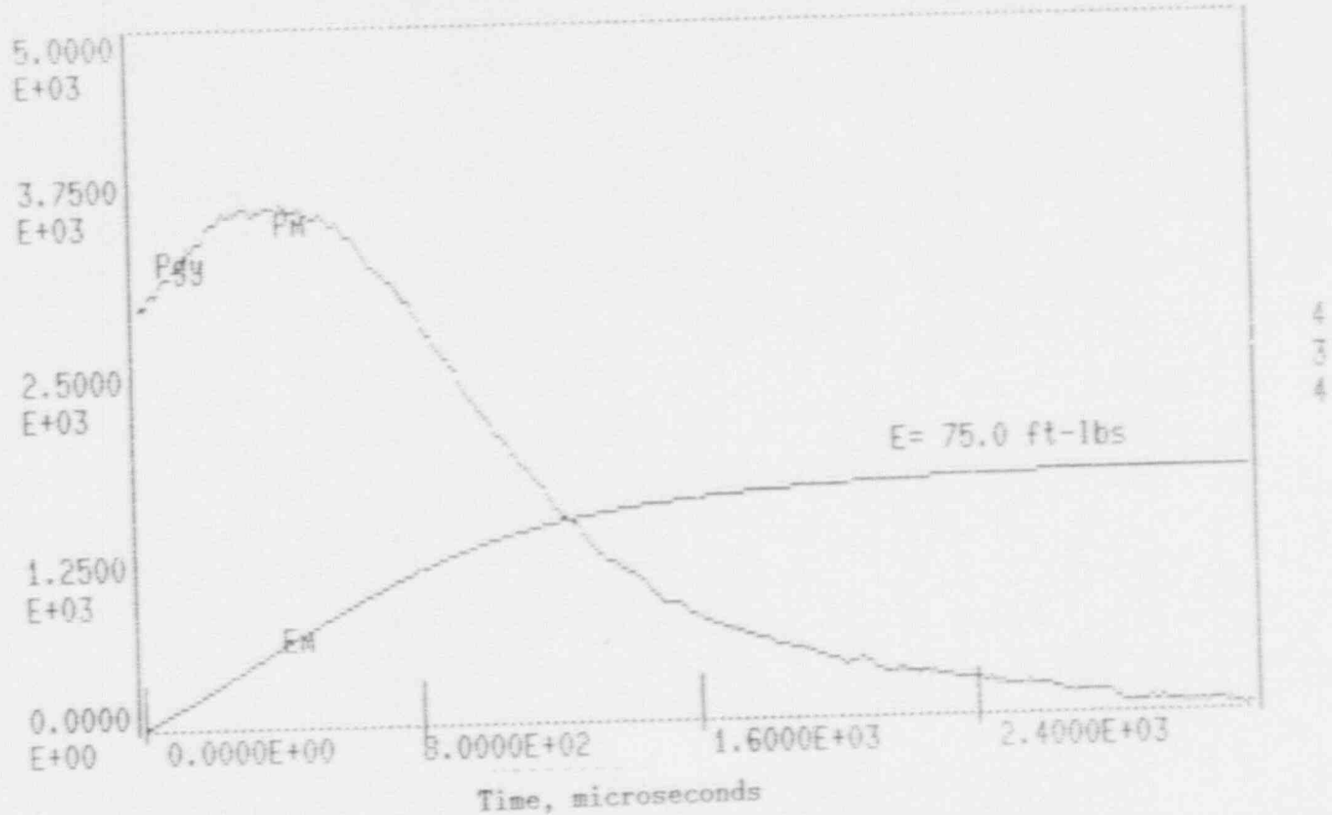

Figure A-44. Charpy impact test load-time record for Specimen 434.

ENCLOSURE B

APPLICABILITY OF HEAT AFFECTED ZONE MATERIAL IN CALCULATING REACTOR VESSEL NIL-DUCTILITY REFERENCE TEMPERATURE (RT_{NDT})

ENCLOSURE B

APPLICABILITY OF HEAT AFFECTED ZONE MATERIAL IN CALCULATING NIL-DUCTILITY REFERENCE TEMPERATURE (RT_{NDT}) SAN ONOFRE UNIT 3

Background Information

The original Unit 3 limiting beltline material based on the 1979 Combustion Engineering (CE) analysis of unirradiated surveillance capsule specimens was the heat-affected-zone (HAZ) metal. On June 12, 1989, Southern California Edison (SCE) submitted Proposed Change Number (PCN) NPF-15-292 revising Technical Specification (TS) 3/4.4.8, "Pressure/Temperature Limits," to be effective up to 8 Effective Full Power Years (EFPY) of operation. In the submittal, SCE noted the HAZ was no longer the limiting material based on the Battelle materials test report, and that the limiting material is now intermediate shell plate C-6802-1.

Discussion

From the original CE HAZ metal V-Notch Charpy impact energy test data, three data points appeared to be anomalous in comparison to the other data (see Figure 1). These anomalous data points led CE to use conservative bounding values (low values) for the HAZ metal Charpy Upper Shelf Energy (USE). As a result, the calculated RT_{NDT} in the CE analysis was believed to be high and overly conservative.

The Battelle materials test performed in 1989 re-evaluated the conservatism of the CE analysis. Battelle fabricated new specimens from archive HAZ metal, which was the limiting material at that time, and tested these samples. The results of the Battelle material test indicated much higher Charpy USE values for the HAZ metal than determined by CE (see Figure 2). We believe the inconsistencies were due to the use by CE of only 2 data points per test temperature and the three anomalous data points. Other factors contributing to the inconsistencies could have been from the non-standardized techniques in the preparation of the samples, the location of the machined notch relative to the HAZ metal, and an off-centered impact for some specimens.

The 1991 Westinghouse data from the first Unit 3 irradiated surveillance capsule specimens did not consider the HAZ metal data in the calculation of RT_{NDT}. This is consistent because HAZ metal is not limiting. Also, HAZ data shows significant scatter and, therefore, may not be representative of the strength of the full thickness of the HAZ material.

Results of SCE Evaluation

The Westinghouse Charpy USE curve for the HAZ metal is consistent with the CE Charpy USE curves with the exception of the three anomalous CE data points. The Battelle Charpy USE test results indicated values up to 59 ft-lbs higher than the Westinghouse values.

ENCLOSURE B

Table 1, Figure 1, and Figure 2, provide specific information on HAZ metal Charpy impact properties, initial RT_{NDT}, and the irradiated specimen test data RT_{NDT}. Table 1 predicted values were based on CE unirradiated specimen data. These values will be updated based on the irradiated surveillance capsule test results. As shown in Table 1, the Battelle unirradiated specimen initial RT_{NDT} is -40°F and the Westinghouse irradiated specimen test data indicated an RT_{NDT} shift of 45°F. We believe this -40°F RT_{NDT} is appropriate because of the care taken by Battelle in preparing (machining, cutting, and notching relative to the HAZ) their specimens. The Battelle data in Figure 2 shows very little scatter compared to CE's data in Figure 1 which shows significant scatter, including three data points considered to be anomalous.

However, as indicated in the transmittal letter, we used the CE unirradiated specimen data in conjunction with the Westinghouse irradiated specimen data to determine the RT_{NDT} shift for the HAZ metal. We believe this is appropriate because both surveillance capsule specimens were prepared by CE. HAZ metal was determined to be not limiting, therefore, HAZ metal is not a factor in determining RT_{NDT}.

TABLE 1

SAN ONOFRE NUCLEAR GENERATING STATION
UNIT 3

Predicted Values of RT_{NDT} for Reactor Vessel Beltline Materials at 8 EFPY

NOTE: The predicted values in this Table were based on CE unirradiated specimen data. The predicted values need to be updated based on the surveillance capsule irradiated specimen test results.

Description	Plate or Block No.	Cu %	Ni %	Intl. RT_{NDT}	Adj RT_{NDT}	RT_{NDT} Shift	Margin
Inter. Shell	C-6802-1	0.05	0.57	+40	92.4	27.3	25.1
Inter. Shell	C-6802-2	0.04	0.55	+0	44.6	22.9	21.7
Inter. Shell	C-6802-3	0.05	0.57	+20	72.4	27.3	25.1
Lower Shell	C-6802-4	0.05	0.57	+55	7.4	27.3	25.1
Lower shell	C-6802-5	0.05	0.57	+10	62.4	27.3	25.1
Lower shell	C-6802-6	0.06	0.62	+20	71.7	32.5	19.2
Long. Weld	2-203A	0.05	1.00	-40	71.2	59.8	51.4
Long. Weld	2-203B	0.05	1.00	-40	71.2	59.8	51.4
Long. Weld	2-203C	0.05	1.00	-40	71.2	59.8	51.4
Long. Weld	3-203A	0.04	0.16	-10	58.1	36.1	32.0
Long. Weld	3-203B	0.04	0.16	-10	58.1	36.1	32.0
Long. Weld	3-203C	0.04	0.16	-10	58.1	36.1	32.0
Circum. Weld	9-203	0.05	0.04	-50	2.4	27.3	25.1
HAZ (Battelle Data)		0.05	0.04	-40	21.7	32.5	29.2
HAZ (CE Data)		-	-	+70			

Predicted Fluence at 1/4 T = 6.51E18 n/cm^2

WESTINGHOUSE DATA

Description	Plate or Block No.	Predicted RT_{NDT} Shift	Test Data RT_{NDT} Shift
Inter. Shell Transverse	C-6802-1	31	55
Inter. Shell Longitudinal	C-6802-1	31	50
Weld Metal		27	32
HAZ Metal		-	45

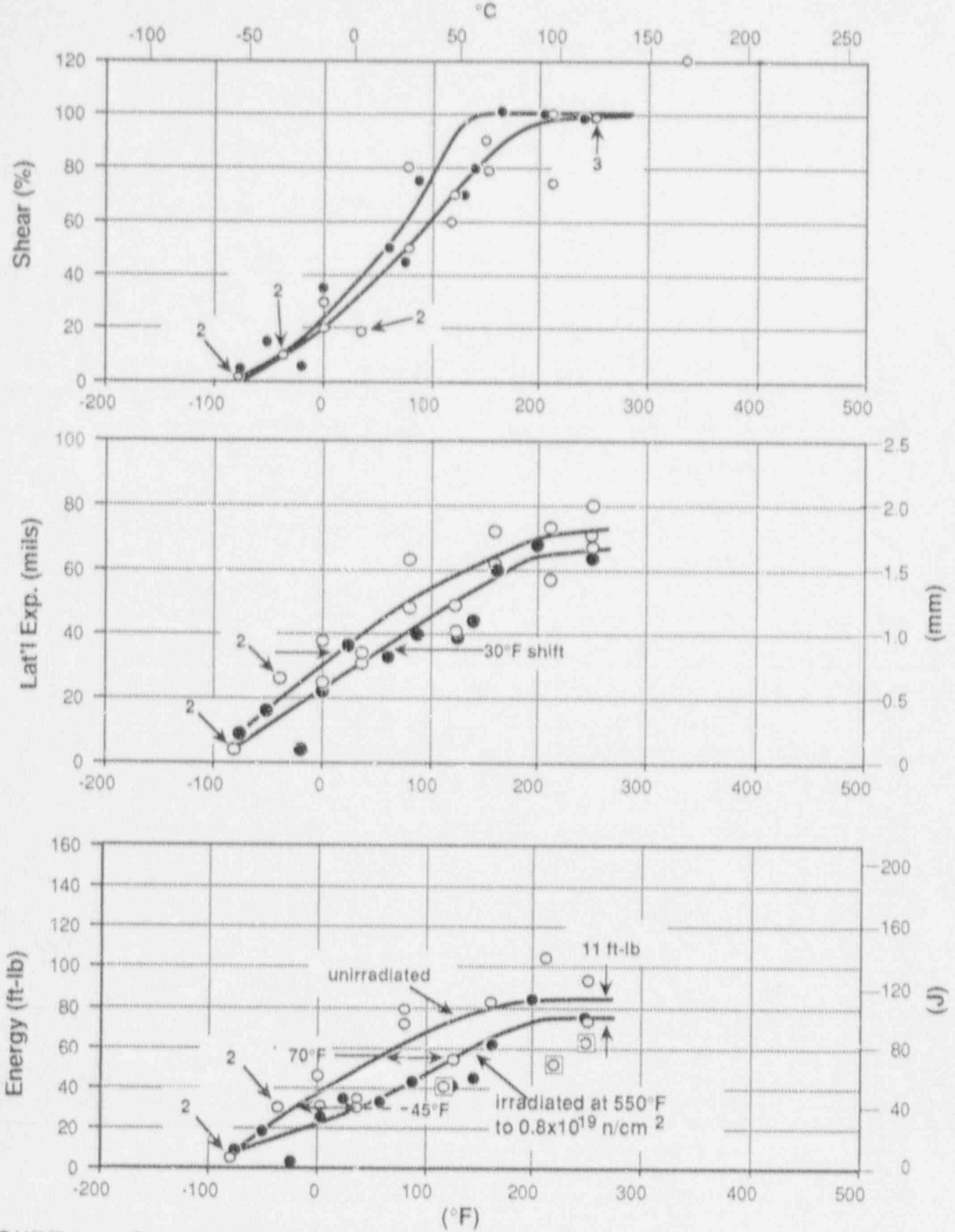

FIGURE 1: Charpy V-Notch Impact Properties for the San Onofre Unit 3 Reactor Vessel HAZ Metal

○ Unirradiated

● Irradiated at 550°F to 0.8 x 10^{19} n/cm^2

⊡ Unirradiated Anomalous Data Points

CE

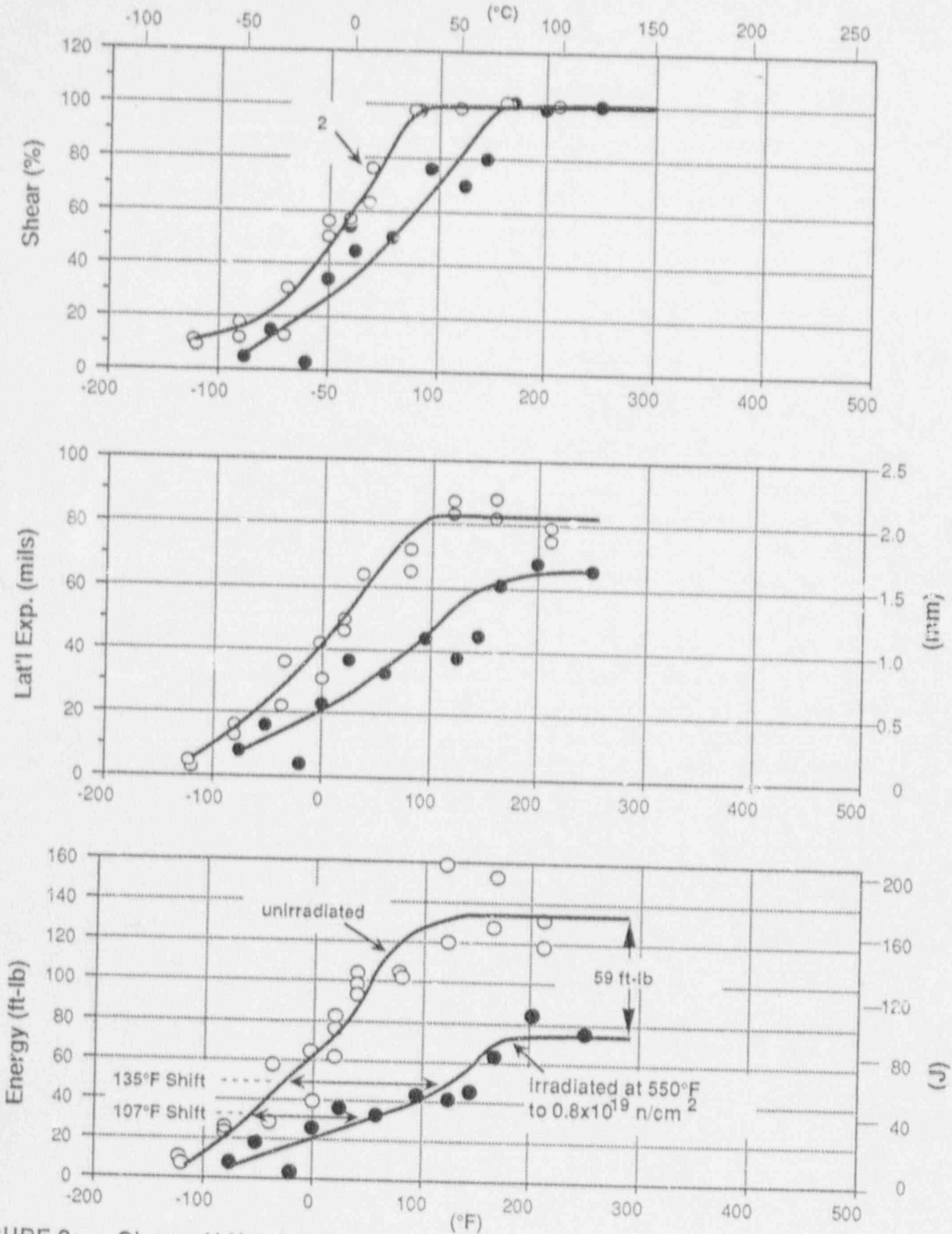

FIGURE 2: Charpy V-Notch Impact Properties for the San Onofre Unit 3 Reactor Vessel HAZ Metal

○ Unirradiated

● Irradiated at 550°F to 0.8 x 10^{19} n/cm^2

Battelle